

INFORMATION TO USERS

This manuscript has been reproduced from the microfilm master. UMI films the text directly from the original or copy submitted. Thus, some thesis and dissertation copies are in typewriter face, while others may be from any type of computer printer.

The quality of this reproduction is dependent upon the quality of the copy submitted. Broken or indistinct print, colored or poor quality illustrations and photographs, print bleedthrough, substandard margins, and improper alignment can adversely affect reproduction.

In the unlikely event that the author did not send UMI a complete manuscript and there are missing pages, these will be noted. Also, if unauthorized copyright material had to be removed, a note will indicate the deletion.

Oversize materials (e.g., maps, drawings, charts) are reproduced by sectioning the original, beginning at the upper left-hand corner and continuing from left to right in equal sections with small overlaps.

Photographs included in the original manuscript have been reproduced xerographically in this copy. Higher quality 6" x 9" black and white photographic prints are available for any photographs or illustrations appearing in this copy for an additional charge. Contact UMI directly to order.

**ProQuest Information and Learning
300 North Zeeb Road, Ann Arbor, MI 48106-1346 USA
800-521-0600**

UMI[®]

UNIVERSITY OF ALBERTA

**CAPILLARY ELECTROCHROMATOGRAPHY AND CAPILLARY
ELECTROPHORESIS FOR THE ANALYSIS OF BIOLOGICAL AND
ENVIRONMENTAL ANALYTES**

BY

MING QI



**A thesis submitted to the faculty of graduate studies and research in partial fulfillment
of the requirements for the degree of DOCTOR OF PHILOSOPHY**

DEPARTMENT OF CHEMISTRY

Edmonton, Alberta

SPRING 2002



**National Library
of Canada**

**Acquisitions and
Bibliographic Services**

**395 Wellington Street
Ottawa ON K1A 0N4
Canada**

**Bibliothèque nationale
du Canada**

**Acquisitions et
services bibliographiques**

**395, rue Wellington
Ottawa ON K1A 0N4
Canada**

Your file Votre référence

Our file Notre référence

The author has granted a non-exclusive licence allowing the National Library of Canada to reproduce, loan, distribute or sell copies of this thesis in microform, paper or electronic formats.

The author retains ownership of the copyright in this thesis. Neither the thesis nor substantial extracts from it may be printed or otherwise reproduced without the author's permission.

L'auteur a accordé une licence non exclusive permettant à la Bibliothèque nationale du Canada de reproduire, prêter, distribuer ou vendre des copies de cette thèse sous la forme de microfiche/film, de reproduction sur papier ou sur format électronique.

L'auteur conserve la propriété du droit d'auteur qui protège cette thèse. Ni la thèse ni des extraits substantiels de celle-ci ne doivent être imprimés ou autrement reproduits sans son autorisation.

0-612-68614-0

Canada

UNIVERSITY OF ALBERTA

LIBRARY RELEASE FORM

NAME OF AUTHOR: **Ming Qi**

TITLE OF THESIS: **Capillary Electrochromatography And Capillary
Electrophoresis For The Analysis Of Biological And
Environmental Analytes**

DEGREE: **Doctor of Philosophy**

YEAR THIS DEGREE GRANTED: **2002**

Permission is hereby granted to the University of Alberta Library to reproduce single copies of this thesis and to lend or sell such copies for private, scholarly or scientific research purposes only.

The author reserves all other publication and other rights in association with the copyright in the thesis, and except as hereinbefore provided, neither the thesis nor any substantial portion thereof may be printed or otherwise reproduced in any material from whatever without the author's prior written permission.



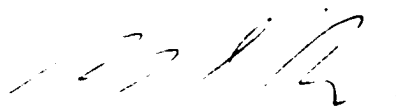
C9, 2329 Hudson Terrace
Fort Lee, NJ, 07024

Mar 31, 2002


UNIVERSITY OF ALBERTA

FACULTY OF GRADUATE STUDIES AND RESEARCH

The undersigned certified that they have read, and recommended to the Faculty of Graduate Studies and Research for acceptance, a thesis entitled **CAPILLARY ELECTROCHROMATOGRAPHY AND CAPILLARY ELECTROPHORESIS FOR THE ANALYSIS OF BIOLOGICAL AND ENVIRONMENTAL ANALYTE** Submitted by **MING QI** in partial fulfillment of the requirements for the degree of **DOCTOR OF PHILOSOPHY**



Dr. Norman J. Dovichi



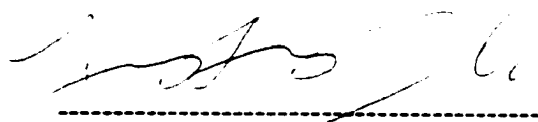
Dr. Liang Li



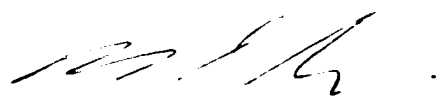
Dr. Mark T. McDermott



Dr. Rik R. Tykwinski



Dr. Xing-Fang Li



Dr. David D. Y. Chen

January 18, 2002

***To my loving grandmother, parents
and in memory of my mother***

Abstract

Capillary electrochromatography (CEC) offers the combined attributes of micro-high performance liquid chromatography (HPLC) and capillary zone electrophoresis (CZE). In the thesis technical aspects in CEC were explored including column-packing techniques, frit fabrication, column performance stability, and durability. A simplified slurry-packing procedure was refined for making 50 μm I.D. CEC columns that produced comparable performance to commercial columns. Evaluation of a single column over an extended period gave precision of 0.6-5.6% RSD for k' value, and 3.7-10% RSD for N value, with N from 60,000 - 213,000 plates/m. The variation from column to column (n=5) gave precision within 0.94% RSD in migration time, 17% RSD in theoretical plates and 6.9% RSD in resolution. The influences of sample loading, solvent ionic strength, organic solvent concentration, buffer pH, electric field and gap formation on separation efficiency and migration time were investigated.

CEC methods for analysis of 19 phenylthiohydantoin amino acids (PTH-AAs), 4 testosterone metabolites and 16 polycyclic aromatic hydrocarbons (PAHs) have been developed using thermo-optical UV absorbance detection (TOAD). A quantitative analysis of *in vitro* testosterone metabolites, transformed by Cytochrome P450 isozymes, was included to show the applicability of CEC in pharmacokinetics studies. CEC was demonstrated as a viable alternative technique to both HPLC and CZE in analysis of a certain range of hydrophobic compounds.

Non-aqueous CE coupled with electrospray ionization and mass spectrometric detection (CE/ESI/MS) was developed for drug screening of *Fritillaria* alkaloids. The

method allowed baseline resolution of 10 stereoisomeric alkaloids and simultaneous quantitation in much shorter analysis times than GC/MS or LC/MS methods.

Micellar electrokinetic chromatography (MEKC) using bile salts and organic modifiers was shown as applicable, efficient and cost-effective in separation of PAHs. Multiconformational bile salt aggregates and organic modifiers were found to play a significant role in determination of the electrophoretic mobilities of PAH.

Two mathematical approaches were proposed to correct the migration time variations of multiple analytes in MEKC. By using the migration markers, the precision of migration was dramatically improved to less than 0.6% for PTH-AAs, 0.4% for FTH-AAs, and 0.03% for oligosaccharides compared to 1%, 4%, and 3% respectively, without correction.

Acknowledgement

I would like to express my sincere gratitude to my supervisor, Dr. Norman J. Dovichi, for providing excellent scientific guidance, endless encouragement on my graduate research, and enormous patience on my process of thesis writing.

I would like to acknowledge everyone in the northern light laser lab. I felt lucky to have known so many talented colleagues and fellow students, who made my five-year graduate study in Canada meaningful and memorable. I thank you all for everything.

I am glad to express my heartfelt appreciation to my Ph.D. committee members, especially Dr. Y. K. Tam, who guided and supported me in the drug metabolite analysis and herbal medicine screening studies (Chapter 3 and 4). Dr. Xingfang Li, who initiated my interests in capillary electrophoresis. I thank the machine shop, electronic shop, and glass shop for all their assistance in constructing all sorts of instrumentation for my experiments. I also want to express my thankfulness to Ms. Kym Schreiner for numerous reviews and suggested corrections on my thesis drafts.

My special appreciation goes to my dear parents for their encouragement, understanding and years of patience, allowing their daughter to pursue her own way of life far away from home, to whom I am indebted for my whole life, To my dear brother for his cheerful remarks to his sister. Finally, I want to thank my dear grandmother, whose love and strength brought me the most encouragement in my life.

Table of Contents

CHAPTER 1 INTRODUCTION TO CAPILLARY ELECTROCHROMATOGRAPHY WITH THERMO-OPTICAL DETECTION AND MASS SPECTROMETRIC DETECTION	1
1.1 CAPILLARY ELECTROPHORESIS (CE)	2
1.1.1 CE Apparatus	3
1.1.2 Electroosmosis and Electrophoresis	4
1.1.3 CE Modes.....	7
1.1.3.1 Capillary Zone Electrophoresis (CZE)	7
1.1.3.2 Capillary Electrochromatography (CEC)	8
1.1.3.3 Micellar Electrokinetic Chromatography (MEKC)	8
1.1.3.4 Other CE Techniques - CGE, CIF, CTPP.....	11
1.1.3.5 Chip-Based CE.....	13
1.2 CAPILLARY ELECTROCHROMATOGRAPHY.....	13
1.2.1 History and Current Achievements.....	14
1.2.2 Technical Advantages.....	14
1.2.3 Problems and Solutions.....	15
1.2.4 Applications	16
1.2.5 CEC Columns	17
1.2.5.1 Column Types.....	17
1.2.5.2 Column Packing Techniques	19
1.2.5.3 Frit.....	22
1.2.6 Mobile Phase in CEC.....	22
1.2.7 Instrumentation	23
1.3 DETECTION SCHEMES.....	24
1.3.1 Thermo-Optical UV Absorbance Detection (TOAD).....	27
1.3.1.1 Thermal Lens Effect	30
1.3.1.2 Crossed-Beam TOAD.....	32

1.3.2 Electrospray Ionization Mass Spectrometric Detection (ESI/MS)	33
1.3.2.1 Electrospray Ionization	35
1.3.2.2 Practical Aspects of ESI.....	37
1.3.2.3 ESI Mass Spectrometer.....	39
1.3.2.3.1 ESI Sprayer	39
1.3.2.3.2 Vacuum Interfacing Region	43
1.3.2.3.3 Quadrupole Mass Analyzer.....	44
1.3.2.3.4 Mass Detector	47
1.3.2.4 CE/ESI/MS Current Development and Limitations	47
REFERENCES	49

CHAPTER 2 DEVELOPMENT OF CAPILLARY ELECTROCHROMATOGRAPHY COLUMN MANUFACTURE 62

2.1 INTRODUCTION	63
2.2 EXPERIMENTAL	65
2.2.1 Material and Reagents.....	65
2.2.2 Column Preparation	66
2.2.3 Frit Fabrication.....	68
2.2.4 Apparatus	70
2.3 RESULTS AND DISCUSSION	71
2.3.1 Packing Procedures and Frit Manufacture	71
2.3.2 Separation Efficiency.....	72
2.3.2.1 Loading Effect	76
2.3.2.2 Solvent Effect.....	76
2.3.2.3 Gap Formation	79
2.3.3 EOF and Velocities of Analytes	80
2.3.4 Effect of Organic Solvent	82
2.3.5 Effect of Buffer pH	85
2.3.6 Reproducibility	88
2.3.6.1 Reproducibility on a Single Column.....	88

2.3.6.2 Reproducibility from Column to Column.....	92
2.3.7 Application of CEC-TOAD	93
2.3.7.1 Analysis of Polycyclic Aromatic Hydrocarbon (PAHs).....	93
2.3.7.2 Analysis of Phenylthiohydantoin Amino Acids (PTH-AAs).....	99
2.3.8 Photothermal Absorbance Detection	105
2.4 CONCLUSIONS.....	107
REFERENCES	109

**CHAPTER 3 SEPARATION OF TESTOSTERONE METABOLITES IN
MICROSOMAL INCUBATES USING CAPILLARY
ELECTROPHORESIS.....**

.....	113
3.1 INTRODUCTION	114
3.2 EXPERIMENTAL	115
3.2.1 Materials and Instrumentation	116
3.2.2 Preparation of Standards	116
3.2.3 Preparation of Testosterone Metabolites <i>in Vitro</i>	117
3.2.4 CEC Conditions	118
3.3 RESULTS AND DISCUSSION	118
3.3.1 CEC Method development.....	118
3.3.2 Calibration and Quantification.....	123
3.4 CONCLUSIONS.....	125
REFERENCES	126

**CHAPTER 4 DEVELOPMENT OF NON-AQUEOUS CE/MS METHOD FOR
ANALYSIS OF ALKALOIDS FROM *FRITILLARIA***

.....	128
4.1 INTRODUCTION	129
4.2 EXPERIMENTAL	132
4.2.1 Chemicals and Materials.....	132
4.2.2 Instrumentation	132

4.2.3 Flow Injection Analysis (FIA).....	133
4.2.4 NACE/MS.....	133
4.2.4.1 Optimization	134
4.2.4.2 Calibration Curves	135
4.2.4.3 Analysis of Active Extract and Crude Extract from <i>Fritillaria</i> Species	135
4.3 RESULTS AND DISCUSSION.....	136
4.3.1 Influence of Spray parameter on Mass Spectra of Verticine	136
4.3.2 Ion Suppression.....	139
4.3.3 NACE/MS Condition Optimization.....	140
4.3.4 Calibration, LOD, Precision and Assays	146
4.4 CONCLUSIONS.....	151
REFERENCES	153

**CHAPTER 5 CAPILLARY ELECTROPHORETIC SEPARATION OF
POLYCYCLIC AROMATIC HYDROCARBONS USING SODIUM CHOLATE IN
MIXED AQUEOUS - ORGANIC BUFFERS..... 154**

5.1 INTRODUCTION.....	155
5.2 EXPERIMENTAL	157
5.2.1 Reagents and Materials	157
5.2.2 Instrumentation	158
5.2.3 Calculations.....	159
5.3 RESULTS AND DISCUSSION.....	159
5.3.1 Effect of Bile Salt Type and Condition.....	159
5.3.2 Effect of Organic Modifiers.....	162
5.3.3 Effect of Buffer Concentration and pH.....	167
5.4 CONCLUSION.....	168
REFERENCES	169

CHAPTER 6 MIGRATION TIME CORRECTION FOR ANALYSIS OF DERIVATIZED AMINO ACIDS AND OLIGOSACCHARIDES USING MICELLAR ELECTROKINETIC CHROMATOGRAPHY	171
6.1 INTRODUCTION	172
6.2 THEORY	174
6.2.1 Method 1	174
6.2.2 Method 2	176
6.3 EXPERIMENTAL	178
6.3.1 PTH-Amino Acids	178
6.3.2 FTH-Amino Acids	178
6.3.3 Tetramethylrhodamine-Labeled Oligosaccharides	180
6.4 RESULTS AND DISCUSSION	181
6.4.1 PTH-Amino Acids	181
6.4.2 Between-Day Precision.....	183
6.4.3 FTH-Amino Acids	186
6.4.4 Oligosaccharide Analysis.....	188
6.5 CONCLUSIONS.....	188
REFERENCES	190
CHAPTER 7 CONCLUSIONS AND FUTURE WORKS	192

List of Figures

Figure 1.1 Schematic diagram of capillary electrophoresis.....	4
Figure 1.2 Diagram of capillary inner surface and the electrical double layer.....	6
Figure 1.3 Migration of micelle and neutral analyte in MEKC.....	10
Figure 1.4 Diagram of a crossed-beam photothermal detection.....	29
Figure 1.5 Diagram of thermo-Optical UV absorbance detection system.....	33
Figure 1.6 ESI Ion formation process.....	36
Figure 1.7 API 100 Ion optic path.....	40
Figure 1.8 Sciex IonSpray interface.....	42
Figure 1.9 A: Schematic diagram of quadrupole mass filter; B: Cross section of rods and their DC and AC potential.....	45
Figure 2.1 Slurry packing set up.....	67
Figure 2.2 Column manufacture procedure.....	69
Figure 2.3 Plot of the plate height measured with thiourea, and PTH derivatives of asparagine, leucine, tryptophan vs. electroosmotic flow.....	75
Figure 2.4 CEC separation of EOF marker and PTH-Amino acids mixture.....	77
Figure 2.5 Plot of plate counts vs. injection amount using the product of injection voltage and time.....	78
Figure 2.6 Electrochromatograms of PTH-W with different sample media.....	79
Figure 2.7 A: Plot of test compound velocity vs. electric field strength. B: Plot of retention factor vs. electric field strength.....	83
Figure 2.8 Dependence of electroosmotic flow (EOF) velocity vs. acetonitrile content ..	84

Figure 2.9 Electrochromatograms of test mixture at increasing acetonitrile content	86
Figure 2.10 Plot of $\log(k')$ vs. acetonitrile content at constant ionic strength.....	87
Figure 2.11 Electrochromatograms of test mixture using mobile phase containing acetonitrile and buffer at different pH values	89
Figure 2.12 Plot of (A) electroosmotic mobility and (B) retention factor of PTH – amino acids as a function of buffer PH.....	90
Figure 2.13 Migration time stability of electroosmotic flow marker (thiourea) and its RSD over nine days	92
Figure 2.14 Reproducibility of migration time, plate height, and resolution on five columns	94
Figure 2.15 Molecular structures of 16 EPA priority pollutants: polycyclic aromatic hydrocarbons.....	95
Figure 2.16 Electrochromatogram of 16 polycyclic aromatic hydrocarbons	97
Figure 2.17 Electrochromatograms of polycyclic aromatic hydrocarbons at different sample concentrations.....	98
Figure 2.18 Electrochromatograms of phenylthiohydantoin amino acids by CEC using buffers (A) MES, (B) NaAC/HAc.....	101
Figure 2.19 Electrochromatogram of 19 Phenylthiohydantoin amino acids	103
Figure 2.20 Electrochromatograms of 19 phenylthiohydantoin amino acids using buffers with different concentrations	104
Figure 2.21 Electrochromatogram of 19 phenylthiohydantoin amino acids.....	105

Figure 3.1 Structure of testosterone with possible monohydroxylation sites by CYPs...	120
Figure 3.2 Electrochromatograms of standard mixture of 7 α , 6 β , 2 α , 16 α - hydroxy-testosterone and testosterone by 10 mM MES buffer with 50 to 80% acetonitrile	121
Figure 3.3 Electrochromatograms of standard mixture by using a: HEPES, b: MES buffers	122
Figure 3.4 Electrochromatograms of standard mixture by using a: C8, b: C18 stationary phase	123
Figure 3.5 Separation of in-vitro testosterone metabolites from rat hepatic microsomes	125
Figure 4.1 Structures of <i>Fritillaria</i> alkaloids	130
Figure 4.2 A: Influence of ionspray voltage on the total ion current and the extracted ion current of the molecular species of verticine	137
Figure 4.2 B: Influence of orifice voltage on the extracted ion current of molecular species of verticine and of its fragment ion	138
Figure 4.3 Matrix ion composition of NH ₄ ⁺ on signal level of the total ion current and the extracted ion current of molecular species of verticine in electrokinetic infusion using NACE/ESI/MS.....	140
Figure 4.4 Effect of ionic strength on separation selectivity	141
Figure 4.5 Effect of alkaloids stacking	143
Figure 4.6 Effect of composition of MeOH and ACN on separation efficiency	145
Figure 4.7 NACE/ESI/MS separation three major alkaloids	147
Figure 4.8 Analysis of extract of active fraction of Zhebei herb	149

Figure 4.9 Analysis of crude extract of Zhebei herb	151
Figure 5.1 Structure of bile salts.....	157
Figure 5.2 Plot of migration times vs. sodium cholate concentration.....	161
Figure 5.3 Plot of electrophoretic mobility vs. sodium cholates concentration.....	162
Figure 5.4 Plot of analyte electrophoretic mobility vs. percent of methanol in separation buffer.....	164
Figure 5.5 Plot of analyte electrophoretic mobility vs. percent of acetonitrile in separation buffer.....	165
Figure 5.6 Electropherograms of PAHs using two optimized separation conditions at the same electric field strength	166
Figure 6.1 Relative standard deviation of migration times for 19 PTH-amino acids, DMPTU, DPTU, and DPU before correction, after one-marker correction, and after two- marker correction	182
Figure 6.2 Comparison of electropherograms for raw data, one-marker corrected data, and two-marker corrected data for separation of PTH-amino acids	184
Figure 6.3 Relative standard deviation of migration times of 19 PTH-amino acids, DMPTU, DPTU, DPU before correction, after one-marker correction, and after two- marker correction from 10 runs obtained over two months.....	185
Figure 6.4 Relative standard deviation (RSD) of migration times for 19 FTH-Amino acids and unknown by-product before correction, after one-marker correction, and after two-marker correction.....	187
Figure 6.5 Relative standard deviation of migration times of five oligosaccharides before correction, after one-marker correction, and after two-marker correction	189

List of Tables

Table 1.1 Literature of column packing protocols.....	21
Table 1.2 Detection methods for capillary electrophoresis	25
Table 2.1 Average and RSD (n=110) of retention factor (k'), efficiency (N), and resolution on a single column	91
Table 2.2 Data of migration time and plate count for each polycyclic aromatic hydrocarbon	99
Table 2.3 LODs of 13 resolved PTH - amino acids using CEC and MEKC with TOAD	107
Table 3.1 Calibration curve data for the quantitation of testosterone metabolites (2 α , 6 β , 7 α , hydroxylate).....	124
Table 4.1 Calibration data for the quantitation	146
Table 4.2 Identification of alkaloids in the active fraction extract	150

LIST OF ABBREVIATIONS

AA	Amino acid
ACE	Affinity capillary electrophoresis
ACN	Acetonitrile
AMI	Amitriptyline
API	Atmospheric pressure ionization
APCI	Atmospheric pressure chemical ionization
CE	Capillary electrophoresis
CEC	Capillary electrochromatography
CEM	Channel electron multiplier
CGE	Capillary gel electrophoresis
CID	Collision-induced dissociation
CMC	Critical micelle concentration
CIEF	capillary isoelectric focusing
CITP	Capillary isotachophoresis
CZE	Capillary zone electrophoresis
DABSYL	4,4-Dimethylaminoazobenzene-4'-sulfonyl
DMPTU	N,N-dimethyl-N'-phenylthiourea
DNA	Deoxyribonucleic acid
DMPTU	Dimethylphenylthiourea
DPTU	Diphenylthiourea
DPU	Diphenylurea
EI	Electron ionization
EOF	Electroosmotic flow
EPA	Environmental protection agency
ES	Electrospray
ESI	Electrospray ionization
FIA	Flow injection analysis
FID	Flame ionization detection
FTICR	Fourier transform ion cyclotron resonance

GC	Gas chromatography
HEPES	N-2-hydroxyethylpiperazine-N'-2-ethanesulfonic acid
HPLC	High performance liquid chromatography
ID	Inner diameter
IT	Ion trap
LIF	Laser induced fluorescence
LOD	Limit of detection
MALDI	Matrix-assisted laser desorption ionization
MEKC	Micellar electrokinetic chromatography
MeOH	Methanol
MES	4-morpholinoethanesulfonic acid
MS	Mass spectrometry
NACE	Non-aqueous capillary electrophoresis
NADPH	Nicotinamide adenine dinucleotide phosphate
OD	Outer diameter
ODS	Octadecylsulfonic acid
ODSS	Octadecylsulfonated silica
TMR	tetramethylrhodamine
PAH	polycyclic aromatic hydrocarbon
PAGE	Polyacrylamide gel electrophoresis
PEEK	Polyether ether ketone
PTFE	Polytetrafluoroethylene
psi	pounds per square inch
PTH	Phenylthiohydantoin
SCX	Strong cation exchange
SDS	Sodium dodecyl sulphate
TLC	Thin layer chromatography
TOAD	Thermal-optical UV absorbance detection
TOF	Time of flight
TRIS	Tris (hydroxymethyl)aminomethane
UV	Ultraviolet

The common amino acids:

A	alanine
R	arginine
N	asparagine
D	aspartic acid
C	cysteine
E	glutamic acid
Q	glutamine
G	glycine
H	histidine
I	isoleucine
L	leucine
K	lysine
M	methionine
F	phenylalanine
P	proline
S	serine
T	threonine
W	tryptophen
Y	tyrosine
V	valine

CHAPTER 1

INTRODUCTION TO CAPILLARY ELECTROCHROMATOGRAPHY WITH THERMO-OPTICAL DETECTION AND MASS SPECTROMETRIC DETECTION

1.1 CAPILLARY ELECTROPHORESIS

Electrophoresis was first introduced as an analytical technique for separation of blood plasma proteins by Tiselius in 1930 [1], who was awarded the Nobel Prize for his pioneering work. Electrophoresis is the movement of electrically charged molecules in a conductive liquid medium under the influence of an electric field.

Capillary electrophoresis (CE), based on the principle of electrophoresis for separation of charged species in a capillary tube, can be traced back several decades. Hjertén in 1967 exploited the performance of open tube electrophoresis in a rotating glass column to minimize convective diffusion due to Joule heating commonly observed in electrophoresis [2]. Mikkers *et al.* demonstrated the use of a small-diameter, 200 μm inner diameter, Teflon[®] capillary for electrophoresis and UV absorbance and conductivity for detection [3]. Jorgenson *et al.* in 1981 demonstrated the use of a fused silica capillary tube of 75 μm i.d. for the separation column [4]. Jorgenson's several research works renovated CE into an analytical technique in aspects of instrumentation in the early 1980's[5-6]. Since then, CE has expanded largely on various aspects and applications in the last two decades (1981-2000).

CE has received tremendous interest because of its high efficiency, fast separation speed, ability to deal with minute amount of analytes, and compatibility with miniaturization and automation of analytical instrumentation. The most recent technical developments, application accomplishments, and future prospects of this technique have been reviewed in an issue of *Electrophoresis* in 1999 [7] and recently by several groups in the past year [8-10].

Capillary electrophoresis has made great contributions and still plays an important role in human genome research such as DNA sequencing [11-14], in proteomics [15-18],

and in new drug discovery [19]. CE is now widely used for traditional chemical separation and analysis in different fields, such as analytical chemistry [20-21], molecular biology [22-23], clinical chemistry [24], the pharmaceutical industry [19, 25-26], forensic chemistry [27], and food science [28]. Affinity capillary electrophoresis (ACE) is also used to study molecular interactions based on differential electrophoretic mobility of a complex and a free ligand, such as the binding constant, K_b , of a receptor protein to a drug molecule [29-30].

1.1.1 CE Apparatus

Capillary electrophoresis can be performed in a simple device as shown in Figure 1.1. The apparatus consists of several major components: a capillary column, two buffer vials, named as inlet vial and outlet vial respectively, two electrodes called anode and cathode, a high voltage supply, a detector, and a data system. The buffer-filled fused-silica capillary commonly of 10 to 100 μm inner diameter, 150 to 360 μm outer diameter and about 40 to 100 cm in length is placed between two vials. After the sample is introduced in the capillary, the high potential is applied across the capillary via the two electrodes. Under the electrical field across the capillary, the positively charged species migrate to cathode, whereas the negatively charged species move to anode, the process of which is termed as electrophoresis. Besides, the buffer solution also moves through the capillary column from inlet to outlet due to the electroosmosis. The charged species are thus separated in the order of electrophoretic mobility and are detected by the appropriate detector. The signal is digitized and recorded by a data system.

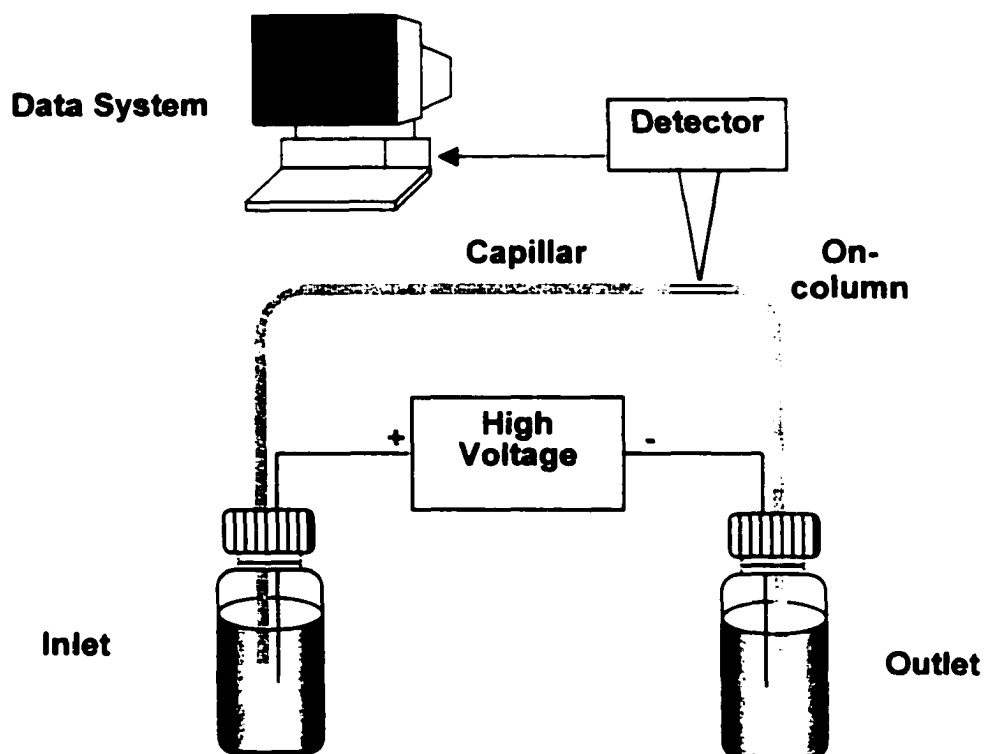


Figure 1.1 Schematic diagram of capillary electrophoresis

1.1.2 Electroosmosis and Electrophoresis

Electroosmosis and electrophoresis are the two main phenomena that are responsible for separation of both charged and neutral analytes. Electroosmosis arises from the solid-liquid interface at the inner surface of fused-silica capillary wall. The ionization of silanol groups at the inner capillary surface results in a negatively charged surface layer, which influences the distribution of the nearby ions in the solution. The counter-ions are attracted to the surface to maintain the charge balance, whereas the co-ions are repelled. The counter-ions are arranged into two layers, stagnant and diffuse.

defined as an electrical double layer [31]. The surface of the shear is located at beyond the interface of two layers. The electric potential at the surface of the shear is known as zeta potential, ζ . The potential falls exponentially to zero in the diffuse layer, as depicted in the Figure 1.2. The applied high voltage across the capillary causes the solvated cations at the diffuse layer to move toward the cathode by the electric force, dragging the solvent molecules along with them. The zeta potential is given by [32]:

$$\zeta = 4\pi\delta\sigma/\varepsilon_0\varepsilon_r \quad (1.1)$$

where δ is the thickness of the diffuse double layer, σ is the charge density at the surface of the shear of the electrical double layer, ε_0 is the permittivity of vacuum, and ε_r is the dielectric constant of the mobile phase.

The electroosmosis flow (EOF) velocity is determined by the Smoluchowski equation as follow [33]:

$$v_{eo} = \varepsilon_0\varepsilon_r\zeta E/4\pi\eta \quad (1.2)$$

where E is the electric field strength, and η is the viscosity of the mobile phase. EOF can be diminished to zero or reverse in direction by modifying the surface of the capillary wall, including covalent bonding [34] or dynamic coating [35].

Electrophoresis is the movement of charged molecules in a conductive liquid medium under the influence of an electric field. The positively charged cations will migrate toward the cathode, and the anions will migrate toward to anode. The rates at which they migrate depend on their charge to size ratio and are defined as the following equation [36].

$$v_{ep} = q/6\pi\eta a \quad (1.3)$$

where q is the charge of the ion, a is the radius of a spherical ion.

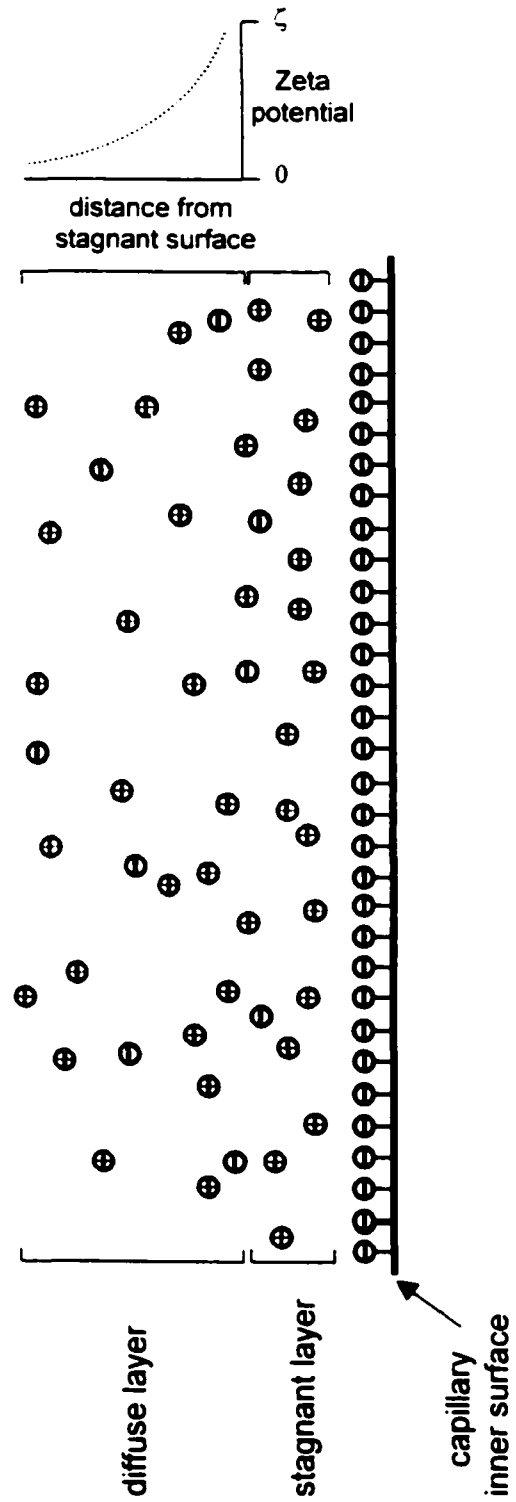


Figure 1.2 Diagram of the capillary inner surface and the electrical double layer

1.1.3 CE Modes

Based on the concept of electrokinetic separation, several separation modes have been explored including capillary zone electrophoresis (CZE), micellar electrokinetic chromatography (MEKC), capillary electrochromatography (CEC), and other CE modes such as capillary isotachopheresis (CITP), capillary isoelectric focusing (CIEF), and capillary gel electrophoresis (CGE). Recently, another format of capillary electrophoresis, chip-based CE (chip-CE), performed on a planar glass, has created enormous excitement [37-39].

1.1.3.1 Capillary Zone Electrophoresis

Capillary zone electrophoresis (CZE) is the simplest form of CE method in terms of separation mechanism. It is widely used to directly resolve charged analytes according to the charge to mass ratio.

In CZE, separations occur in an open tubular capillary filled with aqueous solution. Both electroosmosis and electrophoresis occur in a separation. However, electrophoresis is the only mechanism responsible for the separation, because the electroosmosis process pushes all the analytes to the cathode at the same rate. As a result, the ions move at the rate of a sum of electroosmotic and electrophoretic velocities. Assuming the inlet vial is applied with a positive electric potential, positive ions migrate fastest with the electroosmotic and electrophoretic mobility having the same direction, while the negative ions move slowest with EOF and electrophoretic velocity in opposite direction. Neutral molecules move at the rate of the electroosmotic flow.

1.1.3.2 Capillary Electrochromatography

Capillary electrochromatography (CEC) is a hybrid technique of micro-high performance liquid chromatography (HPLC) and capillary zone electrophoresis (CZE). In CEC, the capillary column is packed with micron sized chromatographic packing material to obtain high selectivity. The mobile phase is driven by a high voltage supply instead of using an HPLC pump. Neutral analytes are separated based on their differential partition between the stationary and mobile phases, whereas charged compounds are separated by differential partition as well as differential electrophoretic mobility.

CEC is the most recently developed method in the CE area. Most research work in the field of CEC has been done in the last decade. Numerous applications of CEC have been demonstrated recently in pharmaceutical analysis [40-45].

CEC is reviewed in more detail in Section 1.2. The CEC separation of phenylthiohydantoin amino acids is reported in Chapter 2. One of my CEC applications was an analysis of testosterone metabolites in microsomal incubates for a pharmacokinetics study, and it is described in Chapter 3.

1.1.3.3 Micellar Electrokinetic Chromatography

Micellar electrokinetic chromatography (MEKC) was developed by Terabe *et al.* in 1984. MEKC allows CE to separate neutral analytes [46]. In MEKC, a surfactant with a higher concentration than its critical micelle concentration (CMC) is incorporated in the separation buffer to attain selectivity. Surfactants contain both a hydrophobic moiety and a hydrophilic functional group within the molecule. Surfactants can aggregate to form

micelles when the concentration is higher than the CMC. There is a distribution of size and shape of micelles in solution dependent on aggregation number.

Sodium dodecyl sulphate (SDS) is the most popular surfactant used in MEKC. The SDS molecule has a hydrophobic aliphatic chain with a polar functional group (sulphate) at one end of the carbon chain. The aliphatic tails aggregate via hydrophobic interactions to form spherical micelles with polar groups protruding to the surrounding aqueous solution. The CMC of SDS in water is 8.1 mM [47]. The aggregation number of SDS is about 60 [48]. The hydrophobic interior of the micelles can include analyte behaving as a pseudo-stationary phase in the buffer shown in Figure 1.3. The SDS micelle carries negative charges due to the sulfate groups, and thus migrates toward the anode by electrophoresis. The solvent phase migrates to the cathode by electroosmosis. The electroosmotic mobility is stronger than the electrophoretic mobility of SDS micelles. The neutral analyte moves at the EOF rate when it is distributed in solvent phase, or it migrates at the rate of the micelle phase when it is included by the micelle. The differential partition of hydrophobic molecules into the micellar interior facilitates separation of neutral and ionic analytes. The separation principle is based on the micellar inclusion and electrokinetic migration.

According to Terabe [49], the relationship between retention time of the analyte, t_r and capacity factor, k' is described by the following equation:

$$t_r = \frac{1 + k'}{1 + (t_0 / t_{mc})k'} t_0 \quad (1.4)$$

where k' is the capacity factor, defined as the ratio of amount of analytes distributed in the micelle phase and solvent phase. The variable t_0 , t_{mc} are the migration times of the solvent phase and micelle phase, respectively.

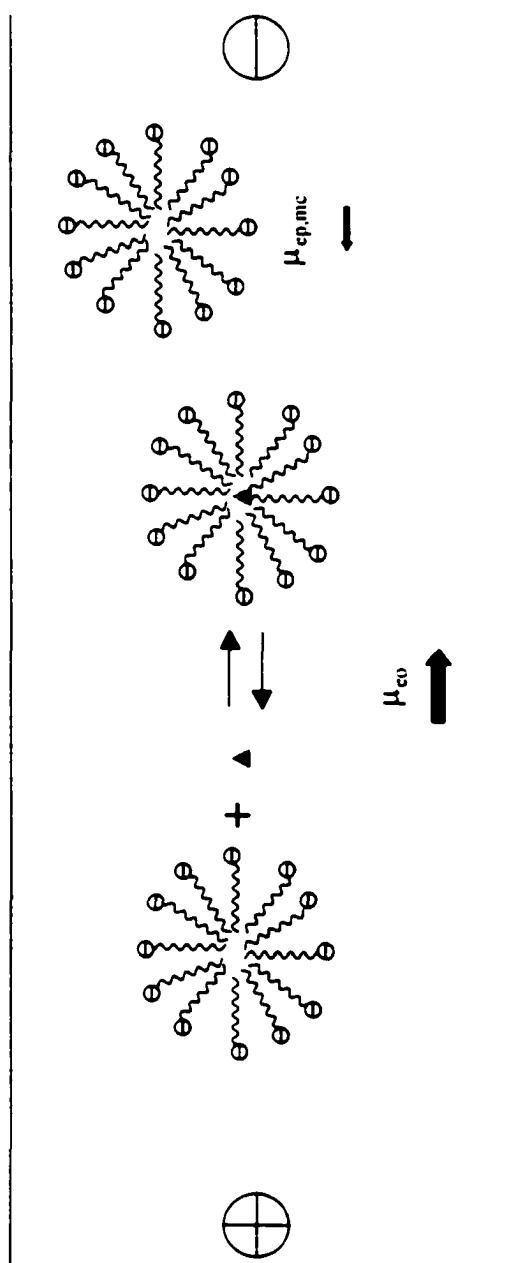


Figure 1.3 Migration of micelle and neutral analyte in MEKC

Chapter 5 describes how MEKC is employed to separate polycyclic aromatic hydrocarbons using bile salts as the micellar phase.

Chapter 6 presents two mathematical models to correct the MEKC migration time variation in analysis of amino acid derivatives and polysaccharides.

1.1.3.4 Other Capillary Electrophoresis Techniques - CGE, CIF, CITP

Capillary gel electrophoresis (CGE) extends the gel electrophoresis technique into a form of capillary scale analysis. Gel electrophoresis is widely used in biological science for DNA and protein analysis as well as purification. However gel electrophoresis experiments are labor-intensive and time-consuming. CGE provides greater automation feasibility than traditional operation. CGE also improves heat dissipation due to the thin capillary wall. In CGE, a capillary tube is filled with viscous polymeric sieving matrix, such as polyacrylamide prior to separation. The pore size of polymer network can be manipulated by altering the ratio of monomer to cross-linking agent in the polymerization mixture. Different sized nucleotides, proteins or peptides migrate through the polymer network, experiencing different extents of restriction. The smaller the size of the nucleotide or protein, the faster it moves. In this way the analytes are resolved in the order of their molecular sizes. CGE is most used for DNA sequencing and protein analysis.

Capillary isoelectric focusing (CIEF) is another form of capillary separation. It is used as one of the dimensions of traditional 2-D SDS gel electrophoresis for protein purification. The analytes are separated based on their isoelectric point, pI. In CIEF the inlet vial, usually a cathodic end, contains the ampholyte with high pH, while the outlet

vial, the anodic end, contains the ampholyte with low pH. The analyte ions are mixed with the carrier ampholytes that define the desired pH range, and the mixture is filled into the capillary before electrophoresis. When the electric field is applied, the ampholytes create a pH gradient across the capillary and concurrently the sample ions migrate under the electric field until they reach the pH point where their net charge reaches zero. The analytes are thus focused in the order of their isoelectric point. The analytes must be eluted from the capillary by hydrodynamic flow, or by adding salt into the buffer [50].

Capillary isotachopheresis (CITP) is performed with two appropriately chosen running buffers, one contains a leading electrolyte, with the fastest electrophoretic mobility among the analytes, and the other buffer contains a terminating electrolyte, with the slowest electrophoretic mobility. Analytes usually are injected hydrodynamically between a leading electrolyte and terminating electrolyte. The analytes migrate at different speeds initially when the high voltage is applied. Because different analytes in the separation media have different conductive properties, the analytes form a set of stack zones based on the uniformity of the current. When a steady-state migration has been established, the discontinuity of the electric field makes all the bands move at an identical velocity. The zones are detected as isotachopheretic steps consisting of height (qualitative information) and width (quantitative information). The width of the zone relates to the absolute quantity of an analyte.

During ITP, the concentration of the analyte zone will adapt to higher concentration of leading ion [51]. Thus CITP allows higher sample volume loading, up to 96% percent of the column volume [52], distinguishing CITP from other CE modes (less than 5%). Transient CITP and CITP-CZE are now employed as on-line concentration and sample preparation approaches for CZE [53-54]. CITP is mostly used for analysis of ion

constituents such as separation of alkali and alkaline earth metal ions or inorganic anions, such as halides, sulfate, sulfite, nitrate, and phosphate [55-56].

1.1.3.5 Chip-based Capillary Electrophoresis

Recently chip-based capillary electrophoresis technology (chip-CE) has been developed and has been predicted to lead the next revolution in chemical analysis [10]. Capillary electrophoresis on a microchip is based on micro-fabrication techniques including photolithography and micromolding to form channels in the glass substrate for CE separation. Chip-CE is essentially a miniaturized CE separation technique. The planar dimensions integrate multiple functions on a single device, such as sample manipulation (reagent delivery, sample purification, and derivatization), separation, and analysis. It is therefore named "lab on a chip". Chip-CE has a promising potential to develop into a multiarray instrument to simultaneously assay hundreds of samples in minutes or less. Numerous applications have been demonstrated for analysis of nucleotides [39, 57], peptides [58-59], and proteins [60-61].

1.2 CAPILLARY ELECTROCHROMATOGRAPHY

Capillary electrochromatography combines attributes of micro-high performance liquid chromatography (μ -HPLC) and CZE. CEC employs a capillary column packed with micron-sized chromatographic packing material to obtain high selectivity. CEC uses plug-profiled electroosmotic flow to transport the mobile phase through the column instead of parabolic hydrodynamic flow. The electrically driven flow results from the

ionization of the surface silanol groups of the capillary and silica-based packing. Neutral analytes are separated based on their differential partition between the stationary and mobile phases, whereas charged compounds are separated by differential partition and electrophoretic mobilities. These two processes allow manipulation of the separation selectivity. Although surface-modified open tubular capillary electrophoresis is classified as CEC as well, the relevant literature cited throughout the thesis only includes packed column CEC.

1.2.1 History and Current Achievements

CEC was first demonstrated by Pretorius *et al.* in 1974 [62]. The interest in CEC was revived in 1981 when Jorgenson and Lucas employed electroosmotic flow (EOF) to drive the solvent in packed capillary electrophoresis for separating some neutral molecules [4]. Several groups [63-66] pioneered the early research focusing on instrumental modification and CEC column preparation. Extensive progress has been made in the last decade in the areas, such as theoretical interpretation [67-74], instrumentation development [75-79], column technology [80-90], and applications in the analysis of a large variety of compounds. Such compounds included small organic molecules [91-94], biological compounds [81, 95-98] and pharmaceuticals [40-45]. However, today this technique is still at the research laboratory stage rather than being fully accepted in good laboratory practice regulated industry due to practical problems during its operation as described in Section 1.2.3.

1.2.2 Technical Advantages

One major advantage of CEC is high separation efficiency. An increase of 50% in efficiency has been reported when CEC is compared to nano-HPLC under the same conditions [78]. High efficiency is essential to resolve complex mixtures. High separation efficiency in CEC is attributed to the plug-like flow profile of electroosmotic flow. In contrast to the parabolic flow observed in HPLC, plug flow generates more uniform flow across the column. The band broadening arising from interparticle channel diffusion and eddy diffusion is minimized. Due to the high surface area of the silica packing, the electroosmotic flow is mainly generated via the electrical double layer on the liquid–solid interface of the reverse phase-modified silica packing rather than on the capillary wall. The second attribute is that the flow in CEC is independent of the particle diameter, so that it is possible to realize higher efficiency by using smaller particles, such as 1.5 μm or smaller. Long columns can be avoided in CEC because of the high voltage power supply limit, analogous to the problem encountered in HPLC because of the limitation of high-pressure pumps. CEC has enormous potential advantages for coupling to mass spectrometry due to the simplicity of the mobile phase system. Therefore it offers a viable alternative to micellar electrokinetic capillary chromatography (MEKC) for the separation of neutral compounds using electrically driven flow. The surfactants critical for separation in MEKC are problematic in mass spectrometric detection such as ion source contamination and signal suppression.

1.2.3 Problems and Solutions

The wide acceptance of CEC is deterred by several practical difficulties. Column manufacture involves multi-step procedures and sophisticated equipment. The packing procedures are not well characterized and standardized [99]. CEC columns are fragile

compared to the more robust HPLC columns. The technical aspects related to column packing techniques and frit fabrication have been explored during the initial development of CEC [65-66, 91, 100]. Different approaches for producing CEC columns will be discussed in detail in Section 1.2.5.2.

The most often criticized problem in CEC is the difficulty in obtaining a stable flow condition. Bubble formation inside the CEC column, due to Joule heating or pressure discontinuity between the frit portion and open tube, results in electrical current cut-off during the separation process. The problem has been overcome by applying supplementary pneumatic pressure on the both inlet and outlet buffer vial (up to 200 psi) to suppress the bubble formation [63, 66]. This pressure-assisted system is also useful for column conditioning.

1.2.4 Applications

CEC has been successfully used to separate small organic molecules such as aromatic hydrocarbons. The hydrophobicity of the reversed-phase particles and the mobile phase composition preferred by CEC make it possible to simply adopt the conditions employed in HPLC for those analytes.

The separation of biopolymers such as peptides has not been extensively studied for the following reasons. (1) The high content of acetonitrile and basicity of buffer commonly used is not suitable for biological compounds such as proteins, polypeptides, and oligosaccharides. For HPLC separations, the above compounds are separated in a buffer of relative low pH (containing 0.5 to 5% trifluoroacetic acid) and wide range of organic content (from 5 to 100%) by gradient elution. In CEC, high pH and high organic

content are essential to produce sufficient EOF to drive the mobile phase. (2) Polar surface adsorption of analytes is another factor preventing CEC separation of biopolymers. The interaction between the negatively charged silanol group on the surface of the silica and positively charged peptides results in significant band broadening, thus reducing the separation efficiency. To extend the popularity and realize the benefits of CEC to biological samples, extensive efforts have been made to develop novel packing materials [81-82] and to implement of pressure-assisted CEC [96]. The latter combines hydrodynamic and electrokinetic forces to transport the mobile phase.

1.2.5 CEC Columns

1.2.5.1 Column Types

Currently, CEC column types can be classified by the properties of the packing materials. These include (1) Conventional HPLC silica-based packing with particle size of 1.5 to 5 μ m bonded with C18, C8, phenyl, strong cation exchange groups (SCX) and chiral materials. (2) Novel mixed-mode packing, designed specifically for CEC, incorporating both reverse phase alkyl chains such as C18, and SCX, such as propanesulfonic acid. (3) Monolithic columns. Monolithic columns are fritless and composed of one piece of silica or organic polymer formed by *in situ* polymerization in a chromatographic column.

In mixed-mode packing, the sulfonic acid group is linked to silica via a propyl group. The sulfonic acid carries a negative charge even in low pH mobile phases. Therefore the column can maintain stable flow over pH ranges from 2 to 5 [40, 101-102]. Another mixed-mode packing created by Yang and El Rassi is octadecylsulfonated silica

(ODSS) [80-81]. ODSS stationary phase is comprised of a three-layered coating. The first hydrophilic layer (sublayer) of γ -glycidoxypropyltrimethoxy-silane is covalently bonded to a silica support. Next, a sulfonated layer is sandwiched via covalent bonding between the sublayer and an ODS top layer.

There are mainly two types of monolithic materials, inorganic porous silica and organic polymers. An ODS-modified porous silica monolith was first demonstrated for conventional HPLC and μ -HPLC [103-104]. Minakuchi *et al.* reported the preparation of monolithic silica by *in situ* hydrolysis and polycondensation of alkoxysilane in a fused-silica capillary. The porous monolithic silica was then treated with octadecyldimethyl-N,N-diethylaminosilane to impart the retentive property [103, 105]. Asiaie described the preparation of a silica monolith by sintering the silica particles packed in a silica column followed by octadecylation [106]. The significant advantage of monolithic packing obtained in this fashion is the expected higher stability and elimination of gapping generated by dislocation of particles that occurs in an unsintered packed column. Dulay *et al.* adopted procedures used for preparing capillary gas chromatography columns [87]. They demonstrated that ODS particles could be trapped inside the pores or cavities formed by polymerizing tetraethyl orthosilicate (TEOS) under temperature of over 373 K. The monolithic structure was integrally fixed to the walls of the capillary and could not be pushed out with moderate pressure (200 psi). Up to 80,000 theoretical plates per meter were reported. However this monolithic CEC column suffers from having a fragile physical structure and poor chromatographic reproducibility from column to column.

The organic monolith is prepared *in situ* by thermo- or photo-polymerization of monomers, cross-linkers, porogens, and catalysts to obtain a highly cross-linked, microporous polymeric network. Organic monolith based CEC has grown tremendously

owing to its simple preparation, versatility and designability. The polymer structure, the porosity, and the level of charged moieties can be tailored by the choices of monomers and porogens. Porogens are used to generate pores in the monolith structure during polymerization. Molecules such as alcohol, alcohol mixture, or imprinting molecules with more specific structure are chosen as porogens in column preparation. These types of monolithic CEC columns are specifically created to circumvent the tedious steps of frit fabrication required by the first two types of columns. Fujimoto *et al.* described a continuous bed made of cross-linked polyacrylamide with attached sulfonate group by radical copolymerization of N-isopropylacrylamide and 2-acrylamido-2-methylpropanesulfonic acid cross-linked by N, N'-methylenebisacrylamide [107]. Peters *et al.* reported the performance of monolithic poly-(butyl methacrylate-co-ethylene-dimethacrylate-co-2-acrylamido-2-methyl-1-propanesulfonic acid) columns for CEC [89, 108-109]. A column efficiency of 120,000 plates/m was achieved at optimal flow velocity. Such monolithic columns have been reported and proven to be effective in high-speed separation of polypeptides [110-112]. By choosing the buried molecule, a "mould", into the polymer network during polymerization, molecular imprinting is especially useful for chiral separation [90, 113].

1.2.5.2 Column Packing Techniques

The procedure of manufacture differs based on the column type. Particle-packed CEC columns may be manufactured by high-pressure slurry packing [64, 66, 91, 114-115], electrokinetic packing [116-117], and by supercritical fluid packing [77, 118-119].

Slurry packing is the most popular approach to the manufacture of CEC columns owing to the experiences gained from making micro-HPLC capillary columns. The reverse phase modified particles are suspended in acetonitrile [31,120], acetone [66], isopropanol [99], or hexane [121], which are also used as packing solvents. Other additives such as ethylene glycol and SDS are used to increase the solvent density or impart surface charge to the particles. Sonicating the slurry reservoir and the capillary to be packed is sometimes employed during the slurry packing process. Sonication was reported to be effective for particle rearrangement to make a well-distributed bed [119]. Although the choice of the packing solvent polarity, density, viscosity, and the pressure could be crucial during the preparation of slurry-packed HPLC columns, it was found that the composition of packing solvent playing a more important role than slurry liquid [112]. Acetonitrile is a widely accepted packing solvent for both micro-HPLC columns and CEC columns. Table 1.1 summarizes the studies done to optimize column packing based on slurry solvent, slurry ratio, and type of packing solvent. The effects of slurry density, type of packing solvent, geometric shape or size of the packing material on chromatographic performance were investigated in the 1980s when micro-bore HPLC gained increasing popularity [115].

Phenomena such as particle coagulation or aggregation in the slurry during packing have been recognized as being important and have been characterized by some research groups [122-126]. The theoretical rate of spherical particle suspension sedimentation can be determined with modified Stokes equations by taking the particle porosity and a hindered settling function into account [120, 122].

In electrokinetic packing, the slurry chamber serves as an inlet and is attached to an ultrasonic shaker. The particles are transported by EOF mobility as well as

electrophoretic mobility from the slurry chamber into the capillary column. All the packing facilities are kept in a Faraday cage to prevent electric shock [116].

Table 1.1 Literature of capillary column packing protocols

Capillary I.D. (μm)	Packing Material	Slurry Solvent	Slurry Ratio Particle:Solvent (mg/ml)	Packing solvent	Ref.
12~33	5 μm C18	hexane	(3~17)/1	isopropanol	[121]
15-50	5 μm C8	ACN/Triton X-100	(33~250)/1	ACN	[120]
50	4 μm	ACN	100/1	ACN	[91]
50	3 μm C18	propanol-2-ol	30/1	propanol-2-ol	[99]
50	3, 5 μm C18	MeOH, or ACN/Toluene (1:1)	30/1	MeOH, ACN, Acetone	[65]
200	3, 5 μm C18	ACN, MeOH, Ethylene Glycol/MeOH	182/1	ACN/H ₂ O	[115]
340	3, 5 μm C18	ACN/PEDE ^a	Not listed	Not listed	[114]

^a: polyoxyethylene dodecyl ether.

Supercritical carbon dioxide media has been used as a packing carrier in preparation of capillary columns [77, 118-119]. The advantage of supercritical fluid packing is that much longer and higher stability columns can be packed owing to the low viscosity of carbon dioxide. Up to 10 meters of packed column can be made at a time by

this method [119]. The supercritical fluid packing system is subjected to high pressure (up to 400 atm) so that special equipment for safety protection is required. All three packing methods give equivalent column performance with a minimum reduced plate height of close to 2 for capillaries in the range of 50–200 μm I.D.

1.2.5.3 Frit

Two frits are made so that the particles inside the capillary form a packed bed. Frits can be prepared by sintering the silica gel that has been wetted by potassium silicate solution. Alternatively, frits for a CEC column can be a polymer plug that is the same as the material of monolithic columns, *in situ* polymerized potassium silicate solution containing silicon dioxide [66, 127] or organic monomers [128]. The most common method for making frits is by heating the packed reverse phase particles using electrical heating wires or a fiber optic splicer [64-65, 91, 99-100]. The latter method employs an arc between a pair of electrodes that is capable of heating a small area at a controlled temperature. The fiber optic splicer is also equipped with a microscope to visualize the process of frit formation.

1.2.6 Mobile Phase in CEC

The mobile phase used for CEC commonly contains 5-20 mM electrolyte and about 80% organic solvents such as acetonitrile or methanol. The electrolytes commonly used are of two types. One type are inorganic compounds, such as sodium phosphate, sodium borate, ammonium acetate, acetic acid, or ammonium bicarbonate. Due to the precipitation of inorganic electrolytes in the high organic content separation media, the

maximum concentration of the buffer is limited to 5 mM, greatly limiting the optimization of selectivity. Another type of electrolyte are zwitterionic compounds, including 4-morpholinoethanesulfonic acid (MES), N-2-hydroxyethylpiperazine-N'-2-ethanesulfonic acid (HEPES), and tris (hydroxymethyl)aminomethane (TRIS). Zwitterionic buffers are better for CEC because they have low conductivity and relatively high solubility in organic solvents [65].

The pH of the mobile phases cited in the literature is the pH of the aqueous buffer before mixing with the organic solvent. The apparent pH may shift after mixing because the dissociating constant K_a value of buffer differs in aqueous versus organic media [129-130].

1.2.7 Instrumentation

CEC can be performed on any CE instrument without modification. Most CEC studies reported in the literature have been carried out on commercial CE instruments. The newly designed Hewlett-Packard CE instrument (HP 3D) equipped with a pressurization system on both inlet and outlet vials of up to 200 p.s.i. is useful for CEC operations. Liquid pressure-assisted CEC has been employed to manipulate the selectivity by tuning the hydrodynamic flow and electrokinetic flow [96-97]. This approach also has broadened the possibility of using a buffer with low pH or high aqueous content in CEC. Gradient elution CEC by use of an HPLC solvent delivery system [76] or by mixing of two electrically pumped solvents [75] has reduced the total analysis time. Most instruments employ on-column detection using transmission UV absorbance or fluorescence. Post-column detection is only used for CEC coupling to mass spectrometry detection.

The two current instrument configurations for gradient CEC have limitations. One type used by Schemeer *et al.* equips an HPLC pump system to deliver gradient elution and a pneumatic gas line for sample injection [131]. This design is capable of performing low volume sample analysis like common CE. But the instrument consists of three separate units, a high voltage power supply, a high-pressure liquid system, and a gas system, which makes it bulky and complicated. Also the mobile phase delivered from the HPLC pump needs to be split (ratio of 1/2000) prior to CEC column. 99.95% of solvent is wasted. Another design, developed by Horváth and coworkers, can perform gradient elution without a liquid pressure assisted or pneumatic system for injection, but the system consumes a large volume of sample for injection [76].

1.3 DETECTION SCHEMES

The detection method is a technology integrated in the CE separation technique. Because of the small detection volumes in CE, high sensitivity is essential for the detection system. Various detection schemes have been developed to adapt to this CE separation scale and can be characterized into four classes: optical, electrochemical, mass spectrometric, and other detection methods. Each class can also be further sub-characterized to several methods based on principle and system configuration. Table 1.2 summarizes the four classes of detection methods currently used in CE, their sub-categories, limit of detection (LOD) for each method, and representative literature [15, 60-61, 132-151]. However, each detection method has its advantages as well as inherent drawbacks. Kelly and Bornhop recently have reviewed the on-line detection methods for capillary electrophoresis [153].

Table 1.2 Detection methods for capillary electrophoresis

Class	Category	LOD (M)	Ref.
Optical	UV-Vis absorbance	10^{-5} - 10^{-6}	[132-133]
	LIF	10^{-13} - 10^{-16}	[134-137]
	Photo thermal	10^{-7} - 10^{-9}	[138-139]
	Refractive index	10^{-3} - 10^{-6}	[140-142]
Electrochemical	Potentiometric	10^{-7} - 10^{-8}	[143]
	Voltammetric	10^{-5} - 10^{-6}	[144]
	Amperometric	10^{-7} - 10^{-8}	[145-146]
	Conductivity	10^{-7} - 10^{-8}	[147-148]
Mass spectrometric	Ionspray. Microionspray	10^{-7} - 10^{-8}	[15. 60. 149]
	Nanospray	10^{-8} - 10^{-9}	[61]
Miscellaneous	Radioisotope	10^{-10}	[150]
	NMR	10^{-3}	[151]
	Raman	10^{-5} - 10^{-7}	[152]

Optical detection is carried out by ultraviolet (UV) absorbance, laser-induced fluorescence (LIF), photo-thermal detector, or refractive index detectors. On-column

ultraviolet (UV) absorbance detection is most widely applied in commercial CE instruments due to its simplicity, robustness and universality to wide range of molecules. However, it has a poor limit of detection due to the short optical path length determined by the tube diameter of the detection cell.

Laser-induced fluorescence (LIF) is the most sensitive detection method, and may be used on-column and post-column to detect extremely low quantities of analytes. LIF can detect single molecules [154]. Yet most analytes do not generate appreciable fluorescence, thus derivatization of a fluorescent tag to the non-fluorescent molecule is required. Furthermore, the high sensitivity of LIF makes it prone to the problems of background interference and tedious alignment.

Electrochemical methods are a class of detection techniques suitable for CE. The scales of micro-fabricated electrodes are almost ideally compatible to CE for detecting minute amount of analytes. All the electrochemical detection methods are generally based on the same electrochemical phenomenon, that the presence of analyte molecules at the electrode-sensing region produces an electrical signal. Electrochemical detection can be characterized into four categories based on which variable is being sensed including potentiometric, voltammetric, amperometric, and conductimetric detection. Electrochemical detection involves complicated fabrication and handling procedures of microelectrodes, which make this technique difficult to be widely used.

Mass spectrometric detection is a post-column analysis technique and has received wide interest and effort in the past ten years. An ion source interface is required for producing analyte ions from CE eluent and subsequent introduction to the mass analyzer. Electrospray ionization is the most suitable ion source to couple CE to a mass spectrometer. Based on the flow rate of eluent transported into the ion source and the

sensitivity, there are mainly two groups of interface configurations listed in Table 1.2. More details of the CE/MS technique are described in Section 1.3.2.

The detection methods listed in the miscellaneous group are rarely used. Radioisotopic detection is not a new technique for CE. It is highly sensitive. However, the radioisotope labeling and hazardous radiation makes this technique less attractive. Other detection methods such as NMR and Raman have been demonstrated recently. Although NMR and Raman can provide molecular structure information, the sensitivity of both methods make them poorly compatible to CE.

This thesis utilized mainly two detection methods: optical detection and mass spectrometric detection. I will focus on these two detection schemes. A thermo-Optical UV absorbance detection (TOAD) system is discussed in Chapter 2, 3, 5, and 6. Mass spectrometric detection is demonstrated in Chapter 4.

1.3.1 Thermo-Optical UV Absorbance Detection

Thermo-optical UV absorbance detection (TOAD) is a form of photothermal laser spectroscopy. Basically, it involves the measurement of deflected, refracted, and defocused light after passing through a thermally modulated refractive index gradient. It is also referred to as the thermal lens effect. Waldron reviewed in her Ph.D. thesis the evolution of thermal lens detectors adapted to CE [155]. The theoretical models and mathematical approaches of various thermo-optical spectrophotometries have been reviewed in detail in the literature [156].

The thermal lens effect, first described and discussed by Gordon *et al.* [157] is produced in an experimental arrangement similar to that in common single-beam

absorbance spectroscopy. The major difference is that laser radiation passing through a sample is detected only at the center of the beam by using a pinhole before the transmitted light reaches the detector. The sample causes a thermal defocusing by absorption of the incident laser light [157]. Usually, the laser radiation is modulated to produce a periodic thermal-optical element that modulates the beam intensity profile. The thermal-optical signal is measured with either an intensity- or position- sensitive detector.

Dovichi and Harris applied the thermal lens effects to trace solute determination in static and flowing samples using single beam configuration [158-159]. The crossed beam laser-induced photothermal refraction for the flowing sample detection has been investigated and meanwhile the complicated mathematical models have been proposed to explain the theory behind the basic phenomenon [160-164]. The sample cuvettes used in all the early detector systems are millimeter square-bore tubes. Bornhop and Dovichi built an on-capillary crossed laser beam photothermal detector combining thermal lens effects and refractive index detection techniques [165-167]. because the round-shaped capillary produces more complicated interference refraction fringes under incidence of laser beam. The detector has been successfully applied to microbore liquid chromatography and capillary electrophoresis of DABSYL-amino acids [138, 168-169], PTH-amino acids [170-171], and antidepressants [172]. Several other groups have also published pulsed-laser photothermal reflective index detection for capillary liquid chromatography [139, 173-174]. Due to its complicated optical system, this detection is not so popular as UV-transmission detection method.

The thermo-optical signal is determined by the power of the pump laser, the molar absorptivity of the analyte, and the concentration of analytes. The quantitative model of crossed beam thermo-optical behavior for a sample in a CE column is more complicated

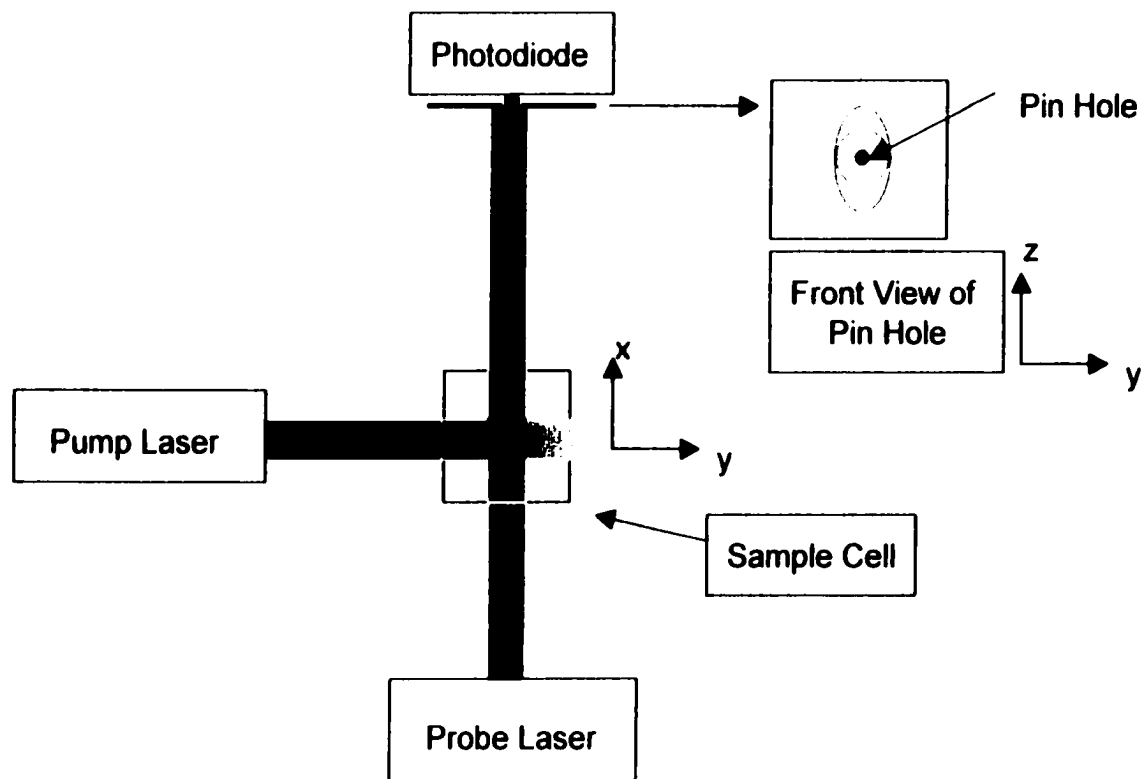


Figure 1.4 Diagram of crossed-beam photothermal detection. The pump beam and the probe beam propagate at a right angle. Refraction of the probe laser is produced at the intersection of the two laser beams. The photo thermal refraction signal is measured as the relative change in the intensity which passed through a pinhole located at the far-field probe beam center.

than the basic model of single beam thermal lens within a rectangular shaped sample cell. This is because the former detection system needs to consider the thermal lens effects, the effect of flowing sample which removes partial heat, the light interference results from refraction and deflection that occur at the interfaces of air to capillary wall and capillary inner surface to flowing liquid media.

Several research groups have modeled the related phenomena in either thermal optical or refractive index detector. For thermal optical detection the spatial temperature rise, ΔT , within the thermal lens region versus time, the focal length of a cylindrical lens, f , and the temporal far-field probe beam center intensity, $I(t)$, generated by crossed beam system have been modeled and summarized by Dovichi *et al.* [160]. Krattiger *et al.* have introduced refractive index-matching fluids to surround the capillary to simplify the interface refraction in a refractive index detector using a position sensitive diode [175-176]. They have provided the model to predict the far field fringe pattern after laser light illuminates the capillary. Tarigan *et al.* measured and modeled the interferometric backscatter of the refractive index detector by slightly tilting a side-illuminated capillary for detection [140]. Though to complete the theory of thermal optical detection is not within the scope of this thesis, a brief explanation of crossed beam thermal lens effects follows to better understand the feature of thermo-optical detection.

1.3.1.1 Thermal Lens Effect

The configuration of a crossed-beam photo thermal detection apparatus is shown in Figure 1.4. It consists of a pump laser and a probe laser intersecting in a right angle. In the coordinate system used in the figure, the probe laser propagates along the X axis and

the pump laser beam propagates along the Y axis. The Z axis is perpendicular to the co-plane of the two laser beams. The modulated pump laser illuminates the sample. The absorption of photons of the pump laser results a heated region, which acts as a cylindrically symmetric lens to defocus the probe beam. A photodiode is placed at far-field of the probe laser beam so that the distance from sample to the photodiode is much larger than the beam waist of the probe beam and the focal length of the thermal lens. The impulse response for the photothermal refraction in absence of flow is governed by the following equations [157]:

$$\Delta I(t) = \frac{I(0)}{(1 + 2t/t_c)^{3/2}} \quad (1.5)$$

where $I(0)$ is

$$I(0) = \frac{4.606 E \varepsilon C (dn/dT) Z_1}{\sqrt{2\pi k t_c} \omega} \quad (1.6)$$

t_c is the time constant defined in the equation:

$$t_c = \frac{\omega^2 C_p \rho}{4k} \quad (1.7)$$

$\Delta I(t)$ is the time-resolved relative intensity change in the far-field probe laser beam center. $I(0)$ is the initial amplitude of the signal for static samples. E is the energy per pump laser pulse. ε is the molar absorptivity. C is the concentration of analyte. dn/dT is the change in solvent refractive index with temperature. Z_1 is the distance from the probe beam waist to the beam intersection region. k is the sample thermal conductivity. t_c is the time constant for the effect. ω is the pump laser beam spot size. ρ is the sample density. C_p is the sample heat capacity.

For flowing sample and impulse excitation, the far-field beam center intensity is described by [161]:

$$\Delta I(t) = \frac{I(0)}{(1 + 2t/t_c)^3} \left(1 - \frac{4(d + Vt)^2 / \omega^2}{1 + 2t/t_c} \right) \exp\left(\frac{-2(d + Vt)^2 \omega^2}{1 + 2t/t_c} \right) \quad (1.8)$$

where d is the half width of the sample cell, and V is the sample flow velocity.

The above equations reveal that the photothermal signal is proportional to the pulsed laser power, molar absorptivity and concentration of analyte, and the refractive index change with temperature. Furthermore the signal is not related to the optical path length.

1.3.1.2 Crossed-Beam Thermo-Optical UV Absorbance Detection

A brief description of a thermo-optical detection system is presented here. Figure 1.5 shows the diagram of the arrangement of components for detection. The two laser beams both are focused on the detection point, which is a window in the capillary. The analytes passing through the detection spot absorb energy provided by the pump laser (UV excimer laser, 249 nm) and subsequently are raised to excited electronic states. The excited molecules release excess energy by several pathways. Nonradiative relaxation is one of the processes through which the analyte gives off heat. This heat causes a temperature increase in the analyte zone, which induces a refractive index change. The probe laser (He-Ne laser, 632.8 nm) beam is reflected within the capillary to produce an interference pattern behind the capillary tube. A photodiode is located after the detection window to detect the forward interference image. Using the pulsed pump laser beam at a suitable frequency allows us to selectively detect the thermo-optical signal by using a lock-in amplifier.

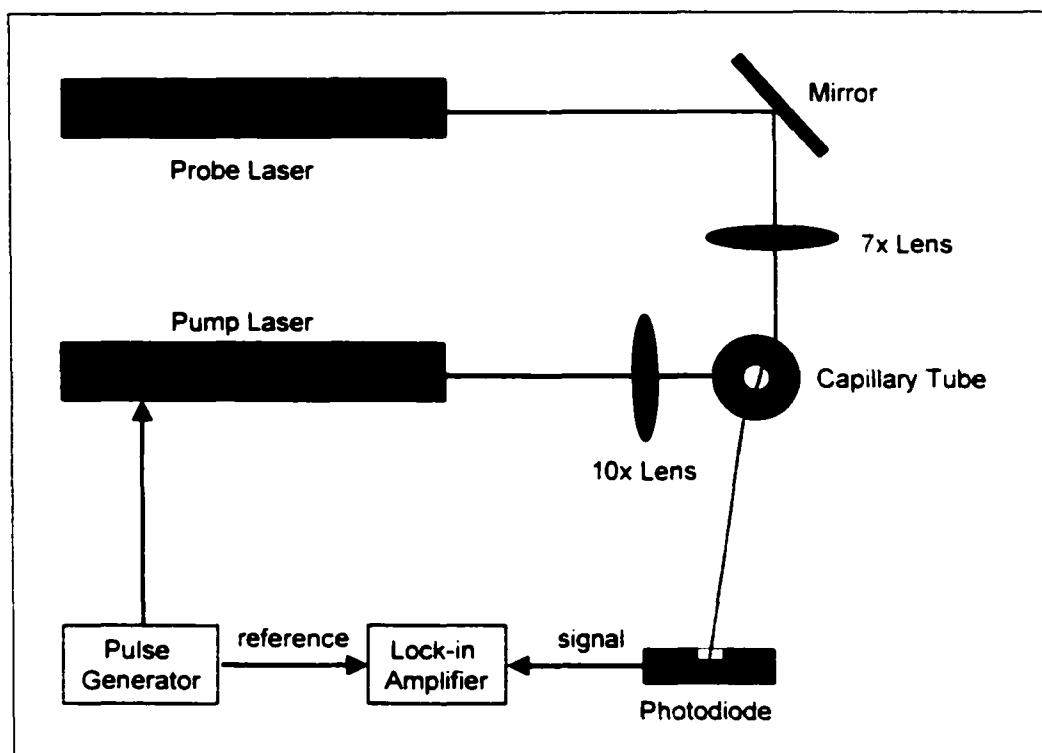


Figure 1.5 Diagram of thermo-optical UV absorbance detection system

This detection system offers several unique features for highly sensitivity detection compared to conventional UV transmittance detection. First, the sensitivity is greatly improved by using a high pump laser power. Second, it eliminates problems arising from short path length. Third, TOAD is universal as well because a large number of analytes absorb light in the UV region, thus no chromophore-labeling chemistry is required for most applications.

1.3.2 Electrospray Ionization Mass Spectrometric Detection (ESI/MS)

Mass spectrometry of analyte ions following separation techniques (LC or CE) has been widely explored for several reasons. First, mass detection provides analyte ion molecular mass information, as well as possible structural information resulting from ion fragmentations. Second, mass spectrometry is a well-developed technology utilizing various sophisticated ionization techniques and highly sensitive and versatile mass analyzers. Third, it is the most powerful tool in current proteome research for protein structure elucidation and identification [177].

Using mass spectrometry for chemical analysis intrinsically requires the analytes to be converted into gas phase ionic species for detection. Electrospray ionization (ESI) is the most feasible ionization method to couple liquid separations to mass spectrometric detection. Electrospray was utilized for electrostatic dispersion of liquids and creation of aerosols for a long time before it was applied to mass spectrometry. The original idea of ESI as a sample introduction method was introduced by Dole *et al.* in the late 1960s [178]. However it was not until the 1980s that a breakthrough took place in this technology, when ESI showed the ability to analyze protein molecules on quadrupole instruments by their detection as multiply-charged species [179-181]. ESI is one of the atmospheric pressure ionization (API) techniques, the other is atmospheric pressure chemical ionization (APCI). Both techniques have been growing quickly and commercial ESI/MS instruments from different vendors appeared in the market in the 1990s [182]. Reviews primarily paying attention to the aspects of API instrumentation [183-185], electrospray mechanism [186], and applications in protein analysis [187-188], can be found in the recently published literature.

ESI coupled to CE separation (CE/MS) was demonstrated by Smith *et al.* [181] in late 80s at the same time when LC/MS instruments became commercialized. The

interface from the CE to MS is more complicated than LC/MS due to several technical difficulties. The much lower typical CE flow rates (nanoliter/min. vs. mL/min. in LC) makes it a challenge to maintain a stable ESI process. Further, the CE/MS system is more complicated due to the two necessary electrical circuits: one for CE current flow and another to supply electrospray current.

The basic phenomena and important aspects of electrospray followed by the major components in CE/ESI/MS instruments will be described in the following sections using the SCIEX API 100 mass spectrometer as a primary example.

1.3.2.1 Electrospray Ionization

Electrospray ionization can generate gas phase ions from liquid phase ions at atmospheric pressure by spraying the analyte-containing solution through a voltage potential difference. The formation of gas-phase analyte ions can be generally divided into three steps: formation of the charged droplets, evaporation of solvent from the droplet and ion desorption [189].

A high electric potential (2 to 5 kV) is maintained between a conductive capillary and the inlet to the mass spectrometer (counter electrode, see Figure 1.6). The high voltage is applied at the end of the capillary and the counter electrode is at ground or *vice versa*. (The figure shows the former case.) The potential difference creates a high electric field at the capillary end that can be determined using the approximate equation [190]:

$$E_c = \frac{2V_c}{r_c \ln(4d/r_c)} \quad (1.9)$$

where E_c is the electric field at the capillary tip, V_c is the applied potential, r_c is the capillary outer radius, and d is the distance from the capillary tip to the counter electrode.

The electric field is about 6×10^6 V/m at a common instrument configuration.

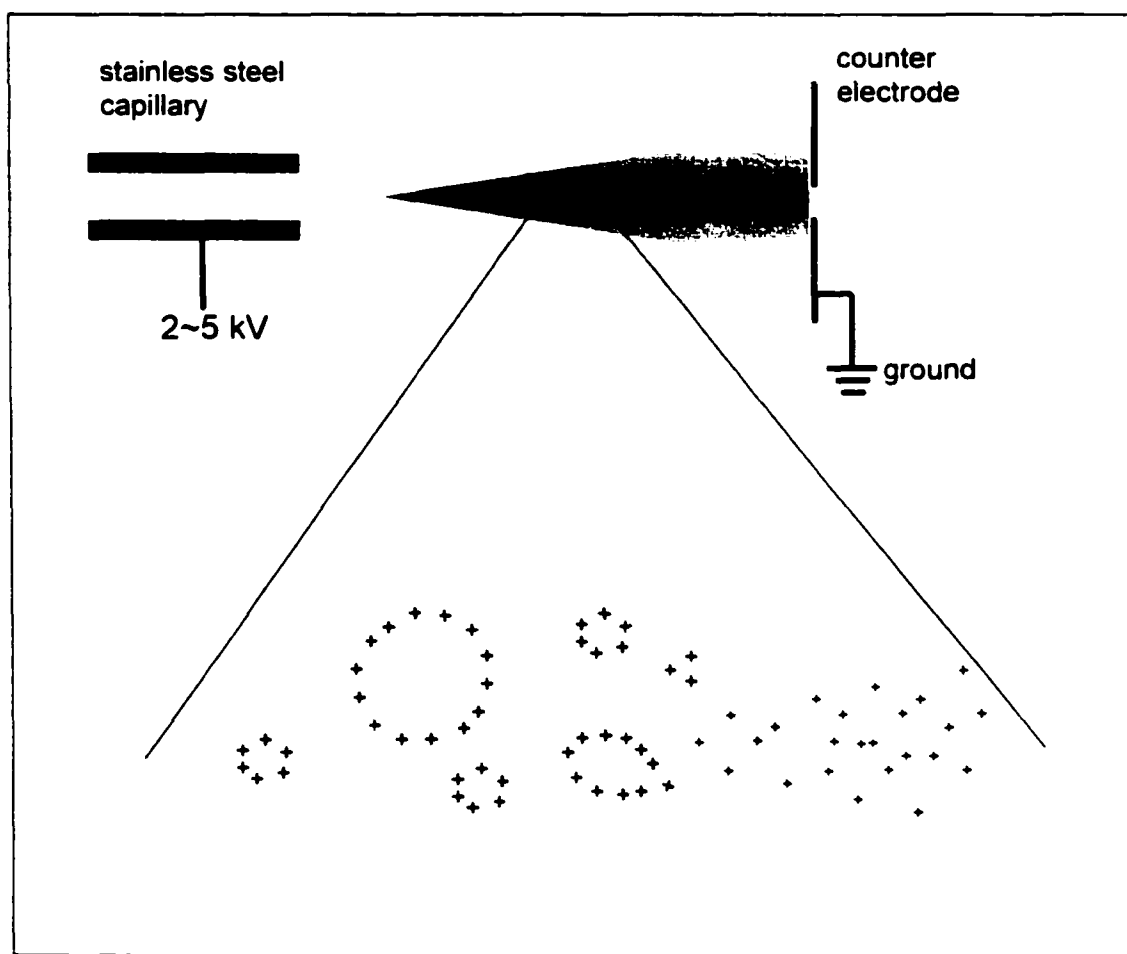


Figure 1.6 ESI ion formation process

The solution present in the capillary may be introduced via a syringe pump or fed from an HPLC or CE column effluent. As the liquid passes the capillary outlet, the electric field draws the positive ions downfield. The surface of the liquid forms a so-called Taylor cone [191] at the exit of the capillary as the applied field is sufficiently high

as a result of a coulomb repulsion process among the positive ions. A fine jet of liquid emerges from the cone tip, which breaks up into an aerosol charged droplets with radius of 0.5 to 1 μm initially containing a large number of analyte and solvent molecules. This jet of charged species is drawn through the counter-plate by the electric field. During the flight to the counter plate, the droplet size continuously reduces as the solvent molecules evaporate. As the droplet size decreases, its electrical density reaches an upper limit. At this point Coulomb repulsion of the ionic species overcomes the droplet surface tension, and the so-called Rayleigh emission process occurs, where the parent droplet breaks into smaller and lower charged droplets [186]. The offspring droplets subsequently evaporate by the same mechanism and continuously shrink until the desolvated quasi-molecular ions are produced.

Different theories have been proposed as to whether the desolvated ions are formed by continuous evaporation of solvent to the naked analyte ion, or by a direct ion emission from the highly charged droplet [190]. In either case, the ESI process produces gas-phase analyte ions for introduction to the mass spectrometer.

1.3.2.2 Practical Aspects of ESI

Several factors affect the ESI process. The shape of the spray liquid at the capillary tip varies depending on the strength of the electric field, which is determined by the bias voltage, the flow rate, and the radius of the sprayer tip [190]. A stable electrospray can be obtained at a voltage when the eluent flow forms the Taylor cone at the spray tip [192]. A much higher electric field can cause discharge in the spray region, which is detrimental to instrument sensitivity and should be avoided.

A pneumatic nebulizer gas flow, usually N_2 , is often used in a sprayer to assist the aerosol formation for highly aqueous solutions or high flow rates (larger than $2 \mu\text{L}/\text{min}$). A sheath liquid may be used to make up for low effluent flows, and to stabilize the electrospray process. Volatile, low surface tension, and polar solvents possess the desired qualities for a sheath liquid. Organic solvents such as methanol, methoxyethanol and acetonitrile modified with aqueous formic or acetic acids are common choices for a sheath liquid.

The operational variables affecting the mass spectrum include ESI sprayer position, spray voltage, nebulizer gas flow rates, sheath liquid and the sample matrix. The ESI mass spectra are less reproducible compared to those from traditional electron impact (EI) and chemical ionization (CI). In-source collision-induced dissociation (CID), induced by increasing the potential on the sprayer, orifice plate, and skimmer, may also produce variable spectra [193-194]. These characteristics of ESI degrades its value for establishing primary ESI mass spectral libraries, such as those utilized effectively for structural confirmation in the fields of conventional EI and CI mass spectrometry.

ESI is characterized as a soft ionization method. It is suitable for ionization of polar, thermally labile molecules, especially of peptides and proteins that are hard to convert into gas phase ions by traditional ionization methods. Generally, for small molecules, "quasi-molecular" ions are produced as protonated species, $(M+H)^+$, in positive mode or deprotonated species, $(M-H)^-$, in negative mode. For peptides and proteins, multiply-charged species tend to form due to ionization of polar amino acid residues. This multiple-charging reduces the m/z magnitude of the large protein ions so that they are even accessible to be measured by quadrupole mass analyzers with a relatively small mass range (1000-4000 amu).

ESI is a continuous ionization method which is most feasibly adapted to the quadrupole mass analyzer, unlike matrix-assisted laser desorption ionization (MALDI) for proteins, which is a pulsed ionization technique for time-of flight (TOF) mass analyzers [195]. However, references have recently reported the coupling of ESI sources to other mass analyzers, including a TOF mass analyzer and an ion-trap (IT) interface [196], in an orthogonal configuration [197]. ESI in conjunction with ion trap or Fourier transform ion cyclotron resonance (FTICR) mass spectrometry has also been utilized [198-199].

1.3.2.3 ESI Mass Spectrometer

Figure 1.7 shows the schematic diagram of SCIEX API 100 mass spectrometer. The mass spectrometer consists of several major components: 1) an electrospray inlet (or sprayer) in the atmospheric pressure region, 2) the intermediate vacuum interfacing region that conducts the sprayed ion to the mass analyzer, 3) quadrupole mass analyzer, 4) mass detector. In the following three sections the major components and their functions will be described.

1.3.2.3.1 ESI Sprayer

The configuration of the sprayer plays a critical role in the performance of CE/ESI/MS. Several approaches have been designed to provide the electric field at the spray tip after CE separations including 1) a coaxial sheath flow technique with or without nebulizing gas [200-201], 2) a liquid junction interface [202-203], 3) a gold or

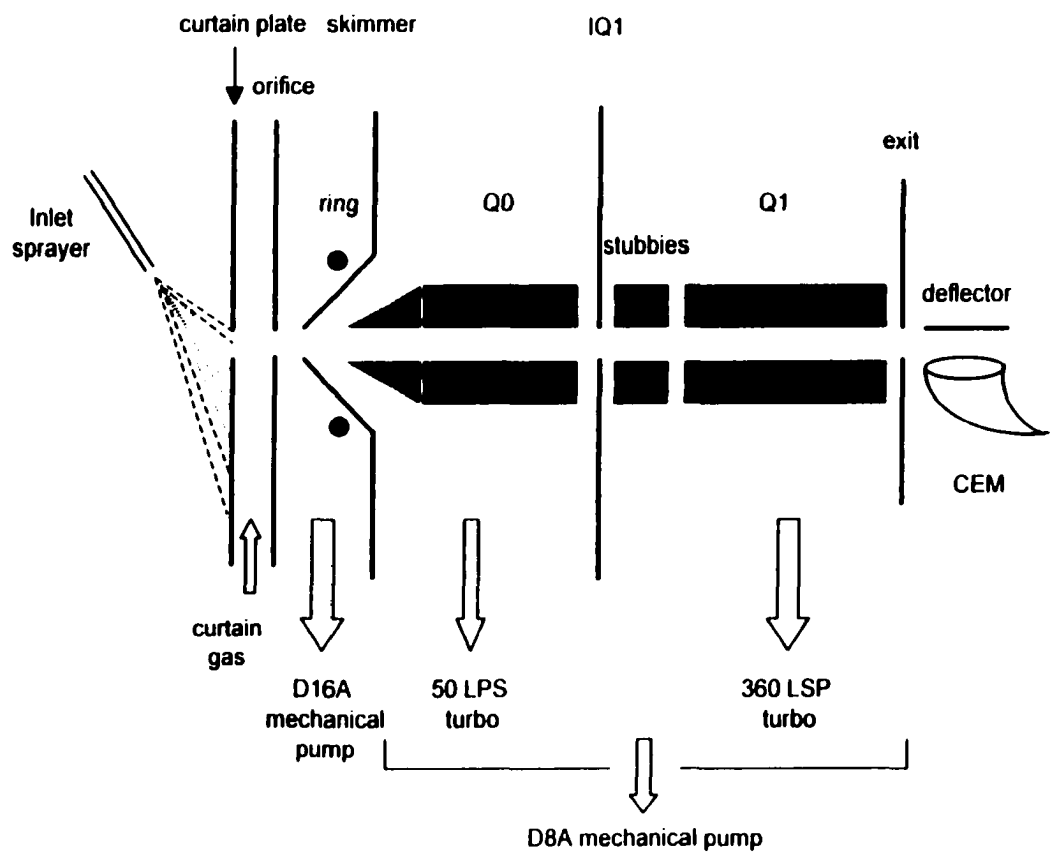


Figure 1.7 API 100 mass spectrometer ion path. The figure is modified from Ref. 208.

carbon-coated tapered sprayer [204-205], or 4) a gold wire electrode inserted in the CE column outlet [206].

The SCIEX API 100 equips an ionspray inlet using a coaxial sheath flow with nebulizer gas assistance, as shown in Figure 1.8. This sprayer consists of two stainless steel tees mounted on a metal bar. The tees are used for introduction of sheath liquid and nebulizer gas respectively. A stainless steel tube is connected to the outlet of the first tee and feeds through the second tee to the end of the sprayer. This metal tube is used as an electrode for applying the ESI voltage. The nebulizer tube, connecting to the outlet of the second tee, has the largest radius. The fused-silica capillary column supplying effluent from the flow injection or CE process is threaded into the inlet of the first tee and through to the ends of the concentric sheath liquid and nebulizer gas tubes. The tip of the capillary is positioned 1 to 2 mm back from the cross end of the electrode tube to allow electric contact with the spray liquid. The sprayer is positioned in diagonal direction to the ion path of the mass spectrometer.

The coaxial sheath liquid inlet has proved to be more reliable, simple to fabricate and easy to implement than other configurations. It is most useful in conjunction with microbore HPLC as well as CE separations, and can be successfully used with a large eluent flow rate.

Sheathless liquid junction, coated electrospray emitters have received significant attention because they overcome the problem of diluting the analyte and are amenable to electrospray at a very low flow rate. They are also classified into micro-ionspray and nanospray depending on the flow rate. However, there are several drawbacks associated with the sheathless inlets. Fabrication of the gold-coated fused silica emitter requires special equipment and the coated tips have a limited lifetime due to the deterioration of

the coating during operation. The small diameter of the emitter tends to clog during the operation. The gold wire electrode needs a highly skilled operator for alignment [207].

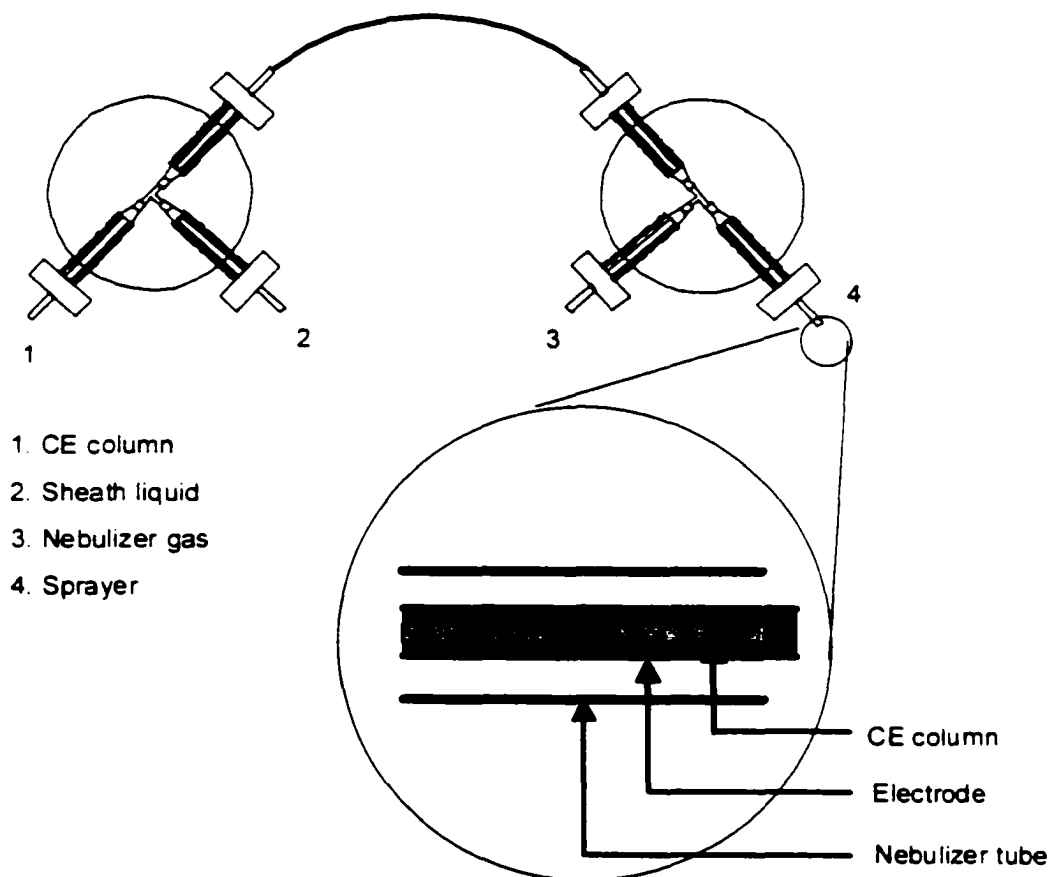


Figure 1.8 IonSpray interface

1.3.2.3.2 Vacuum Interfacing Region

The curtain plate is placed to separate the sample flow from the curtain gas and is also used as a counter electrode. Between the curtain plate and the orifice plate a curtain gas (N_2) is applied to aid desolvation of charged droplets into analyte ions before the ions enter the mass analyzer. The curtain gas is continuously flowing in a counter direction to the electrospray to restrict air, solvent, neutral contaminants, and dusts from entering the orifice. Part of the nitrogen goes through the curtain plate toward the atmospheric region. The other curtain gas portion, carrying neutral solvent molecules, passes through the orifice into the vacuum region and is pumped away. Analyte ions from the sprayer pass through the gas region under the influence of the electric fields between the sprayer and the skimmer plate. The curtain plate is biased at about 1kV with the same polarity of the spray voltage. The orifice plate is usually biased at low voltage (up to 200 V). There is a ring electrode on the skimmer (biased up to 400 V) for keeping the ion beam focussed at the center of the ion path through the skimmer. The first stage of the vacuum between the orifice plate and skimmer is pumped by a mechanical pump (D16A) to about 2 torr. Two TURBO molecular pumps (50 LPS and 360 LPS TURBO D8A) differentially pump the ion optics region to about 10^{-3} torr and the analyzer quadrupole region ultimately to 10^{-5} torr [208].

The ion optics behind the skimmer consist of several focussing elements including the quadrupole lens (Q0), interquadrupole lens (IQ1), and stubby electrodes (quadrupole prefilter) for optimizing ion transfer efficiency before ions enter the quadrupole mass analyzer (Q1).

1.3.2.3.3 Quadrupole Mass Analyzer

The quadrupole mass device consists of an array of four parallel metal rods positioned in a radial arrangement of the cross section shown in Figure 1.9. One pair of opposite electrodes is biased positive dc electric fields, $+U$ (x-direction), superimposed on radiofrequency ac electric fields, $V \cos \omega t$, the other pair is biased negative dc voltage, $-U$ (y-direction), superimposed on a 180 degree phase difference ac component, $-V \cos \omega t$. The quadrupole device functions as a mass filter. The ions injected along the z direction are subjected to a combination of electrical forces, and therefore have complex trajectories. For an ion with a given m/e ratio, the particular trajectory is determined by the dc potential, U , the rf zero-to-peak voltage, V , and the angular frequency, ω , of the oscillating potential. The trajectory can be described by the solutions to the following Mathieu type equations [209]:

$$m \left(\frac{d^2 x}{dt^2} \right) + \frac{2e(U + V \cos \omega t)x}{r_0^2} = 0 \quad (1.10)$$

$$m \left(\frac{d^2 y}{dt^2} \right) + \frac{2e(U - V \cos \omega t)y}{r_0^2} = 0 \quad (1.11)$$

where r_0 is the radial distance to the closest surface of the rods. Two distinct types of solutions exist corresponding to ion motions of bounded (stable ions) and unbounded (lost ions). For the bounded motion, the x or y is periodic with time giving the trajectories in which the maximum distance of excursion of the ion from the z axis is less than r_0 . For the unbounded motion, the x and y increase with time, which results in the collision of the ion onto the rods and neutralization. Thus, only the ions with bounded motion can transit the quadrupole device [210].

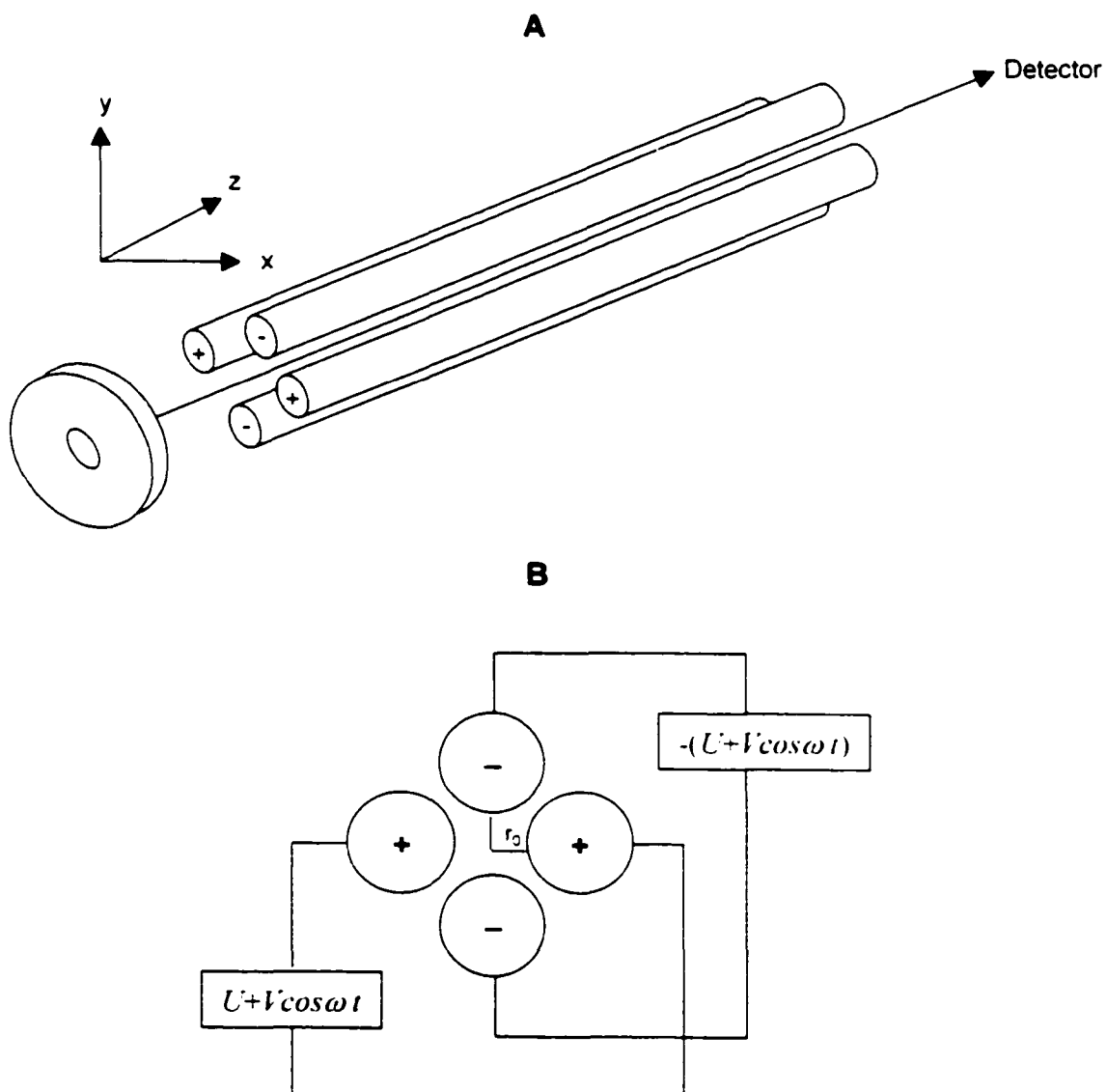


Figure 1.9 A: Schematic diagram of quadrupole mass filter. B: Cross section of rods and their DC and AC potentials.

The solutions of the above equations can be described in terms of a stable diagram that plots parameter “ a ” as a function of “ q ”. The a , q are derived from the procedure when Eq. 1. is converted into the standard Mathieu equation. The a , q are expressed as follows:

$$a = \frac{8eU}{mr_0^2\omega^2} \quad q = \frac{4eV}{mr_0^2\omega^2} \quad (1.12)$$

The values of a , q are proportional to U/m and V/m respectively. The operation of a quadrupole mass analyzer consists of varying the a , q values on the scan line within the stable region, which is realized practically by sweeping the U and V potential value with a constant ratio and a constant rf frequency. Ions within a certain linear mass range are allowed to transit the quadrupole device based on the m/e value. Thus in the quadrupole mass analyzer only ions with one particular m/z at a time can transit Q1, and all the other ions are lost.

Quadrupole mass analyzers offer a number of significant advantages over other more traditional analyzers such as magnetic and electric sector instruments. 1) The former can be operated at comparatively high pressure (5×10^{-5} torr), which leads to wide applications in conjunction with gas chromatography, liquid chromatography, and capillary electrophoresis. It is the most favored mass analyzer for use with an ESI inlet. 2) Rapid scan speeds can be obtained due to the absence of magnets. 3) Quadrupole mass analyzers achieve mass resolution on the basis of their mass/charge ratio rather than the basis of momentum or kinetic energy, as in the case of TOF and magnetic-electric sector instruments. The mass resolution is preserved electronically for the ions even with wide velocity distributions. This feature is useful for the application of successive quadrupole mass analyzer stages in MS-MS experiments. 4) The other useful features of the

quadrupole device are mechanical simplicity, small size, and low cost, in contrast to electric-magnetic sector and FT-ICR instruments.

Unit mass resolution, and high sensitivity for masses up to 1000-4000 m/z makes the quadrupole MS most suitable for quantitative analysis of small to medium size molecules. It is also useful to resolve multiple charged protein ions in a form of a multi-peak envelope.

1.3.2.3.4 Mass Detector

Channel electron multiplier (CEM), a continuous dynode device, is used as a detector for monitoring the ions. Ions exiting the mass analyzer are drawn to CEM by the voltage applied to the entrance of the CEM. Each ion that strikes the CEM generates an electron cascade propagated along the CEM by a potential gradient. The ion current produced by the cumulative number of electrons cascading within a certain period of dwell time is measured and represents the total ion counts, which is proportional to the relative abundance of analyte ions.

1.3.2.4 CE/ESI/MS Current Developments and Limitations

In the last five years CE/ESI/MS has been explored extensively regarding the interface technology and its application to analysis of a large number of molecules. Improvements in CE/MS instrumentation also have been made in interfacing to the time of flight (TOF) mass analyzer to detect the fast eluting ions of CE peaks, especially those of large biomolecules. Most mass analyzers used currently are quadrupole, iontrap, and

TOF instruments. Various experimental conditions have been investigated, including the sheath liquid composition, flow rate, and CE buffer types. ESI/MS shows distinct advantages in analyzing various small to medium size molecules because it provides a simple and easy way to interpret mass spectra.

However, ESI provides multiply-ionized species for peptides and proteins, which are difficult to interpret. Sufficient separation on the first stage is required. Although this problem has been circumvented by tandem mass spectrometric techniques, CE/ESI/MS is restricted by limited choices of solvent or buffer to optimize separation. The salts, acids, and surfactants that are effective in the separation are problematic even at low levels because these substances can form adducts with the analyte, causing ambiguous molecular mass determination. Signal suppression, complicated cluster ion formation, ion source contamination, and high chemical background are also difficulties in analysis.

Chapter 4 describes a nonaqueous CE for separation coupled to ESI/MS detection for drug screening of Chinese herbal medicine.

REFERENCES

1. Tiselius, A., Thesis, *Nova Acta Regiae Societas Scientiarum Upsaliensis* 1930, Ser. IV, 7, Number 4.
2. Hjertén, S. *Chromatogr. Rev.* 1967, 9, 122.
3. Mikkers, F. E. P.; Everaerts, F. M.; Verheggen, Th. P. E. M. *J. Chromatogr.* 1979, 169, 11.
4. Jorgenson, J. W.; Lukacs, K. D. *Anal. Chem.* 1981, 53, 1298.
5. Jorgenson, J. W.; Lukacs, K. D. *Clin. Chem.* 1981, 27, 1551.
6. Jorgenson, J. W.; Lukacs, K. D. *Science.* 1983, 222, 266.
7. *Electrophoresis* 1999, Issue 15-16, 2989-3328.
8. Issaq, H. J. *Electrophoresis* 2000, 21, 1921.
9. Krylov, S. N.; Dovichi, N. J. *Anal. Chem.* 2000, 72, 111R.
10. Dolnik, V.; Liu, S.; Jovanovich, S. *Electrophoresis* 2000, 21, 41.
11. Zagursky, R. J.; McCormick, R. M. *Biotechniques* 1990, 9, 74
12. Swerdlow, H.; Zhang, J. Z.; Chen, D. Y.; Herke, H. R.; Grey, R. Wu, S.; Dovichi, N. J. *Anal. Chem.* 1991, 63, 2835.
13. Zhang, J. Z.; Fang, Y.; Hou, J. Y.; Ren, H. J.; Jiang, R.; Roos, P.; Dovichi, N. J. *Anal. Chem.* 1995, 67, 4589.
14. Schmalzing, D.; Koutny, L.; Salas-Solano, O.; Adourian, A.; Matsudaira, P.; Ehrlich, D. *Electrophoresis* 1999, 20, 3066.
15. Figeys, D.; Oostveen, I. V.; Ducret, A.; Aebersold, R. *Anal. Chem.* 1996, 68, 1822
16. Lyubarskaya, Y. V.; Carr, S. A.; Dunnington, D.; Prichett, W. P.; Fisher, S. M.; Appelbaum, E. R.; Jones, C. S.; Karger, B. L. *Anal. Chem.* 1998, 70, 4761.
17. Manabe, T. *Electrophoresis* 1999, 20, 3116.

18. Zhang, Z.; Krylov, S.; Arriaga, E. A.; Polakowski, R.; Dovichi, N. J. *Anal. Chem.* 2000, 72, 318.
19. Nishi, H. *Electrophoresis* 1999, 20, 3237.
20. de Boer, T.; de Zeeuw, R. A.; de Jong, G. J.; Ensing, K. *Electrophoresis*, 1999, 20, 2989.
21. Haddadian, F.; Shamsi, S.; Warner, I. M. *Electrophoresis* 1999, 20, 3011.
22. Heegaard, N. H. H.; Kennedy, R. T. *Electrophoresis* 1999, 20, 3122.
23. Luga, A. L. *Electrophoresis* 1999, 20, 3145.
24. Flurer, C. L. *Electrophoresis* 1999, 20, 3269.
25. Issaq, H. J. *Electrophoresis* 1999, 20, 3190.
26. Chen, S.; Chen, Y. *Electrophoresis* 1999, 20, 3259.
27. Thormann, W.; Wey, A. B.; Lurie, I. S.; Gerber, H.; Byland, C.; Malik, N.; Hochmeister, M.; Gehrig, C. *Electrophoresis* 1999, 20, 3203.
28. Frazier, R. A.; Ames, J. M.; Nursten, H. E. *Electrophoresis* 1999, 20, 3156.
29. Lin, S.; Tang, P.; Hsu, S. M. *Electrophoresis* 1999, 20, 3388.
30. Okun, V. M.; Ronacher, B.; Blaas, D.; Kenndler, E. *Anal. Chem.* 2000, 72, 4634.
31. Shaw, D. J. in: *Electrophoresis*. Academic Press, London, 1969.
32. Hunter, R. J. in: *Zeta Potential in Colloid Science*. Academic Press, London, 1982. pp 61.
33. Rice, C. L.; Whitehead, R. *J. Phys. Chem.* 1965, 69, 4017.
34. Hjertén, S. *J. Chromatogr.* 1985, 347, 191.
35. Harrold, M. P.; Jo Wajtusik, M.; Riviello, J.; Henson, P. *J. Chromatogr.* 1993, 640, 463.

36. Karger, B. L.; Foret, F. in: *Capillary electrophoresis Technology*. Guzman, N. A. (Ed.) 1993, Marcel Dekker, Inc. pp 7.
37. Harrison, D. J.; Fluri, K.; Seiler, K.; Fan, Z.; Effenhauser, C. S.; Manz, A. *Science* 1993, 262, 895.
38. Jacobson, S. C.; Hergenröder, R.; Koutny, L. B.; Ramsey, J. M. *Anal. Chem.* 1994, 66, 1114.
39. Effenhauser, C. S.; Paulus, A.; Manz, A.; Widmer, H. M. *Anal. Chem.* 1994, 66, 2949.
40. Smith, N. J.; Evans, M. B. *Chromatographia* 1995, 41, 197. (41)
41. Euerby, M. R.; Johnson, C. M.; Bartle, K. R. *LC-GC* 1998, 16, 386.
42. Angus, P. D. A.; Victorino, E.; Payne, K. M.; Demarest, C. W.; Catalano, T.; Stobaugh, J. F. *Electrophoresis* 1998, 19, 2073.
43. Lane, S. J.; Boughtflower, R.; Paterson, C.; Underwood, T. *Rapid Commun. Mass Spectrom.* 1995, 9, 1283.
44. Lim, J.; Zare, R. N.; Bailey, C. G.; Rakestraw, D. J.; Yan, C. *Electrophoresis* 2000, 21, 737.
45. Thiam, S.; Shamsi, S. A.; Henry III, C. W.; Robinsin, J. W.; Warner, I. M. *Anal. Chem.* 2000, 72, 2541.
46. Terabe, S.; Otsuka, K.; Ichikawa, K.; Tsuchiya, A.; Ando, T. *Anal. Chem.* 1984, 56, 111.
47. Hinze, W. L. in: *Chemical Separations*, Hinze, W. L.; Armstrong, D. L. (Eds.) American Chemical Society, Washington, D. C., 1987.
48. Rosen, M. J. *Surfactants and Interfacial Phenomena*, 2nd Ed., Wiley, New York, 1989, pp 108.

49. Terabe, S.; Otsuka, K.; Ando, T. *Anal. Chem.* 1985, 57, 834.
50. Carchon, H.; Eggermont, E. *Amer. Lab.* 1992, Jan, 67.
51. Bocek, P.; Deml, M.; Gebauer, P.; Dolinik, V. in: *Analytical Isotachopheresis*, Radola, B. J. (Ed.) VCH, Weinheim, 1988, pp 40-57.
52. Witte, D.; Någård, S.; Larsson, M. *J. Chromatogr.* 1994, 687, 155.
53. Chen, S.; Lee, M. L. *Anal. Chem.* 2000, 72, 816.
54. Larsson, M.; Mareike Lutz, E. S. *Electrophoresis* 2000, 21, 2859.
55. Blatny, P.; Kvasnicka, F.; Loucka, R.; Safarova, H. *J. Agric. Food Chem.* 1997, 45, 3554.
56. Kvasnicka, F. *Electrophoresis* 2000, 21, 2780.
57. Liu, S. R.; Shi, Y. N.; Ja, W. W.; Mathies, R. A. *Anal. Chem.* 1999, 71, 566.
58. Zhang, B.; Liu, H.; Karger, B. L.; Foret, F. *Anal. Chem.* 1999, 71, 3258.
59. Li, J.; Thibault, P.; Bings, N. H.; Skinner, C.; Wang, C.; Colyer, C.; Harrison, J. D. *Anal. Chem.* 1999, 71, 3036.
60. Figeys, D.; Ning, Y.; Aebersold, R. *Anal. Chem.* 1997, 69, 3153.
61. Li, J.; Kelly, J. F.; Chernushevich, I.; Harrison, J. D.; Thibault, P. *Anal. Chem.* 2000, 72, 599.
62. Pretorius, V.; Hopkins, B. J.; Schieke, J.D. *J. Chromatogr.* 1974, 99, 23.
63. Rebscher, H.; Pyell, U. *Chromatographia* 1996, 42, 171. (63)
64. Smith, N. J.; Evans, M. B. *Chromatographia* 1994, 38, 694.
65. Boughtflower, R. J.; Underwood, T.; Paterson, C. J. *Chromatographia* 1994, 40, 329.
66. Behnke, B.; Grom, E.; Bayer, E. *J. Chromatogr. A.* 1995, 716, 207.
67. Rebscher, H.; Pyell, U. *Chromatographia* 1994, 38, 737.

68. Dittmann, M. M.; Wienand, K.; Bek, F.; Rosing, G. P. *LC-GC* 1995, 13, 800
69. Rathore, A. S.; Horváth, Cs. *J. Chromatogr. A* 1996, 743, 231.
70. Choudhary, G.; Horváth, Cs. *J. Chromatogr. A* 1997, 781, 161.
71. Rathore, A. S.; Horváth, Cs. *J. Chromatogr. A* 1997, 781, 185.
72. Rathore, A. S.; Horváth, Cs. *Anal. Chem.* 1998, 70, 3069.
73. Rathore, A. S.; Horváth, Cs. *Anal. Chem.* 1998, 70, 3271.
74. Wen, E.; Asiaie, R.; Horváth, Cs. *J. Chromatogr. A* 1999, 855, 349.
75. Yan, C.; Dadoo, R.; Zhao, H.; Zare, R. H.; Rakestraw, D. J. *Anal. Chem.* 1995, 67, 2026.
76. Huber, C. G.; Choudhary, G.; Horváth, Cs. *Anal. Chem.* 1997, 69, 4429.
77. Xin, B.; Lee, M. L. *Electrophoresis* 1999, 20, 67.
78. Alexander, J. N.; Poli, J. B.; Markides, K. E. *Anal. Chem.* 1999, 71, 2398.
79. Johansson, J.; Owens, P. K. *Anal. Chem.* 2000, 72, 740.
80. Zhang, M.; El Rassi, Z. *Electrophoresis* 1998, 19, 2068.
81. Zhang, M.; Yang, C.; El Rassi, Z. *Anal. Chem.* 1999, 71, 3277.
82. Huang, P.; Jin, X.; Chen, Y.; Srinivasan, J. R.; Lubman, D. L. *Anal. Chem.* 1999, 71, 1786.
83. Cikalo, M. G.; Bartle, K. D.; Myers, P. *Anal. Chem.* 1999, 71, 1820.
84. Wei, W.; Luo, G.; Yan, C. *Amer. Lab.* 1998, 20C.
85. Ye, M.; Zou, H.; Liu, Z.; Ni, J.; Zhang, Y. *Anal. Chem.* 2000, 72, 616.
86. Ishizuka, N.; Minakuchi, H.; Nakanishi, K.; Soga, N.; Nagayama, H.; Hosoya, K.; Tanaka, N. *Anal. Chem.* 2000, 72, 1275.
87. Dulay, M. T.; Kulkarni, R. P.; Zare, R. N. *Anal. Chem.* 1998, 70, 5103.
88. Wang, D.; Chong, S. L.; Malik, A. *Anal. Chem.* 1997, 69, 4566.

89. Peters, E. C.; Petro, M.; Svec, F.; Fréchet, J. M. J. *Anal. Chem.* 1998, 70, 2296.
90. Peters, E. C.; Lewandowski, K.; Petro, M.; Svec, F.; Fréchet, J. M. J. *Anal. Commun.* 1998, 35, 83.
91. Yamamoto, H.; Baumann, J.; Erni, F. *J. Chromatogr.* 1992, 593, 313.
92. Dadoo, R.; Yan, C.; Zare, R. N.; Anex, D. S.; Rakestraw, D. J.; Hux, G. A. *LC-GC* 1997, 15, 630.
93. Bailey, C. G.; Yan, C. *Anal. Chem.* 1998, 70, 3275.
94. Warriner, R. N.; Craze, A. S.; Games, D. E.; Lane, S. J. *Rapid Commun. Spectrom.* 1998, 12, 1143.
95. Ding, J.; Vouros, P. *Anal. Chem.* 1997, 69, 379.
96. Wu, J.; Huang, P.; Li, M. X.; Lubman, D. M. *Anal. Chem.* 1997, 69, 2908.
97. Huang, P.; Wu, J.; Lubmann, D. M. *Anal. Chem.* 1998, 70, 3003.
98. Yang, C.; El Rassi, Z. *Electrophoresis* 1998, 19, 2061.
99. Frame, L. A.; Robinson, M. L.; Lough, W. J. *J. Chromatogr. A* 1998, 798, 243.
100. Dulay, M. T.; Yan, C.; Rakestraw, D. J.; Zare, R. N. *J. Chromatogr. A* 1996, 725, 361.
101. Euerby, M. R.; Gilligan, D.; Johnson, C. M.; Roulin, S. C. P.; Myers, P.; Bartle, K. *D. J. Microcolumn Sep.* 1997, 9, 373.
102. Dittmann, M. M.; Rozing, G. P. *J. Microcolumn Sep.* 1997, 9, 399.
103. Minakuchi, H.; Nakanishi, K.; Soga, N.; Ishizuka, N.; Tanaka, N. *Anal. Chem.* 1996, 68, 3498.
104. Fields, S. M. *Anal. Chem.* 1996, 68, 2702.
105. Minakuchi, H.; Ishizuka, N.; Nakanishi, K.; Soga, N.; Tanaka, N. *J. Chromatogr. A* 1998, 828, 83.

106. Asiaie, R.; Huang, X.; Faman, D.; Horváth, Cs. *J. Chromatogr. A* 1998, 806, 251.
107. Fujimoto, C.; Fujise, Y.; Matsuzawa, E. *Anal. Chem.* 1996, 68, 2753.
108. Peters, E. C.; Petro, M.; Svec, F.; Fréchet, J. M. J. *Anal. Chem.* 1998, 70, 2288.
109. Peters, E. C.; Petro, M.; Svec, F.; Fréchet, J. M. J. *Anal. Chem.* 1997, 59, 3646.
110. Xie, S.; Allington, R. W.; Svec, F.; Fréchet, J. M. *J. Chromatogr. A* 1999, 865, 169.
111. Xie, S.; Svec, F.; Fréchet, J. M. *J. Chromatogr. A* 1997, 775, 65.
112. Gusev, I.; Huang, X.; Horváth, Cs. *J. Chromatogr. A* 1999, 855, 273.
113. Schweitz, L.; Andersson, L. I.; Nilsson, S. *Anal. Chem.* 1997, 69, 1179.
114. Takeuchi, T.; Ishii, D.; Nakanishi, A. *J. Chromatogr.* 1984, 285, 97.
115. Gluckman, J. C.; Hirose, A.; McGuffinn, V. L.; Novotny, M. *Chromatographia* 1983, 17, 303.
116. Yan, C. Electrokinetic Packing of Capillary Columns. *US Pat.* 5453163, 1995.
117. Stol, R.; Mazereeuw, M.; Tjaden, U. R.; van der Greef, J. *J. Chromatogr. A* 2000, 873, 293.
118. Robson, M. M.; Roulin, S.; Shariff, S. M.; Raynor, M.W.; Bartle, K. D.; Clifford, A. A.; Myers, P.; Euerby, M. R.; Johnson, C. M. *Chromatographia* 1996, 43, 313.
119. Koivisto, P.; Danielsson, R.; Markides, K. E. *J. Micro. Sep.* 1997, 9, 97.
120. Kennedy, R. T.; Jorgenson, J. M. *Anal. Chem.* 1989, 61, 1128.
121. Hsieh, S.; Jorgenson, J. W. *Anal. Chem.* 1996, 68, 1212.
122. Vissers, J. P. C.; Claessens, H. A.; Laven, J.; Cramers, C. A. *Anal. Chem.* 1995, 67, 2103.
123. Shelly, D. C.; Edkins, T. J. *J. Chromatogr.* 1987, 411, 185.

124. Shelly, D. C.; Antonucci, L.; Edkins, T. J. Dalton, T. J. *J. Chromatogr.* 1989, 458, 267.
125. Wang, H.; Hartwick, R. A.; Miller, N. T.; Shelly, D. C. *J. Chromatogr.* 1990, 523, 23.
126. Verzele, M.; Dewaele, C. *LC-GC* 1986, 4, 614.
127. Chen, Y.; Gerhardt, G.; Cassidy, R. *Anal. Chem.* 2000, 72, 610.
128. Chen, J.; Dulay, M. T.; Zare, R.; Svec, F.; Peters, E. *Anal. Chem.* 2000, 72, 1224.
129. Cikalo, M. G.; Bartle, K. D.; Robson, M. M.; Myers, P.; Euerby, M. R. *Analyst* 1998, 123, 87R.
130. Janini, G. M.; Chan, K. C.; Barnes, J. A.; Muschik, G. M.; Issaaq, H. J. *Chromatographia* 1993, 35, 497.
131. Schemeer, K.; Behnke, B.; Bayer, E. *Anal. Chem.* 1995, 67, 3656.
132. Chevret, J. P.; Van Soest, R. E. J.; Ursem, M. *J. Chromatogr.* 1991, 543, 439.
133. Caslavaska, J.; Gassmann, E.; Thormann, W. *J. Chromatogr. A* 1995, 147.
134. Cheng, Y.F.; Dvichi, N.J. *Science* 1988, 242, 562.
135. Chen, D. Y.; Swerdlow, H. P.; Harke, H R.; Zhang, J. Z.; Dovichi, N. J. *J. Chromatogr.* 1991, 559, 237.
136. Gassman, E.; Kuo, J. E.; Zare, R. N. *Science* 1985, 230, 813.
137. Kuhr, W. G.; Yeng, E. S. *Anal. Chem.* 1988, 60, 1832.
138. Yu, M.; Dovichi, N. J. *Anal. Chem.* 1988, 61,37.
139. Saz, J. M.; Krattiger, B.; Bruno, A. E.; Díez-Masa, J. C.; Widmer, H. M. *J. Chromator. A* 1995, 319-322.
140. Tarigan, H. J.; Neill, T; Kenmore, C.K.; Bornhop, D.J. *Anal. Chem.* 1996, 68, 1762.
141. Krattiger, B; Bruin, G. J. M.; Bruno, A. E. *Anal. Chem.* 1994, 66, 1.

142. Burggraf, N.; Kratiger, B.; deMello, A. J.; deRoos, N. F.; Manz, A. *Analyst* 1998, 123, 1443.
143. Nann, A.; Pretsch, E. *J. Chromatogr. A* 1994, 676, 437.
144. Swanek, F. D.; Chen, G.; Ewing, A. G. *Anal. Chem.* 1996, 68, 3912.
145. Wallingford, R. A.; Ewing, A.G. *Anal. Chem.* 1987, 59, 1762.
146. Colon, L. A.; Dadoo, R.; Zare, R. N. *Anal. Chem.* 1993, 65, 476.
147. Gordon, M. J.; Huang, X.; Pentoney, S. L.; Zare, R. N. *Science* 1988, 63, 224.
148. Kar, S.; Dasgupta, P. K.; Liu, H.; Hwang, H. *Anal. Chem.* 1994, 66, 2537.
149. Banks, J. F.; Dresch, T. *Anal. Chem.* 1996, 68, 1480.
150. Pentoney Jr., S. L.; Zare, R. N.; Quint, J. F. *Anal. Chem.* 1989, 61, 1642.
151. Olson, D. L.; Lacey, M. E.; Webb, A. G.; Sweedler, J. V. *Anal. Chem.* 1999, 71, 3070.
152. Walker, P. A.; Morris, M.D.; Burns, M.A.; Johnson, B. N. *Anal. Chem.* 1998, 70, 3766.
153. Swinney, K.; Bornhop, D. *Electrophoresis* 2000, 21, 1239.
154. Pentoney, Jr.; S. L.; Sweedler, J. V. in: *Handbook of Capillary Electrophoresis*. Laders, J. P. (Ed.). CRC Press, Boca Raton, FL 1992, pp 379.
155. Waldron, K. Ph.D. Thesis. *Development of a Miniaturized Peptide Sequencer with Capillary Electrophoresis Separation and Thermo-optical Absorbance detection of derivatized Amino Acides*. 1994, University of Alberta, Edmonton.
156. Dovichi, N. J. in: *CRC Critical Reviews in Analytical Chemistry*. CRC Press, Inc. 1987, 4, 353.
157. Gordon, J. P.; Leite, R. C. C.; Moore, R. S.; Porto, S. P. S.; Whinnery, J. R. *J. Appl. Phys.* 1965, 36, 3.

158. Dovichi, N. J.; Harris, J. M. *Anal. Chem.* 1979, 51, 728.
159. Dovichi, N. J.; Harris, J. M. *Anal. Chem.* 1981, 53, 689.
160. Dovichi, N. J.; Nolan, T. G.; Weimer, W. A. *Anal. Chem.* 1984, 56, 1700.
161. Weimer, W. A.; Dovichi, N.J. *Appl. Spectrosc.* 1985, 39, 1009.
162. Weimer, W. A.; Dovichi, N.J. *Anal. Chem.* 1985, 57, 2436.
163. Nolan, T. G.; Hart, B. K.; Dovichi, N. J. *Anal. Chem.* 1985, 57, 2703.
164. Nolan, T. G.; Dovichi, N. J. *IEEE Circuit Devices Mag.* 1986, 2, 54.
165. Bornhop, D. J.; Dovichi, N. J. *Anal. Chem.* 1986, 58, 504.
166. Bornhop, D. J.; Dovichi, N. J. *Anal. Chem.* 1987, 59, 1632.
167. Bornhop, D. J.; Nolan, T. G.; Dovichi, N. J. *J. Chromatogr.* 1987, 384, 181.
168. Nolan, T. G.; Dovichi, N. J. *Anal. Chem.* 1987, 59, 2803.
169. Yu, M.; Dovichi, N. J. *Appl. Spectrosc.* 1989, 43, 196.
170. Waldron, K. C.; Dovichi, N. J. *Anal. Chem.* 1992, 64, 1396.
171. Chen, M.; Waldron, K. C.; Zhao, Y.; Dovichi, N. J. *Electrophoresis* 1994, 15, 1290.
172. Li, X. F.; Liu, C. S.; Roos, P.; Hansen Jr.; E. B.; Cerniglia, C. E.; Dovichi, N. J. *Electrophoresis* 1998, 19, 3178.
173. Kettler, C. N.; Sepaniak, M. J. *Anal. Chem.* 1987, 59, 1733.
174. Krattiger, B.; Bruno, A. E.; Widmer, H.M.; Dändliker, R. *Anal. Chem.* 1995, 67, 124.
175. Bruno, A. E.; Krattiger, B.; Maystre, F.; Widmer, H. M. *Anal. Chem.* 1991, 63, 2689.
176. Krattiger, B.; Bruno, A. E.; Widmer, H. N.; Geiser, M.; Dändliker, R. *Appl. Optics* 1993, 32, 956.
177. Yates, III, J. R. *J. Mass Spectr.* 1998, 33, 1.

178. Dole, M.; Hines, R. L.; Mack, L. L.; Mobley, R. C.; Ferguson, L. D.; Alice, M. B. *J. Chem. Phys.* 1968, 49, 2240.
179. Fenn, J. B.; Mann, M.; Meng, C. K.; Wang, S. F.; Whitehouse, C. M. *Science* 1989, 6, 64.
180. Covey, T. R.; Bonner, R. F.; Shushan, B. I.; Henion, J. D. *Rapid Commun. Mass Spectrom.* 1988, 2, 249.
181. Olivares, J. A.; Nhung, N. T.; Yonker, C. L. R.; Smith, R. D. *Anal. Chem.* 1987, 59, 1230.
182. Balogh, M. P. *LC-GC* 1998, 16, 135.
183. Chernushevich, I. V.; Ens, W.; Standing, K. G. *Anal. Chem. News & Features* 1999, 453A.
184. Niessen, W. M. A. Review: Advances in Instrumentation in Liquid Chromatography-Mass Spectrometry and Related Liquid-Introduction Techniques. *J. Chromatogr. A* 1998, 794, 407.
185. Henry, C. *Anal. Chem. News & Features* 1997, 427A.
186. Bruins, A. P. Review: Mechanism Aspects of Electrospray Ionization. *J. Chromatogr. A* 1988, 794, 345.
187. Lahm, H-W.; Langen, H. *Electrophoresis* 2000, 21, 2105.
188. Patterson, S.; Aebersold, R. *Electrophoresis* 1995, 16, 1791.
189. Kebarle, P.; Tang, L. *Anal. Chem.* 1993, 65, 972A.
190. Kabarle, P.; Ho, Y. in: Cole, R. B. (Ed.) *Electrospray Ionization Mass Spectrometry: Fundamentals, Instrumentation, and Applications*. Wiley, New York, 1997.
191. Taylor, G. I. *Proc. R Soc. London A* 1964, A280, 383.

192. Bailey, A. G.; *Electrostatic Spraying Liquids*. Wiley, New York, 1988.
193. Loo, J. A.; Udseth, H. R.; Smith, R. D. *Rapid Commun. Mass Spectrom.* 1988, 2, 207.
194. Weinmer, W.; Wiedemann, A.; Eppinger, B.; Renz, M. Svoboda, M. *J. Am. Soc. Mass Spectrom.* 1999, 10, 1028.
195. Chernushevich, I. V.; Ens, W.; Standing, K. G. *Anal. Chem.* 1999, 452A.
196. Purves, R. W.; Li, L. *J. Am. Soc. Mass Spectrom.* 1997, 8, 1085.
197. Mirgorodskaya, O. A.; Shevchenko, A. A.; Chernushevich, I. V.; Dodonove, A. F.; Miroshnikov, A. I. *Anal. Chem.* 1994, 66, 99.
198. Lin, H-Y.; Voyksner, R. D. *Anal. Chem.* 1993, 65, 451.
199. Henry, K. D.; McLaffery, F. W. *Org. Mass Spectrom.* 1990, 25, 490.
200. Bruins, A. P.; Covey, T. J.; Henion, J. D. *Anal. Chem.* 1987, 59, 2642.
201. Smith, R. D.; Baringa, C. J.; Udseth, H. R. *Anal. Chem.* 1988, 60, 1948.
202. Lee, E. D.; Muck, W.; Henion, J. D.; Covey, T. R. *J. Chromatogr.* 1989, 458, 313.
203. Reinhoud, N. J.; Niessen, W. M. A.; Tjaden, U. R.; Gramberg, L. G. Verheij, E. R.; van der Greeg, J. *Rapid Commun. Mass Spectrom.* 1989, 3, 87.
204. Kelly, J. F.; Ramaley, L.; Thibault, P. *Anal. Chem.* 1997, 69, 51.
205. Chang, Y. Z.; Her, G. R. *Anal. Chem.* 2000, 72, 626.
206. Fang, L.; Zhang, R.; Williams, E. R.; Zare, R. N. *Anal. Chem.* 1994, 66, 3696.
207. Banks, Jr. J. F. *J. Chromatogr.* 1995, 712, 245.
208. *API 100 LC/MS System Reference's Manual*. 1995, pp 4-8. Perkin-Elmer Sciex Instruments, Foster City, CA. 94404.
209. Miller, P. E.; Denton, M. B. *J. Chem. Educ.* 1986, 63, 617.

210. March, R. E.; Hughes, R. J.; Todd, J.F. in: *Quadrupole Storage Mass Spectrometry*, vol. 102 of *Chemical Analysis*, Wiley, NewYork, 1989.

CHAPTER 2

DEVELOPMENT OF CAPILLARY ELECTROCHROMATOGRAPHY COLUMN MANUFACTURE*

* A version of this chapter has been published. *J. Chromatogr. A* **1999**, 853, 131-140.

2.1 INTRODUCTION

Capillary electrochromatography (CEC) is a hybrid technique combining both the high selectivity of micro-high performance liquid chromatography (HPLC) and the high efficiency of capillary zone electrophoresis (CZE). The high separation efficiency but short history of CEC has created an exciting area for research in separation science. Higher number of theoretical plates, essential for resolving complex mixtures, have been both theoretically predicted and found by experiment [1-2]. Secondly, the electrokinetically driven flow is independent of the particle diameter, which allows the use of smaller particles to enhance the separation efficiency. Thirdly, CEC reduces the cost of materials and consumption of solvent due to its miniaturized separation scale.

The wide acceptance of CEC is deterred by several practical difficulties. Column manufacture involves tedious and demanding manual operations. The packing procedures are not well characterized and standardized [3]. CEC columns are fragile compared to more robust HPLC columns. CEC is mostly criticized for the difficulty in obtaining stable flow conditions due to bubble formation that results in electrical current cut-off during the separation process. Bubble formation can also destroy the integrity of the packed bed. The problem has been dealt with by implementation of pneumatic pressure on both the inlet and outlet buffer vials [4-5].

The production of particle-packed CEC columns has been reported by three main approaches including high-pressure slurry packing [5-9], electrokinetic packing [10-11], and super critical fluid packing [12-14]. In the slurry packing method, a high-pressure column packer and bomb are required. Sonicating the slurry reservoir and the capillary to

be packed is often employed during the slurry packing process. The packing solvent and slurry concentrations have been found to play important roles in a successful packing procedure [15-16].

Frits are reported to be one of the causes of bubble formation and band broadening of polar analytes [17]. Frits are prepared by sintering silica gel or making a monolithic plug. Electrical heating wires are the simplest devices used for sintering [3, 6-7, 18]. A fiber optic splicer has also been employed for frit production [19].

The applications of CEC are mostly in analysis of small molecules, especially pharmaceuticals [20-26]. To my knowledge, only one research group has reported the separation of several phenylthiohydantoin amino acids (PTH-AAs) using gradient CEC [27]. PTH-AAs are generated by Edman degradation, a classical protein sequencing technique. Traditionally, this class of compounds is analyzed by gradient HPLC for protein sequencing [28].

The objectives of this chapter are to address some practical problems in the preparation of CEC columns and to demonstrate the use of a photothermal absorbance detector for CEC separation. The performance of laboratory-made CEC columns has been characterized and evaluated using migration time, theoretical plate numbers, and resolution. The influence of electrical voltage, mobile phase composition (such as buffer type), concentration, buffer pH, organic solvent composition on electroosmotic flow velocity, separation efficiency, and retention factors have been investigated. The value of home-made CEC columns has also been demonstrated in separation of 16 polycyclic aromatic hydrocarbons and 19 PTH - amino acid derivatives using a photothermal ultraviolet absorbance detector.

2.2 EXPERIMENTAL

2.2.1 Materials and Reagents

Enzyme grade 4-morpholinoethanesulfonic acid (MES), N-2-hydroxyethyl-piperazine-N'-2-ethanesulfonic acid (HEPES), and reagent-grade sodium hydroxide (NaOH) were purchased from Fisher Scientific (Fair Lawn, NJ, USA). HPLC-grade acetonitrile (ACN) and methanol (MeOH) were purchased from EM Science (Gibbstown, NJ, USA). Thiourea was purchased from Sigma (Ontario, Canada). The PTH - amino acid kit for protein sequencing was purchased from ABI (Foster City, CA, USA). The individual PTH - amino acids were purchased from Sigma (St. Louis, MO, USA). The 3 μm Supelcosil ODS and 16 polycyclic aromatic hydrocarbons mix were obtained from Supelco (Bellefonte, PA, USA). The individual PAH compounds were purchased from Aldrich (Milwaukee, WI, USA). The Spherisorb ODS1 3 μm packing material was a kind gift from Dr. Henry Chen of Waters Corporation (Milford, MA, USA).

The zwitterionic mobile phases were prepared as follows. The stock buffer solutions of 100 mM MES or HEPES were prepared in deionized water, followed by being titrated with 2 M sodium hydroxide solution to the desired pH value. The buffer was then mixed with different volume percentages of organic solvent. The CEC mobile phase was sonicated for 5 min. and filtered through a 0.2 μm Millex PTFE filter (Millipore) prior to use.

The test mixture contained thiourea, used as an electroosmotic flow marker, and PTH - asparagine (N), PTH - leucine (L), PTH - tryptophan (W), PTH - glutamic acid

(E), N, L, W, E are the codes corresponding to each amino acid. The stock solution of each compound was prepared in acetonitrile at a concentration of 10^{-3} M. The concentration of each compound in the test mixture was 5×10^{-5} M diluted in CEC mobile phase.

2.2.2 Column Preparation

The CEC columns used in this chapter were prepared using 50 μm i.d., 182 μm o.d. fused silica capillaries (Polymicro Technologies, Phoenix, AZ, USA). Our packing procedures were similar to those reported by Smith and Evan [6] with some modifications as follows. Before packing, a temporary frit was made by dipping one end of the capillary into a 5 μm silica gel prewetted with water, and this end was heated mildly on a micro-torch flame after drying at ambient temperature. This frit was used to retain the reverse phase particles during the packing process. The temporary frit was tested for mechanical stability and porosity by pumping acetonitrile at a pressure of 1000 pounds per square inch (p.s.i.) into the capillary (1 p.s.i. = 6894.76 Pa). An HPLC pump (Waters 515) was used for slurry packing. Figure 2.1 demonstrates the packing device used for this study. The slurry of reverse phase material was made by mixing 10 mg of ODS1 3 μm particles with 1 mL of acetonitrile. After 5 min. of sonication, the slurry was transferred into an empty HPLC column with dimensions of 70 mm x 4.6 mm i.d. (Supelco), serving as a slurry reservoir. Sonication of the slurry reservoir was omitted. The capillary was connected to the reservoir with a polyether ether ketone (PEEK) tubing

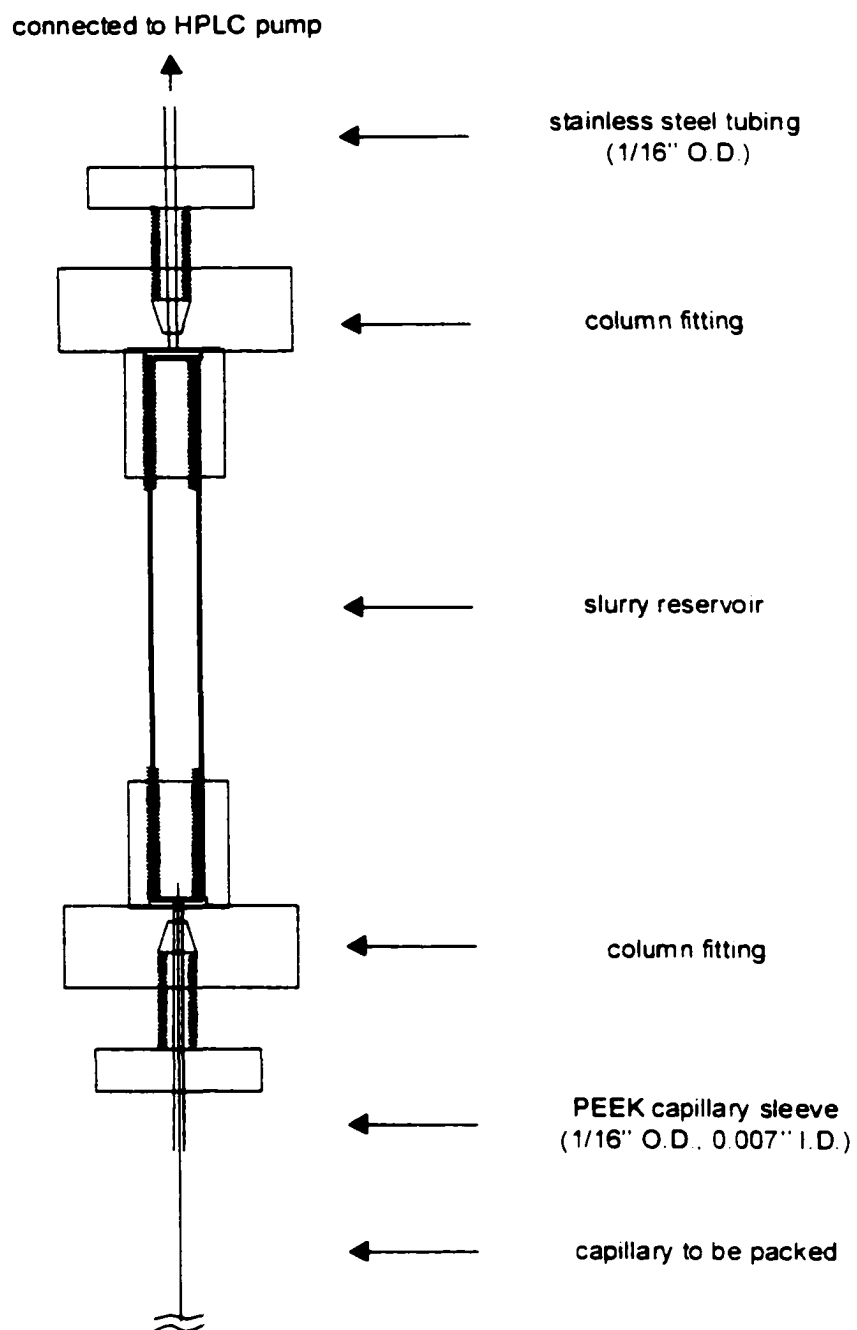


Figure 2.1 Slurry packing set-up

sleeve (1.6 mm o.d. x 180 μm i.d.) and column fittings. The pump was set at pressure limited mode. The C18 particles were pumped into the capillary at pressures up to 5000 p.s.i. The flow was below 0.01 mL/min. without the use of a splitter. The packing process was monitored with a microscope (Unimicro Technology, CA, USA). Successful slurry packing usually took only 5 min for a 30 cm long column. After the capillary was packed for the desired length, the pressure was slowly released to avoid disturbing the packing bed.

2.2.3 Frit Fabrication

A fiber-optic splicer (Orionics FW-301, Scarborough, Canada) with manually controlled heating power was utilized for preparing the frits. The formation of the frit was monitored under a microscope attached on the fiber optic splicer. The steps of packing the column and making both inlet and outlet frits are shown in Figure 2.2. The packed capillary was connected to the HPLC pump via an on-line solvent filter with pore size of 0.2 μm and flushed with HPLC grade water to replace the acetonitrile as shown in step 3 of the Figure. The inlet frit was located 1 cm away from the temporary frit and localized at the center of the two electrodes by adjusting the knobs for three translational stages. The arc power was increased by turning the power knob to a setting of 5.5. During the heating, the polyimide coating was first burnt off, the mobile phase at the heating location was expelled in both directions and the packing turned to white and then to an incandescent red. The temperature was held at the red-hot stage for about 2 sec. before slowly dialing down the power setting. Water was constantly pumped through the

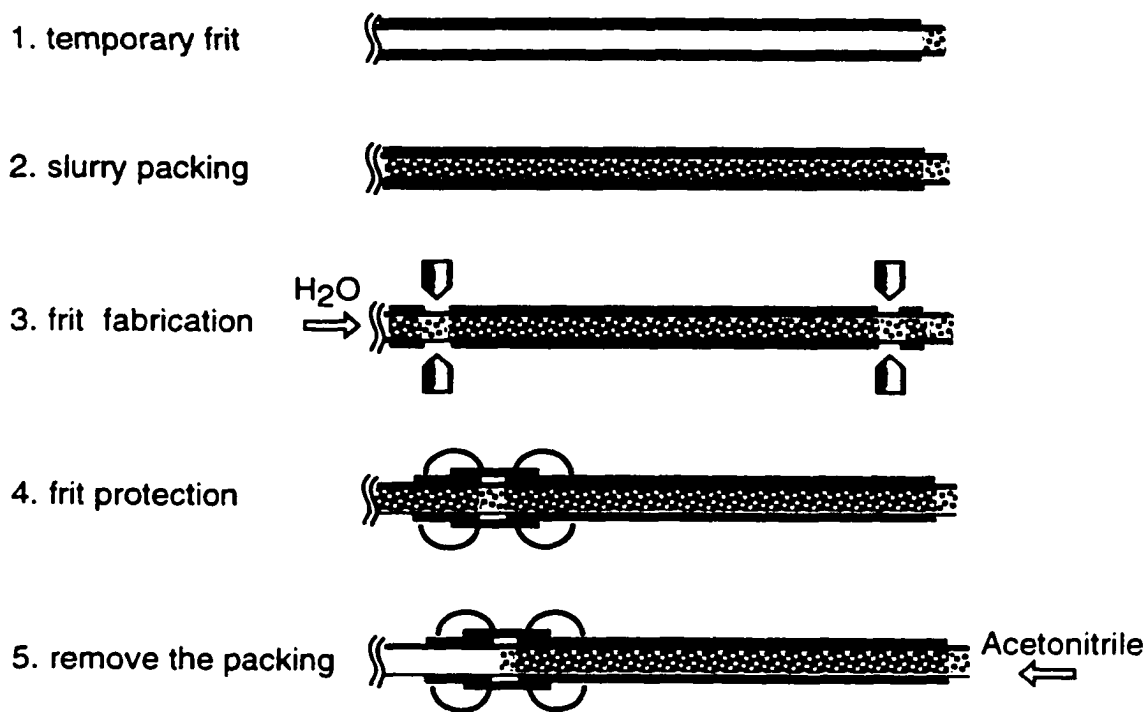


Figure 2.2 Column manufacture procedures

capillary at a pressure of about 2000 to 3000 p.s.i. during the heating process. Overheating must be avoided since it could affect the porosity. The outlet frit was generated in the same manner.

The region near the outlet frit became extremely fragile after the polyimide coating was burnt. To prevent breakage of the column in further experimental steps, the outlet frit was protected by gluing a 1 cm long PTFE sleeve (1.6 mm o.d.; 280 μm i.d.) around it as shown in step 4. The column was dismounted and connected to the HPLC pump in a reverse direction. The mobile phase was switched to acetonitrile and pumped to high pressure to expel the extra packing behind the outlet frit as shown in step 5 of the Figure 2.2. The column was then stored in a box till used. The on-column detection window was made a few centimeters away from the outlet frit. The polyimide coating was burnt by a Ni-Cr coil after the column had been flushed with water.

Columns used for the reproducibility studies were 22 cm of packed bed with a total length of 32.5 cm, with the on-column detection window 5.5 cm from the outlet end (27 cm from inlet end) of the capillary, unless otherwise specified. The evaluation of the columns was carried out by separating the test mixture. The mobile phase contained acetonitrile / 20mM MES at pH 7.0 (80/20, v/v).

2.2.4 Apparatus

All the CEC separations were performed on an in-house designed instrument with a crossed-beam thermo-optic UV absorbance detection system described in Chapter 1. A UV excimer laser (248 nm) was used as a pump laser modulated at a frequency of 625 Hz and a He-Ne laser (632.8 nm) was used as a probe laser. The signal intensity of the

diffraction fringe was monitored by a silicon photodiode and the signal was amplified by a lock-in amplifier, which sent the data to a computer for recording. The chromatograms or electrochromatograms for the separation efficiency study were processed using PeakFit v4.00 (Jandel Scientific, San Rafael, CA, USA).

2.3 RESULTS AND DISCUSSION

2.3.1 Packing Procedures and Frit Manufacture

The effect of the packing liquid on the coagulating behavior of the stationary phase predominantly determines the performance of slurry-packed micro-columns in HPLC [15-16]. It was expected that the longer the packing slurry was in suspension, the more effective would be the slurry packing. Thus, the rate of sedimentation of the reverse phase particles in the slurry determined the success of the packing process. The settling rate of reverse phase particles is determined by gravity, concentration, and particle aggregation. Carbon tetrachloride (CCl_4) was first used as a packing solvent in my experiments because of its high density. However, it was found that no difference was observed in column packing with CCl_4 compared to acetonitrile. THF and acetone were reported to be less effective because the column produced large reduced plate heights [15]. Acetonitrile was used as packing solvent for the rest of the experiments. Occasionally the packing process stopped after only a few-centimeter-long region was packed. Packing could be resumed by turning the slurry reservoir upside-down and tapping it to disturb the particle sedimentation. This approach was more effective than

placing the slurry reservoir and the capillary in a sonication bath because the sedimentation of particles in the slurry reservoir can not be easily avoided even by sonication. By monitoring the capillary with a microscope during packing, I found that the particles were transported through the core of the capillary like a thin "thread" till they impinged on the packed bed and then relocated across the tube. In the packed section, the particles at the core were more densely packed than near the capillary wall, presumably because the parabolic hydrodynamic flow transported particles at maximum speed at the capillary center.

Frit fabrication is a crucial step in column preparation. Both filament heating and an electric arc device were tested for sintering the packing beads. The fiber optic splicer was found to be superior to the heating wire because the arc formed between two electrodes could sinter the packing material and produce better quality frits than the heating wire. Different sintering powers and time intervals were tested to find an optimal condition (data not shown). The thickness of the frit made by this method was less than 2 mm. The frit was intended to be made as porous as possible. Over-heating results in a thicker and less porous plug that degrades the chromatographic performance.

2.3.2 Separation Efficiency

Separation efficiency is one of the parameters that characterizes the column quality. Separation efficiency is described by the number of theoretical plates computed from the retention time of the peak and the peak width at the half height as follows:

$$N = 5.54 \left[\frac{t_r}{\Delta t_{1/2}} \right]^2 \quad (2.1)$$

The retention time t_r is determined by the flow rate of the mobile phase and the interactions of the analyte with both the mobile phase and stationary phase. The peak width, $\Delta t_{1,2}$, is due to the band broadening that occurs in the entire system including injector, column, and the detector. The experimental conditions that can determine peak width include quality of packing and frits, injection amount, sample media, packing types and characteristics, mobile phase composition, and mobile phase flow rate.

In the classical chromatography model, band broadening is measured by plate height that expresses the variance per unit length of the column. The van Deemter equation (Eq. 2.2) was the most popular correlation of plate height to column properties and operational variables.

$$H = A + \frac{B}{u} + Cu \quad (2.2)$$

where H is plate height, u is velocity of mobile phase, and A, B, and C are constants. In pressure-driven liquid chromatography, A is related to interstitial flow inequality arising from the size distribution of intraparticle channels. It is also called eddy diffusion. Eddy diffusion is caused by flow path differences among the channels between particles. B is associated to longitudinal diffusion of the eluting analyte. C is related to resistance to mass transfer of the analyte occurring in the retention process. The equation was based on the additivity of the incremental variances arising from various independent contributions to band broadening.

CEC promises to provide higher separation efficiency than HPLC because of the plug profile of the flow. If the liquid is driven electrically, the flow inequalities should be very small. Dittmann et al. [1] predicted that eddy diffusion, σ_E^2 , in CEC is much lower than in a pressure-driven mode, which results in substantially more plates than in HPLC.

Rebscher and Pyell [29] have proposed that in CEC the overall band broadening of a retained compound is determined by the following factors: eddy diffusion, σ_E ; longitudinal diffusion, σ_L ; resistance to mass transfer, σ_R ; band broadening caused by temperature gradient, σ_G ; and instrumental band broadening, σ_I .

$$\sigma_T^2 = \sigma_E^2 + \sigma_L^2 + \sigma_R^2 + \sigma_G^2 + \sigma_I^2 \quad (2.3)$$

They described a method to experimentally estimate σ_E^2 , σ_L^2 , σ_R^2 , and σ_I^2 band broadening contributions and the values corresponding were 0.46 mm², 0.74 mm², 1.08 mm², and 1.02 mm². They concluded that all of the above band broadening factors were non-negligible except for temperature gradient band broadening. The percentage of eddy diffusion was 14% of the total. Recently, Wen *et al.* [2] have systematically compared the column efficiency in microscale HPLC and CEC in terms of the three constants in the van Deemter equations derived from HPLC mode and CEC mode in otherwise the same conditions. They found with voltage driven flow, the A and C parameters were approximately two to four times lower than pressure-driven flow, which strongly supported the widely observed higher efficiency obtained in CEC vs. μ -HPLC.

The main intent in my study was to investigate the influence of mobile phase flow rate on the separation efficiency rather than to evaluate the variance of each factor contributing to band broadening. Figure 2.3 shows the van Deemter plot from CEC mode for four selected compounds including an EOF marker (thiourea), PTH - asparagine (N), PTH - leucine (L), and PTH -tryptophan (W). The height equivalent to a theoretical plate (HETP) was plotted as a function of EOF linear velocity under running voltages up to 30 kV. Because the power supply was limited to a 30 kV maximum, only a narrow region of the profile could be described. From the figure, one can find that the working range

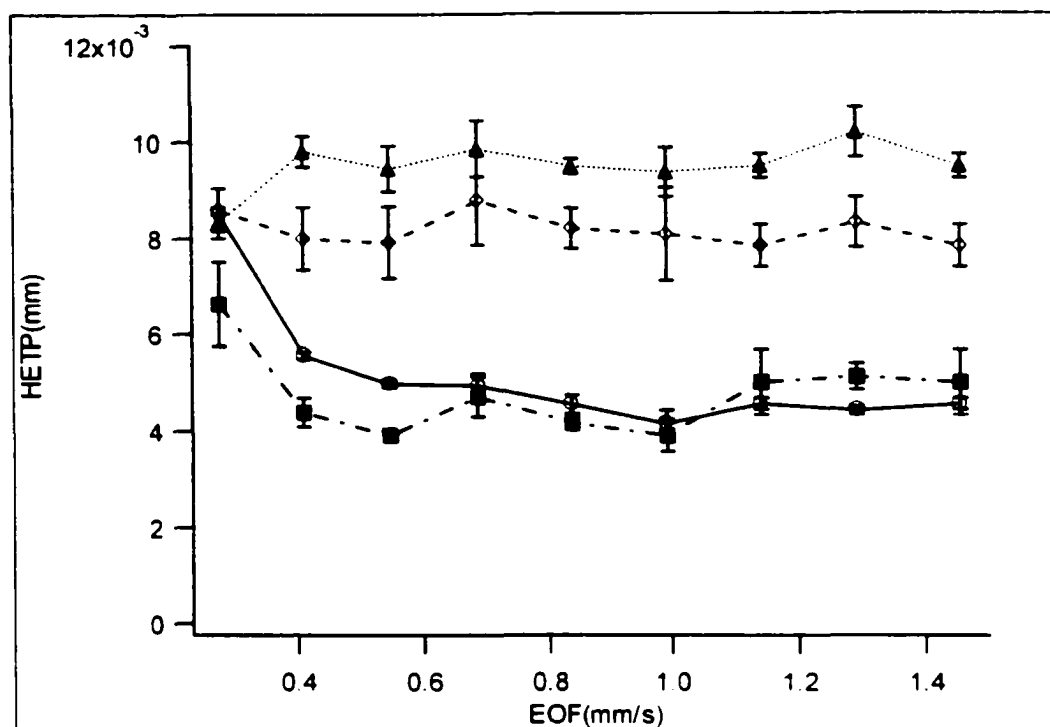


Figure 2.3 Plot of plate height measured with (○) thiourea, and PTH derivatives of (■) Asparagine, (◇) Leucine, and (▲) Tryptophan vs. electroosmotic flow. Column, 23/27.5/33.5 cm, which indicates the length of packed bed / capillary length to the detection window / total column length. The same convention is used in the following figure captions. Packing, 3 μ m Spherosorb-ODS1, Mobile Phase, Acetonitrile/20 mM MES (20/80, v/v) (pH 6.5). Electrokinetic injection at 5kV for 10 sec.

covers the portion of reasonably high efficiency. The efficiency for each of these neutral compounds is quite similar in the range of 10 to 25 kV. The plate height of the unretained EOF marker (thiourea), mostly reflects the sum of variances of eddy diffusion and longitudinal diffusion in the absence of resistance to mass transfer and results in lowest plate height. The number of theoretical plates decreases dramatically for the more retained compounds such as PTH-W and PTH-L because of the additional resistance to

mass transfer term. Based on the previous knowledge [1-2, 29] and Figure 2.3, it is confirmed that longitudinal diffusion and resistance to mass transfer are the major factors in band broadening. The best results for reduced plate height, defined as the ratio of plate height to particle diameter, was between 1.4 to 2.8 for the above compounds. The standard deviation of efficiency ($n=3$) for the amidic PTH-N was larger than those of neutral compounds. Under the experimental conditions, PTH - glutamic acid was negatively charged and eluted as a tailed peak, presumably due to a narrower linear range of isotherm and the overloading of the sample. Figure 2.4 presents a typical capillary electrochromatographic separation of the test compounds. The number of the theoretical plates ranges from 2.2×10^5 plates/m for thiourea to 1.2×10^5 plates/m for PTH - glutamic acid.

2.3.2.1 Loading Effect

High mass loading can be done by injecting a high concentration sample, using high injection voltage, or injecting for a longer time. Fig 2.5 shows the number of theoretical plates for four test compounds at different injection amounts expressed as the product of injection voltage and time. The plate number decreased when the injection amount increased, because a wider sample plug was introduced at high injection amount. The more retained compound shows more reduction in plate counts.

2.3.2.2 Solvent Effect

In HPLC, the solvent effect is the use of solvent and modifier(s) in the sample

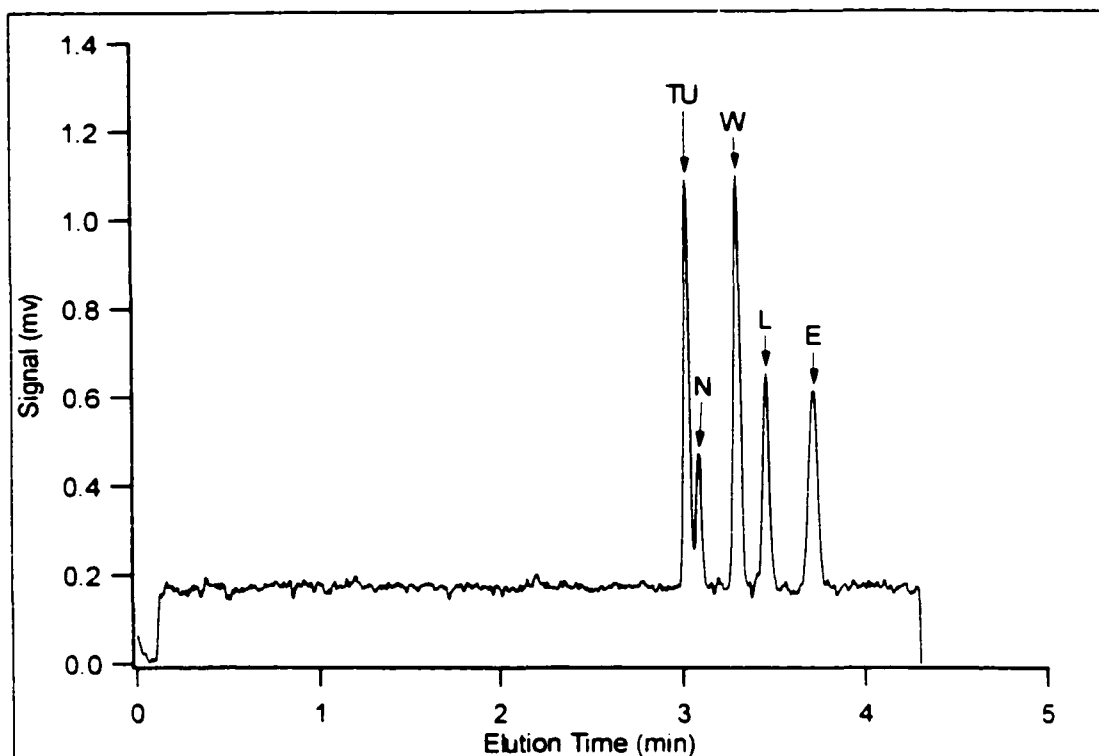


Figure 2.4 CEC separation of EOF marker and PTH-Amino acids mixture. Column, 23/27.5/33.5 cm. Packing, 3 μ m Spherosorb-ODS1. Mobile Phase, Acetonitrile/20 mM MES (20/80, v/v) (pH 6.5). Electrokinetic injection at 5kV for 10 sec. TU: thiourea, N, W, L, E refer to corresponding PTH - amino acids.

media to improve column selectivity and resolution of sample components and to reduce the analysis time of well-retained components. Solvent effects are achieved by either premixing the solvent and its modifier(s) in isocratic operation or by step or gradient elution [30]. In CEC, this mechanism is more complicated. Differences in ionic strength or solvent strength from sample to mobile phase could cause sample loading bias during injection and therefore affect the peak efficiency.

When the ionic strength of the sample is less than that of the mobile phase, electric field amplification occurs as the result of lower conductivity at the sample vial.

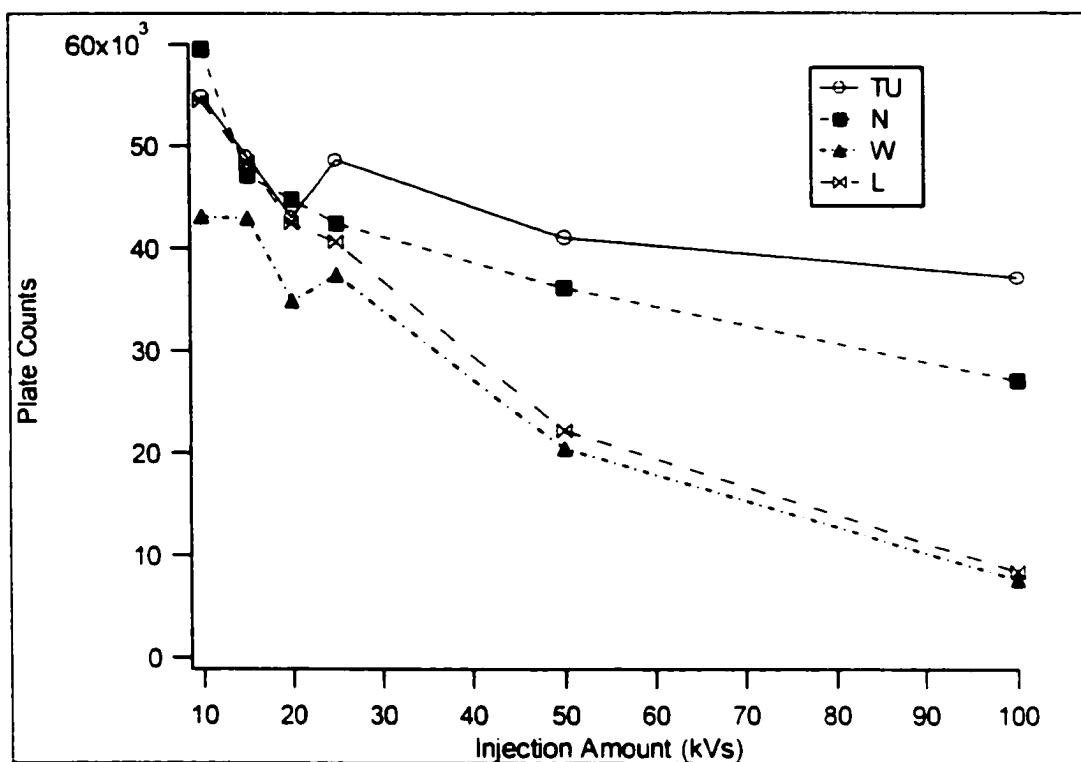


Figure 2.5 Plot of plate counts vs. injection amount using the product of injection voltage and time. Column, 23/27.5/33.5 cm. Packing, 3 μm Spherosorb-ODS1. Mobile Phase, Acetonitrile/20 mM MES (20/80, v/v) (pH 7.0). Electrokinetic injection.

The stronger field induces higher EOF flow, which causes high sample loading into the column. Figure 2.6 demonstrates the example of solvent effect in CEC. The number of theoretical plates decreased by 63% by using lower ionic strength sample buffer (5 mM MES) compared to higher ionic strength buffer (10 mM). The stacking effect to obtain high sensitivity, commonly applied in CZE and MEKC, was not observed here. Instead, similar peak height but greater peak width occurred at higher sample loading.

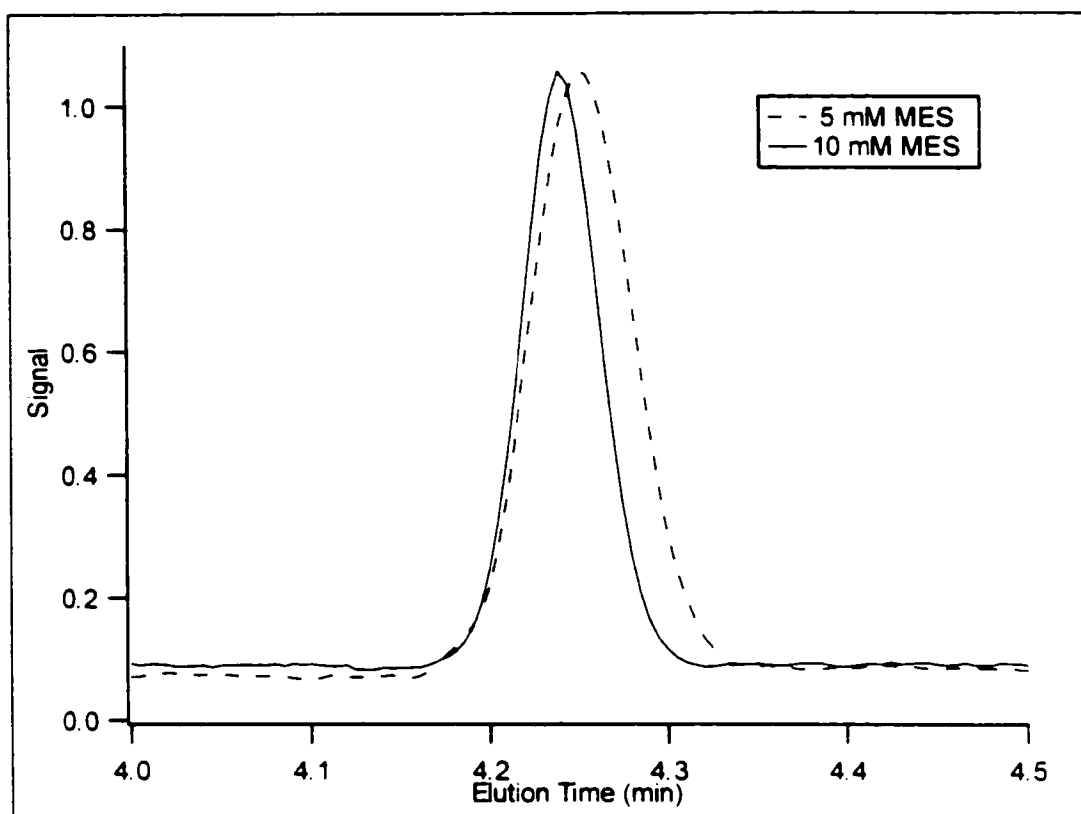


Figure 2.6 Electrochromatograms of PTH-W introduced with different sample media: 10 mM MES, 90% ACN (solid line), 5 mM MES, 90% ACN (dashed line). Mobile Phase, 10 mM MES, 90% ACN, 20 μ M PTH-W concentration.

2.3.2.3 Gap Formation

I observed that after many runs, a gap a few millimeters long was generated behind the inlet frit. This gap might be due to the influence of different characteristics of the mobile phase used in the preparation of the column and separation. A gap shorter than 2 mm did not noticeably affect the migration reproducibility, although the resolution degraded. Damage of the inlet frit often resulted in loss of the packing from the inlet, forced by electrophoretic mobility, which increased the electroosmotic flow dramatically

during the run.

2.3.3 EOF and Velocities of Analytes

Unlike in HPLC, where the velocity of the mobile phase is an independent parameter controlled by the pressure of the pump, in CEC the speed of mobile phase is a result of electroosmotic flow determined by several factors as defined in Eq. 2.4 [31]

$$\mu_{eo} = \frac{\sigma \left[\frac{\epsilon_0 \epsilon_r RT}{2cF^2} \right]^{1/2} E}{\eta} \quad (2.4)$$

where σ is the charge density at the surface of the shear of the electrical double layer, ϵ_r is the dielectric constant of the mobile phase, ϵ_0 is the permittivity of vacuum, R is the gas constant, T is temperature, E is the electric field strength, c is electrolyte concentration, F is the Faraday constant, and η is the viscosity of the mobile phase.

Practically, EOF is mostly affected by the organic content and buffer pH of the mobile phase. Once a suitable buffer is chosen, the velocity of the mobile phase moving through the column is then simply determined by the voltage across the column.

The relationship of the velocity of analyte as a function of electric field can be derived as follows. CEC separation involves the processes of partitioning and electrophoretic mobility. The apparent migration velocity of a charged analyte, u_a , is described by Rathore and Horváth [32] as the sum of its velocities due to electroosmotic flow (u_{eo}) and electrophoretic migration (u_{ep}) in the mobile phase multiplied by the retention factor $1/(1+k')$:

$$u_a = \frac{1}{1+k'} (u_{eo} + u_{ep}) \quad (2.5)$$

where k' is the chromatographic retention factor defined as:

$$k' = \frac{t_r - t_0}{t_0} \quad (2.6)$$

Only for neutral compounds where partition is responsible for the separation, k' obtained from Eq. 2.6 are comparable to those which are obtained from the HPLC method. For charged compounds, k' by the CEC method differs from k' by the HPLC method.

Electroosmotic flow and electrophoretic mobility in CZE is described by Knox [33] as:

$$u_{eo} = \frac{\epsilon_r \epsilon_0 \zeta E}{\eta} = \mu_{eo} E \quad (2.7)$$

The electrophoretic rate of charged solute is described as [34]:

$$u_{ep} = \frac{qE}{6\pi\eta r} = \mu_{ep} E \quad (2.8)$$

where q is the charge of ionized solute, and r is the solute radius. Substituting μ_{eo} , μ_{ep} in Eq. (2.7) and (2.8) into Eq. (2.5), one can obtain

$$u_a = \frac{1}{1 + k'} (\mu_{eo} + \mu_{ep}) E \quad (2.9)$$

Eq. (2.9) reveals that the migration velocity of an analyte in CEC is linearly related to the applied electric field.

The fact of a linear relationship between migration velocity and electric field can be used to examine the stability of CEC column performance. A number of CEC separations for the test mixture were conducted using different electric fields while the other conditions were kept constant. The results are summarized in Figure. 2.7A. The electric field range plotted corresponds to a high voltage range from 5 kV to 25 kV. It illustrates a linear relationship ($r > 0.999$) between the velocity of each analyte and the

electric field. Such a linear relationship indicated that there was no significant Joule heating under the experiment conditions and the column was conditioned for reproducible runs. The plot of k' versus electric field strength from the same experimental data further confirmed the stable k' values of PTH-N, PYH-W, PTH-L, and PTH-E over the range of field strengths in Figure 2.7B. The variances of k' for the above compounds were 4.8%, 2.6%, 1.5%, and 7.4%, respectively. PTH-E migrated slowest, as expected, because it was negatively charged and had a reversed electrophoretic mobility compared to the electroosmotic flow at the pH of the buffer.

At a field strength of 1100 V/cm, the corresponding electroosmotic flow was 1.5 mm/s in the CEC column, whereas the electroosmotic flow in an open tubular capillary was 1.8 mm/s at a field of 200 V/cm with the same buffer. This indicates that CEC requires a much higher electric field strength than CZE in order to obtain the same electroosmotic flow.

2.3.4 Effect of Organic Solvent

It has been reported that increasing the content of acetonitrile in the mobile phase increases electroosmotic flow [29]. A series of CEC separations for the test mixture was carried out using various volume ratios of the acetonitrile to buffer (20 mM MES, pH 7.0) as mobile phases. When the volume ratio of acetonitrile to buffer was increased from 50% to 90%, EOF velocity increased by 74% as shown in Figure 2.8. This enhancement in EOF is attributed to several factors: 1) a higher ratio of dielectric constant to viscosity (ϵ/η) of the mobile phase at a higher concentration of acetonitrile as Eq. 2.7 illustrates. 2)

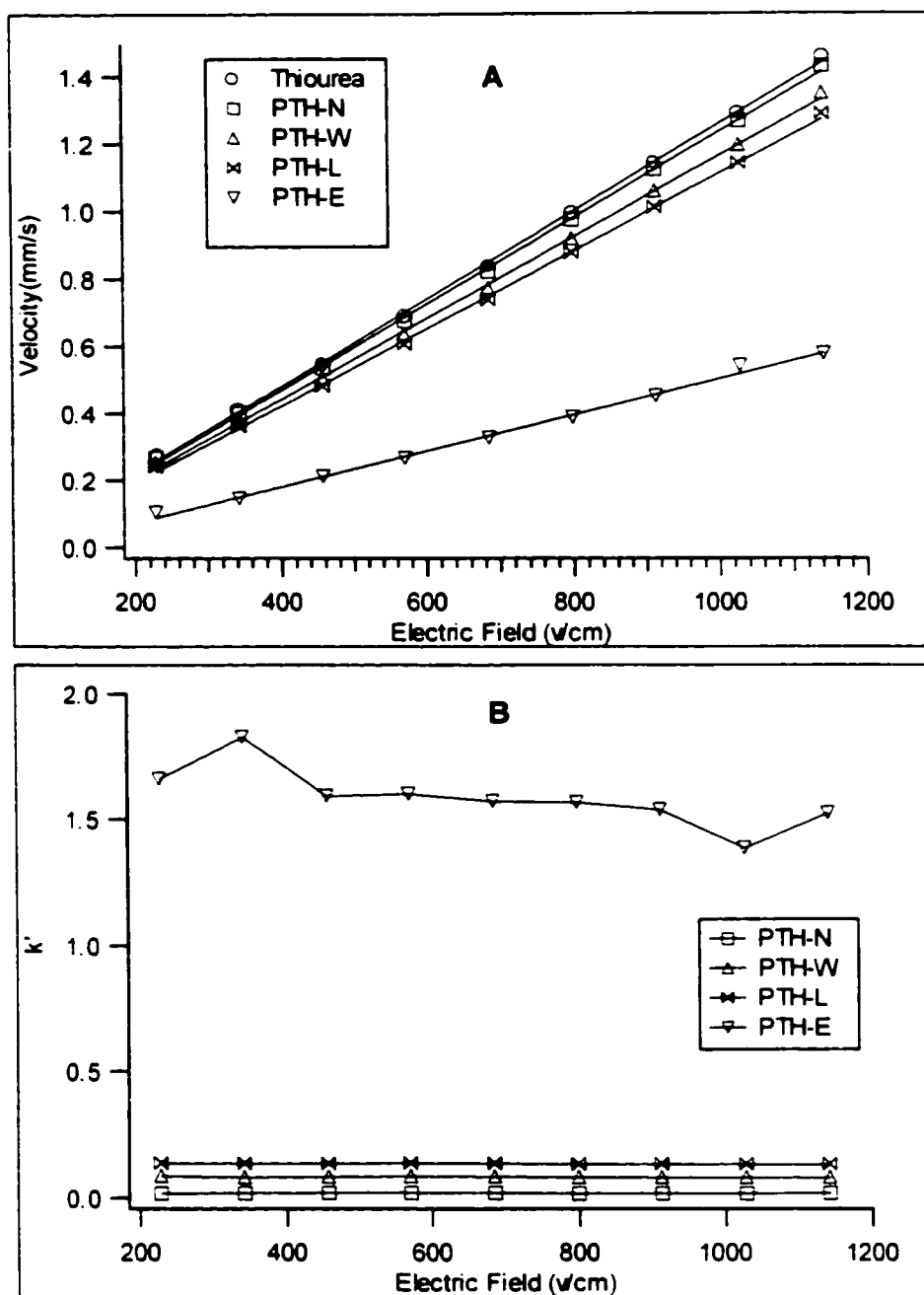


Figure 2.7 A: Plot of test compound velocity vs. electric field strength. B: Plot of retention factor vs. electric field strength. Column, 23/27.5/33.5 cm. Packing, 3 μ m Spherisorb-ODS1. Mobile Phase, Acetonitrile / 20 mM MES (20/80, v/v) (pH 7.0). Electrokinetic injection at 5 kV for 10 sec.

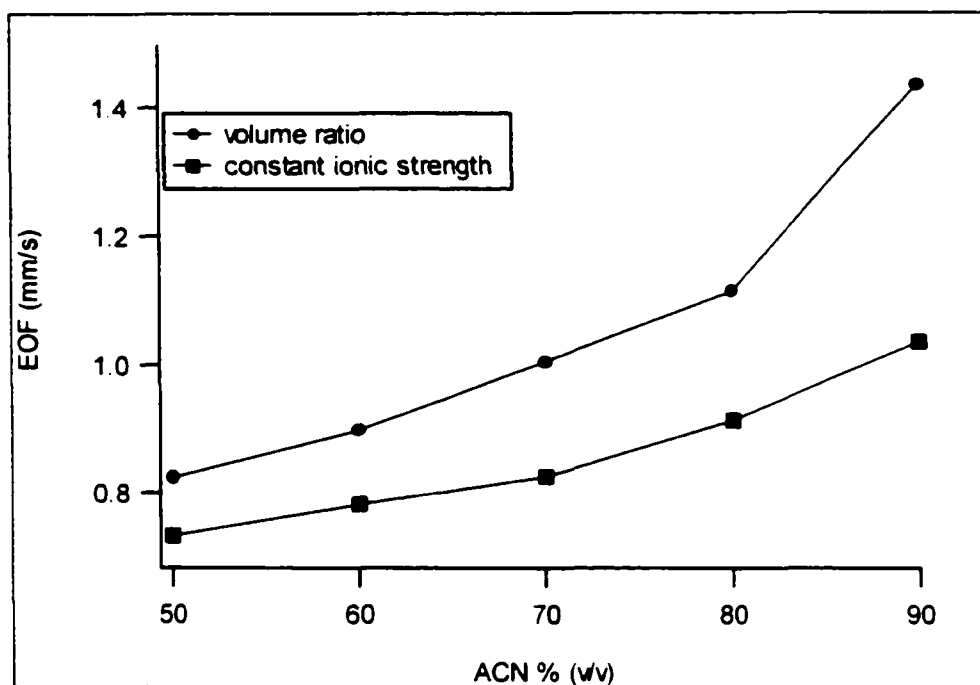


Figure 2.8 Dependence of electroosmotic flow (EOF) velocity vs. acetonitrile content (v/v) (●) with 20 mM MES, pH 7.0. (■) at constant ionic strength of 10 mM MES, pH 6.5. Marker, thiourea. Column, 22/26.5/32.5 cm. Packing, 3 μ m Spherosorb-ODS1.

a lower ionic strength of the mobile phase, which also leads to a higher EOF. The variation of electroosmotic flow was further investigated with changes of the acetonitrile content in the mobile phases while the ionic strength of buffers were kept constant. In order to obtain a constant ionic strength in the mobile phase, a MES (pH 6.3) buffer was used and kept at 10 mM. The result is also shown in Figure 2.8. When the percentage of acetonitrile was increased from 50% to 90%, electroosmotic flow increased by 41%. The above results further demonstrate the dependence of mobile phase velocity on the composition of the solvent system. In the figure at 50% acetonitrile, both mobile phase systems have the same concentration of buffers, but the EOF velocities are different

because of the pH difference in the buffer. Unstable flows in the CEC system were experienced when I attempted to use organic content mobile phase below 50%. The current was unstable and relationship between the current and the voltage applied was nonlinear. This phenomenon was also noticed by others in nonpressurized CEC mode [29], which was explained as insufficient wetting of the C18 surface on the silica with higher aqueous content buffers.

The amount of acetonitrile in the mobile phase not only alters the mobile phase pumping force but also modifies the solvent strength of the mobile phase. Solvent strength affects the separation selectivity by changing the retention factor k' of analyte. Figure 2.9 shows the separation profiles of the test mixture under various percentages of acetonitrile. As the solvent strength decreases, the resolution of the separation improves, whereas the total separation time lasts longer. The mobile phase composed of 70% acetonitrile gives an elution window of about ten minutes from the EOF marker and PTH - glutamic acid. These data provide some hint to further optimize separation conditions for a mixture of all PTH - amino acids. The peak of a charged compound, PTH-E, was not observed due to the extensive band broadening when the percentage of acetonitrile was below 60%. The relationship between the logarithmic retention factor, $\text{Log}(k')$, as a function of percentage of acetonitrile is summarized in Figure 2.10. The linear relation indicated the very similar behavior in CEC as compared to HPLC [34].

2.3.5 Effect of Buffer pH

The pH of the mobile phase plays an important role in the determination of EOF

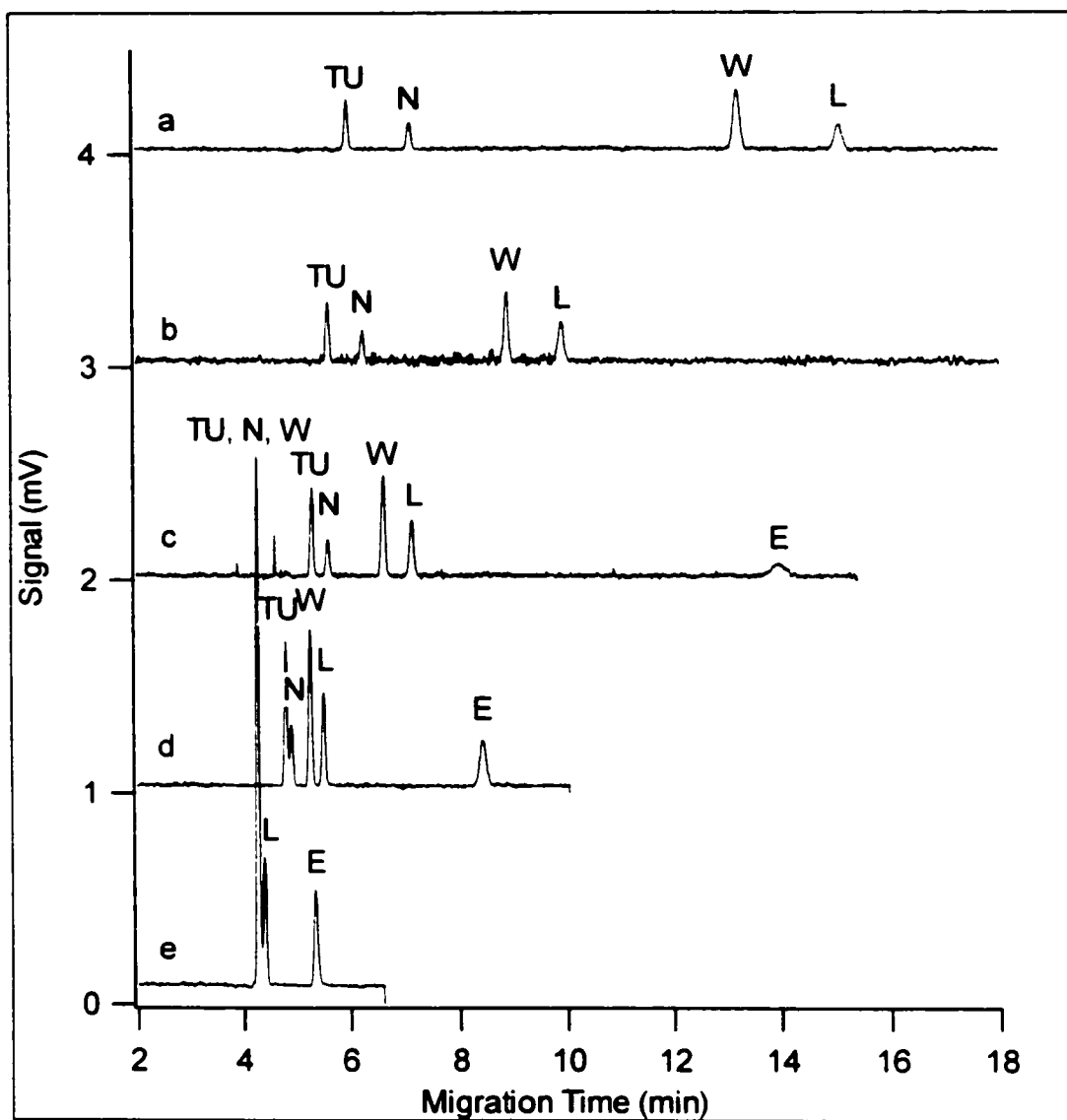


Figure 2.9 Electrochromatograms of test mixture at increasing acetonitrile content (ACN). a: 50% ACN, b: 60% ACN, c: 70% ACN, d: 80% ACN, e: 90% ACN. The ionic strength of the mobile phase was 10 mM MES at pH of 6.5. Electrokinetic injection at 5kV for 10 sec. Applied voltage 20kV. Column. 22/26.5/32.5 cm. Packing. 3 μ m Spherisorb-ODS1.

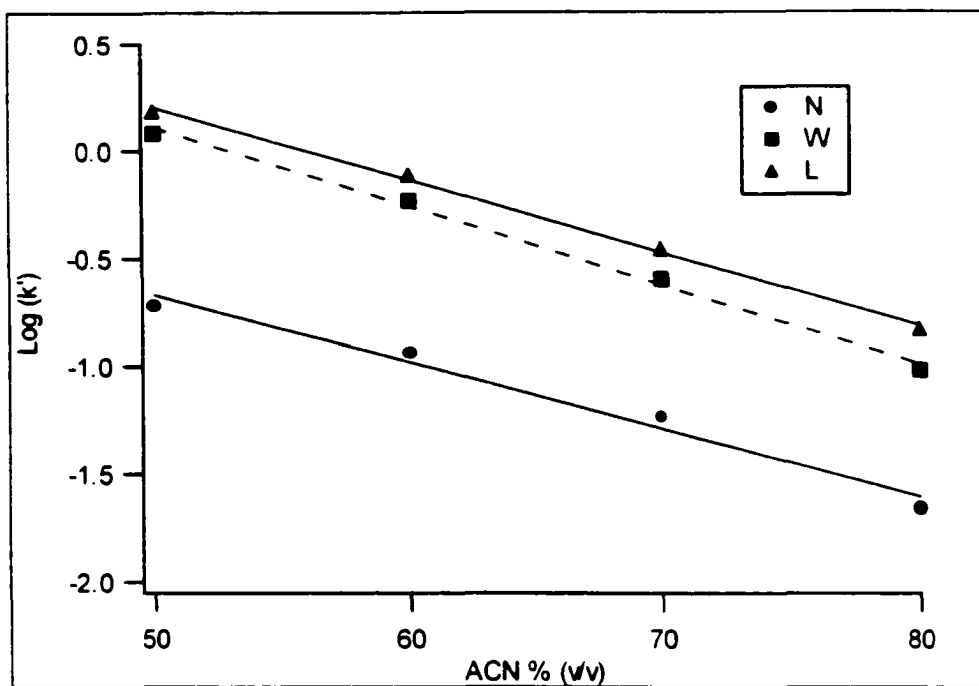


Figure 2.10 Plot of $\text{Log}(k')$ vs. acetonitrile content at constant ionic strength (10 mM MES), pH of 6.5. Electrokinetic injection at 5kV for 10 sec. Applied voltage 20kV. Column, 22/26.5/32.5 cm. Packing, 3 μm Spherisorb-ODS1.

velocity in reverse phase particle-packed CEC. Both the surfaces of the reverse phase modified silica packing and the capillary wall after silanization still possess residual silanol groups owing to steric hindrance during the reaction. These residual silanols generate a broad range of titration curves from pH 3.5 to 9 in water [35]. The presence of the anionic charges induces an electrical double layer. The influence of buffer pH on the EOF is a result of changes in the surface charge density of the double layer. As in almost all of the CEC literature published, I also refer to the apparent pH of the mobile phase mixed with organic solvent as the original buffer pH prepared in water. However, the addition of organic solvents to aqueous electrolytes can alter the ionization equilibrium, analyte solvation, and shift the pK_a values of the silanol group. The effect of organic

solvent on pK_a has been interpreted theoretically by Kenndler [35]. Due to the complication of estimating pK_a in a mixture of organic and water solvents, currently most of the researchers take the aqueous buffer pH as referred pH for the reason of simplicity.

In this study four different types of buffer system were chosen: sodium acetate (NaAc), MES, ammonium acetate, HEPES with aqueous pH values 4.5, 6.3, 6.8, 7.4, and a concentration of 10 mM in 70% acetonitrile. The chromatograms of four test compounds are shown in Figure 2.11. The separation profiles except for PTH - glutamic acid are quite similar at different pH values. The overall mobility of PTH - glutamic acid, $\mu(G)_{\text{overall}}$, consists of the electroosmotic mobility of the neutral form and the reversed electrophoretic mobility superimposed with EOF mobility for the anionic form as described in Eq. 2.10.

$$\mu(G)_{\text{overall}} = [HA]\mu_{\text{eo}} + [A^-](\mu_{\text{eo}} - \mu_{\text{ep}}) \quad (2.10)$$

where [HA] is the fraction of the neutral form, [A⁻] is the fraction of the anionic form as a result of dissociation. The EOF mobility and retention factors calculated versus pH are shown in Figure 2.12. The EOF mobility increases 20% from pH 4.5 to pH 7.4. The retention factor is relatively stable within the experimental pH range for the neutral species, which is as expected.

2.3.6 Reproducibility

2.3.6.1 Reproducibility on a Single Column

One of the major obstacles to CEC becoming a routine analytical tool is the need for reproducible performance of CEC columns. The results of the column performance in

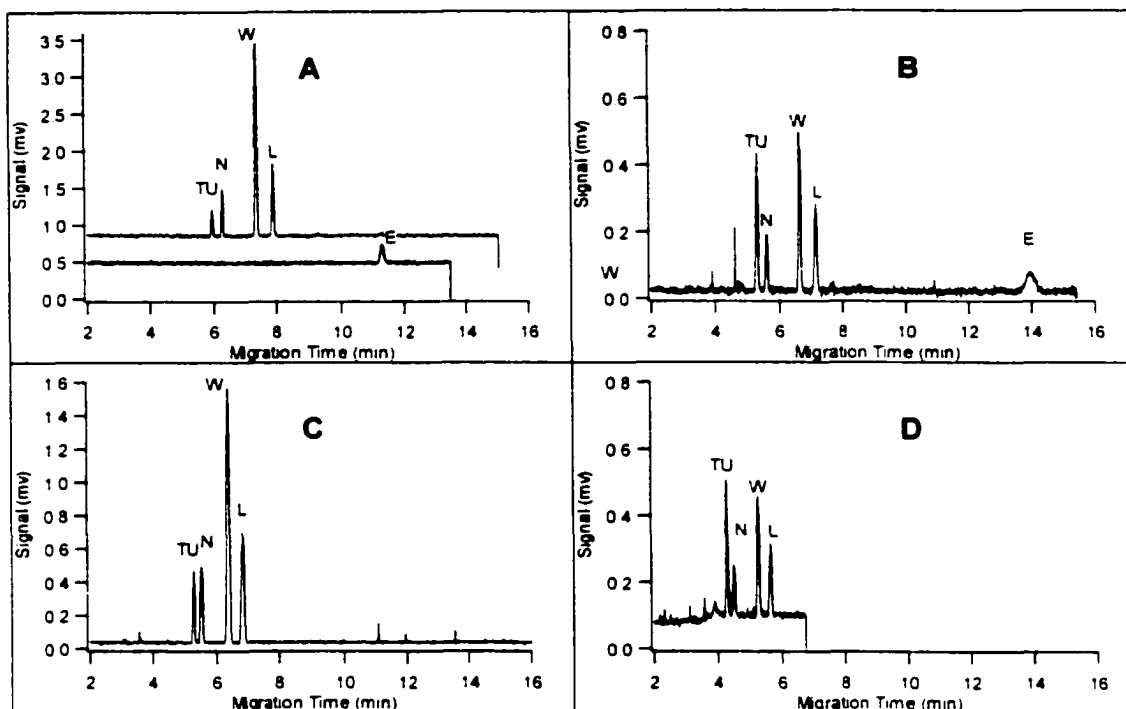


Figure 2.11 Electrochromatograms of test mixture using mobile phase containing acetonitrile / buffer at different pH values (70/30, v/v). Applied voltage 20 kV. (A) 10 mM NaAc/HAc, pH 4.5, current, 2.76 μ A (B) 10m M MES, pH 6.3 current, 1.35 μ A (C) 10 mM NH₄Ac, pH, 6.8 current, 2.76 μ A (D) 10 mM HEPES, pH 7.4 current, 1.45 μ A.

terms of retention factor (k'), theoretical plate numbers, and resolution over nine days were calculated and are summarized in Table 2.1. The relative standard deviations (RSD) of the retention factors vary from 0.6% to 5.6% for over one hundred runs on the same column. The RSD of the retention factors is less than 1.2% for all the well-resolved compounds except PTH-N, which is comparable to the reproducibility of capacity factors reported by others [19]. The middle column in Table 2.1 presents average values of the theoretical plate numbers from 60.500 plates/m for negatively charged compound PTH-E to 212.000 plates/m for the neutral marker, thiourea, along with the RSDs from 10% to

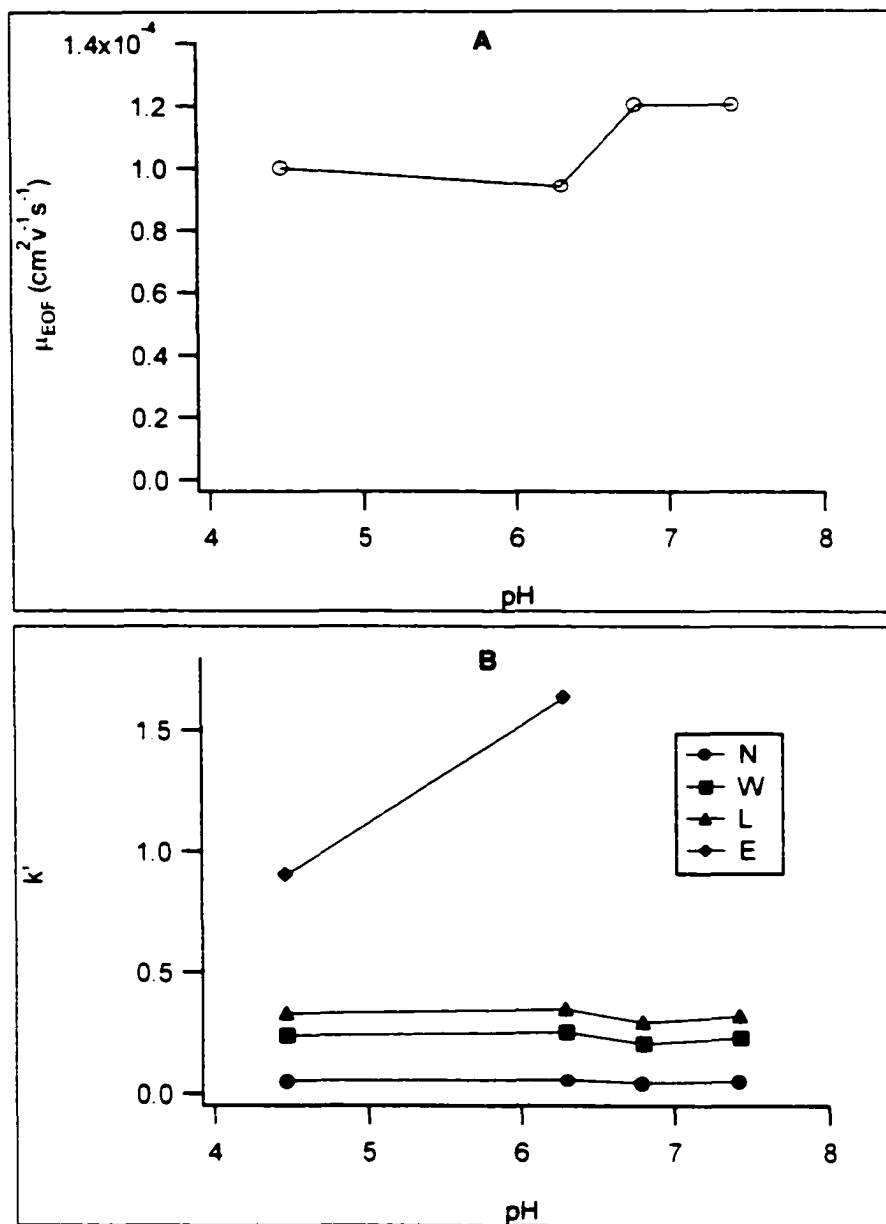


Figure 2.12 Plot of (A) electroosmotic mobility and (B) retention factor of PTH – amino acids (N, W, L, E) as a function of buffer pH. Same experimental conditions as in Figure 2.11.

4%. The results show that the reversed-phase CEC column has a higher separation efficiency for neutral compounds than charged compounds. The reproducible separations obtained using this column were further demonstrated by low RSD values (2 to 4%) of the resolution from 110 runs. The resolution was calculated from two adjacent peaks. The low RSD value indicated the column gave a long lifetime and stable performance.

A stable electroosmotic flow determines the precision in separation efficiency of a column. Therefore, electroosmotic flow is also a crucial parameter for examining the stability of a column. As described above, one column gave reproducible separations over 110 runs. The EOF stability given by this column was demonstrated by measuring the migration time of thiourea over nine days, as shown in Figure 2.13. The largest within-day RSD is less than 1%. Reproducible EOF confirms the day-to-day stable performance of the column.

Table 2.1 Average and RSD (n=110) of retention factor (k'), efficiency (N), and resolution (R) on a single column.

Solute	k'		N (plates/m)		R	
	AVG	RSD(%)	AVG	RSD(%)	AVG	RSD(%)
Thiourea	–	–	213 000	3.7	0.79	2.0
PTH-N	0.018	5.6	178 000	6.8	2.18	2.6
PTH-W	0.081	1.2	107 000	5.9	1.53	2.2
PTH-L	0.132	0.8	115 000	4.2	20.2	3.8
PTH-E	1.515	0.6	60 000	10		

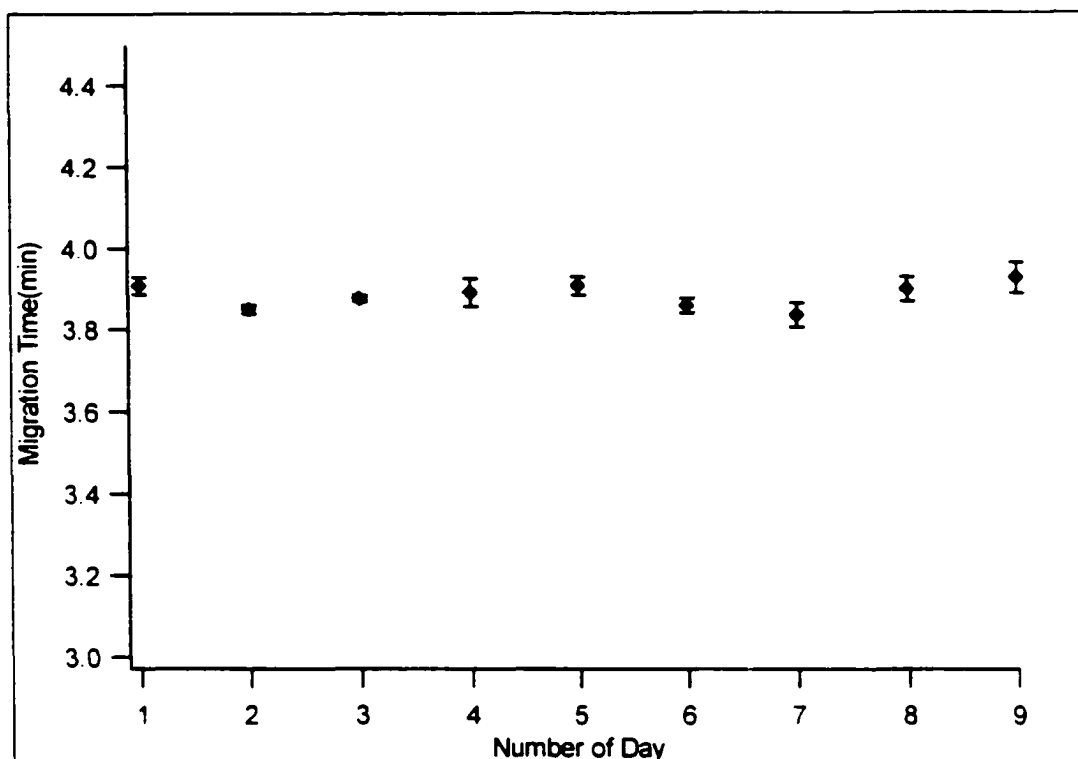


Figure 2.13 Migration time stability of electroosmotic flow marker (thiourea) and its RSD over nine days. Column, 22/26.5/32.5 cm. Packing, 3 μ m Spheresorb-ODS1. Electrokinetic injection at 5kV for 10 sec. Applied voltage 20 kV.

2.3.6.2 Reproducibility from column to column

The reproducibility of the packing procedure was evaluated via the variation in performance from column to column. Five columns were packed with the same slurry concentration and procedure, but were made at different times and in different batches. The performance of each column was evaluated by separating the same test mixture with a buffer of 20 mM MES (pH 7.0) / acetonitrile (20/80, v/v). Migration times, theoretical plate numbers, and resolutions were calculated over six runs for each column. Figure 2.14 shows (A) mean and RSD of migration times and (B) theoretical plate numbers for

thiourea, PTH-L, and PTH-W obtained from the five columns. Figure 2.14 demonstrates the reproducible separations of the test compounds using different columns and confirms that the packing procedure is reproducible. The slightly lower efficiency shown by Columns 2 to 5 might be due to a long time storage of the column in water while over one hundred runs were carried out on Column 1. Reproducible resolutions between adjacent peaks were also obtained and are shown in Figure. 2.14 C.

2.3.7 Applications of CEC – TOAD

2.3.7.1 Analysis of Polycyclic Aromatic Hydrocarbons (PAHs)

PAHs are produced by combustion of fossil fuels and found in automobile exhausts. PAHs can also be produced by the processes of pyrolysis and pyrothesis found in industry. Because these compounds are mutagenic, carcinogenic and resistant to bacterial degradation, they are considered as priority environmental pollutants by the environmental protection agency (EPA). These pollutants are found in air, water, soil, and animal tissue. The routine analytical methods have already been established. Gas chromatography with flame ionization detection or mass detection is the most widely used analytical methods. HPLC with fluorescence detection and micellar electrokinetic electrochromatography for PAH analysis have also been demonstrated [36-38]. HPLC and MEKC are more suitable for analysis of thermally labile and nonvolatile PAHs while GC is useful to separate small and volatile ones. The analysis of PAHs by capillary electrophoresis with thermo-optical detection will be described in Chapter 5. The molecular structures of the analytes are shown in Figure 2.15. They are listed in the order

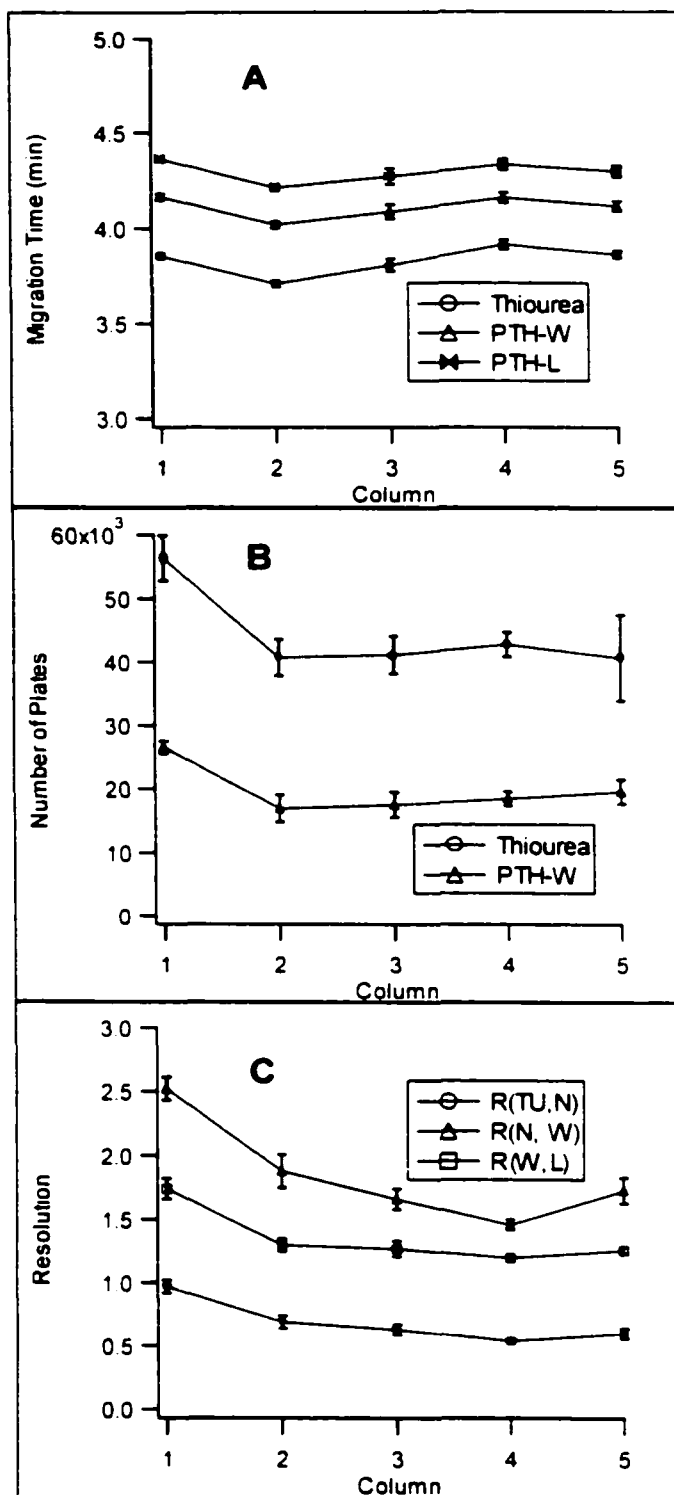


Figure 2.14 Reproducibility of migration time (A), plate height (B), and resolution (C) on five columns. Each data point was calculated from 6 runs on each column.

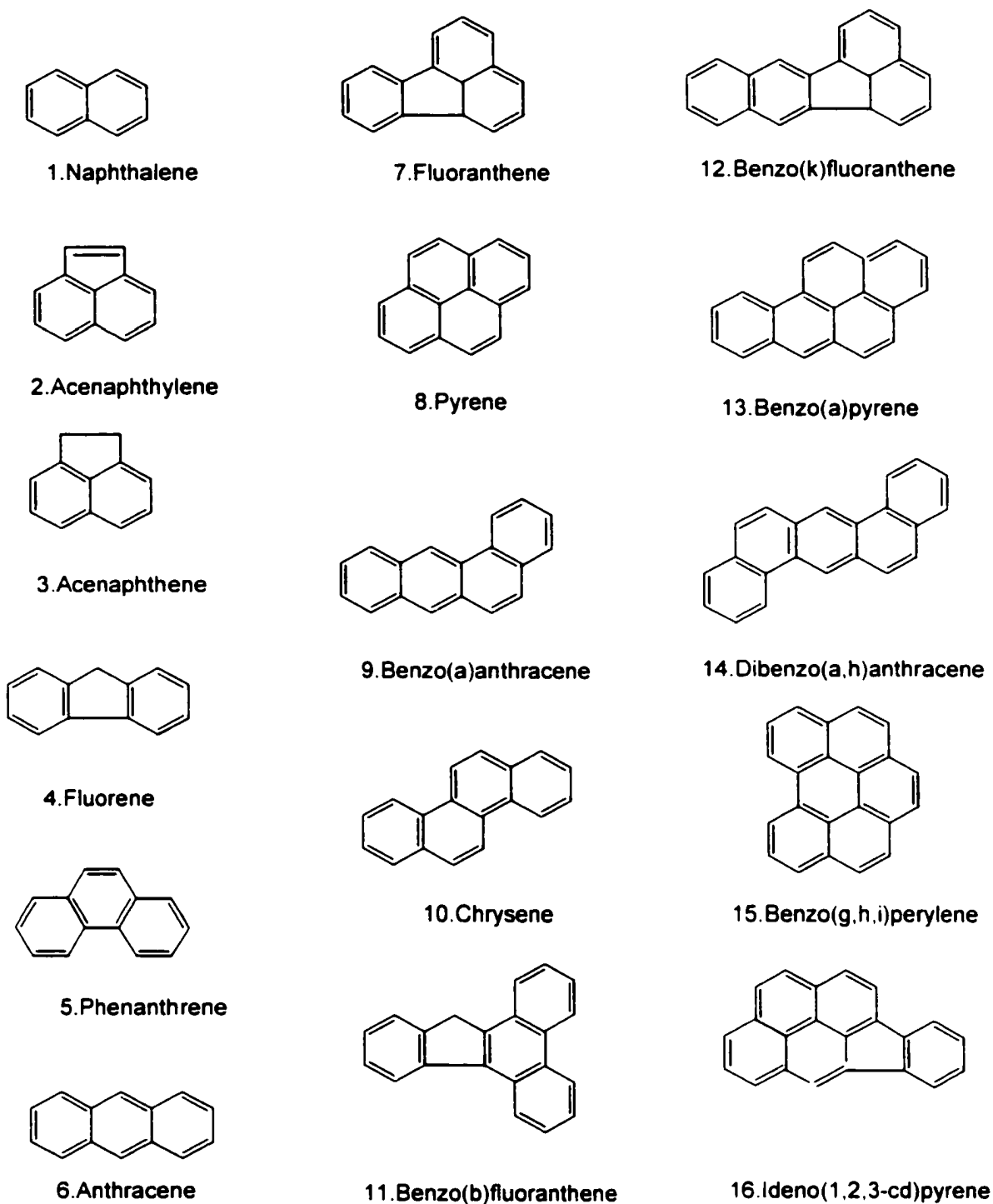


Figure 2.15 Molecular structures of 16 EPA priority pollutants: polycyclic aromatic hydrocarbons.

of hydrophobicity from low to high.

A good quality C18 packing can produce baseline resolution of 16 PAHs. Chao *et al.* [39] published a CEC separation of PAHs using electroosmotic pumping gradient elution and on-column fluorescence detection by 3 μm C18 material. Recently, fast and efficient analysis of seven PAHs in 1 min was performed by using 1.5 μm particles [40]. The theoretical plates reported were around 100,000 to 200,000 plates/m from most publications. I also chose PAHs as model compounds to evaluate the quality of home-made columns. Figure 2.16 shows the chromatogram of 16 PAHs on my CEC column. The dimension of the column was 22 cm packed with 3 μm Supelco C18 reverse phase particles and total length of 33 cm. The migration time and number of theoretical plates are listed in Table 2.2. The maximum number of theoretical plates was over 100,000. 14 compounds were well separated but two compounds, chrycene and benzo(a)anthracene, coelute as a single peak. Both selectivity and separation speed are similar to the results reported for commercial CEC columns [41]. In Figure 2.16 the first peak with the highest intensity was generated by the benzene solvent contained in the commercial PAH standard mixture. Compared to the capillary electrophoretic separation method developed previously [37], CEC produced higher selectivity but lower theoretical plates. Three pairs of isomers, acenaphthylene and acenaphthene, phenanthrene and anthracene, chrycene and benzo(a)anthracene, could not be resolved by CE. By using a longer packed CEC column or reducing the acetonitrile to 70% in the mobile phase, I observed that CEC was able to resolve chrycene and benzo(a)fluoranthrene (data not shown).

In order to estimate the limit of detection (LOD) for PAH compounds by the CEC/TOAD system, a serial dilution of mixture compounds was prepared and subjected

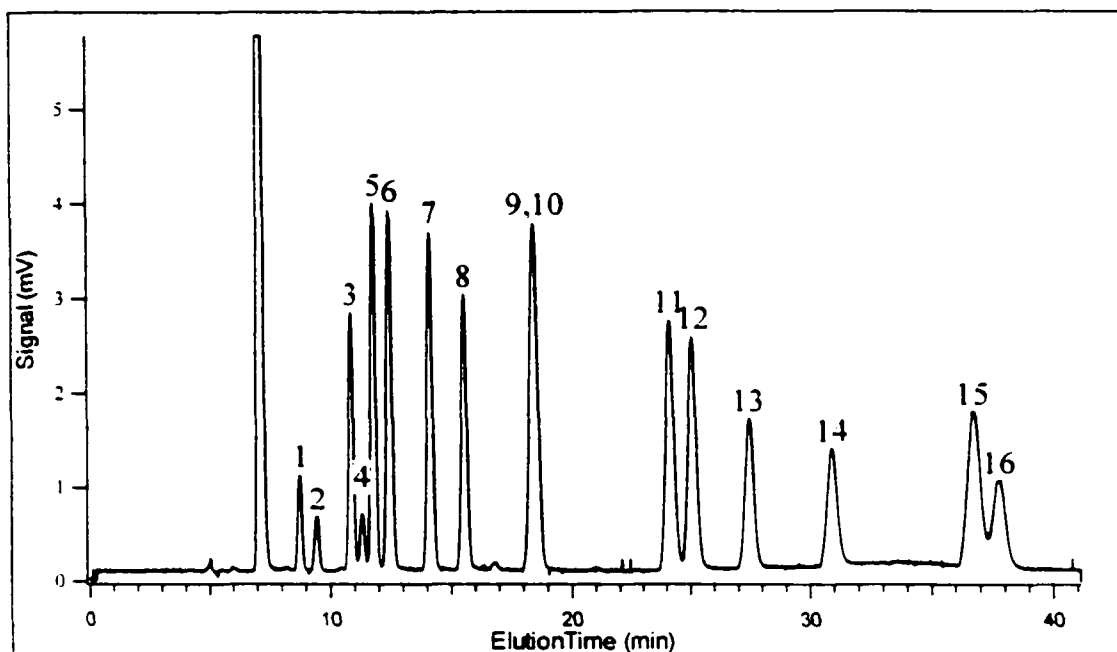


Figure 2.16 Electrochromatogram of 16 polycyclic aromatic hydrocarbons. Column, 22cm/28cm/34cm. Packing, Supelcosil 3 μm ODS. Mobile phase: Acetonitrile / 20 mM MES with pH 7.2 (80/20, v/v). Electrokinetic injection at 10 kV for 10 sec. Applied voltage, 20 kV. Current, 0.85 μA . Concentration of each component was 25 ppm.

to the same method on the same day. Figure 2.17 shows the results. The profiles of the separations look quite similar, though the migration time of each compound at different concentration varies within a certain range, which is partially due to different acetonitrile concentrations introduced during sample preparation. Sample over-loading at a concentration of 40 ppm caused a “fronting” type peak shape for all of the species. The limit of detection of each PAH was estimated from the result at lowest concentration. The LOD (3σ) for the most sensitive compound, anthracene, was 43 ppb, and for the least sensitive compound, fluorene, was 210 ppb.

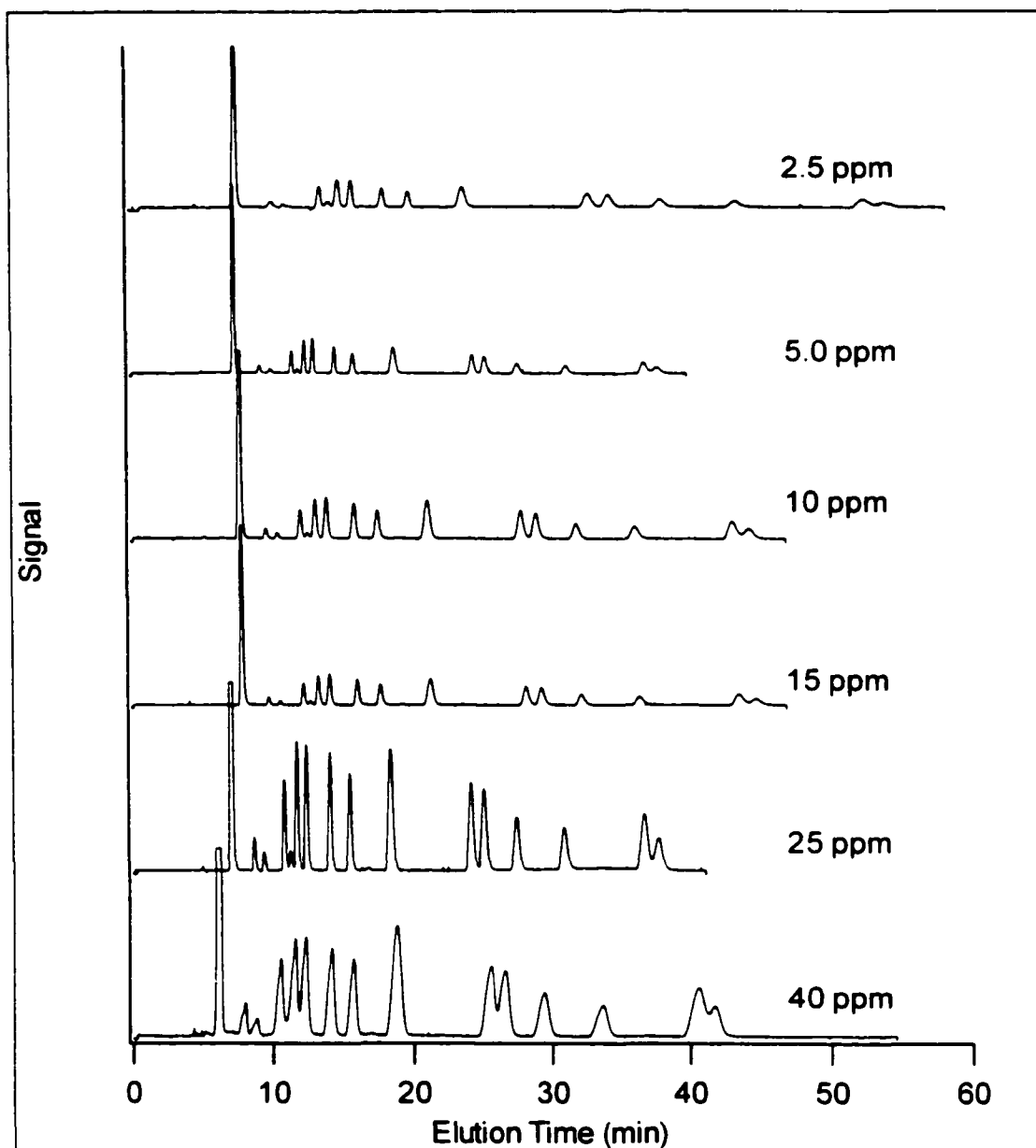


Figure 2.17 Electrochromatograms of polycyclic aromatic hydrocarbons at different sample concentrations as indicated. Column, 22cm/28cm/34cm. Packing, Supelcosil 3 μ m ODS. Mobile phase: Acetonitrile / 20 mM MES with pH 7.2 (80/20, v/v). Electrokinetic injection at 10 kV for 10 sec. Applied voltage, 20 kV.

Table 2.2 Data of migration time and plate count for each polycyclic aromatic hydrocarbon

Peak	PAH	CEC(22/33cm)		CE(35/40cm)
		t_m	Plates/m	Plates/m
1	Naphthalene	8.745	5.5E+04	2.3E+05
2	Acenaphthylene	9.435	6.3E+04	2.9E+05
3	Acenaphthene	10.855	6.7E+04	
4	Fluorene	11.305	7.7E+04	2.8E+05
5	Phenanthrene	11.765	7.2E+04	2.3E+05
6	Anthracene	12.445	7.0E+04	
7	Fluoranthene	14.125	8.4E+04	3.0E+05
8	Pyrene	15.545	9.4E+04	
9	Chrysene	18.445	6.4E+04	
10	Benz(a)anthracene	18.445		2.6E+05
11	Benzo(b)fluoranthrene	24.145	1.1E+05	1.4E+05
12	Benzo(k)fluoranthrene	25.085	1.1E+05	
13	Benzo(a)pyrene	27.455	1.2E+05	3.1E+05
14	Dibenzo(a,h)anthracene	30.895	1.0E+05	2.6E+05
15	Benzo(g,h,i)perylene	36.765	1.0E+05	2.3E+05
16	Indeno(1,2,3-c,d)pyrene	37.785	1.1E+05	2.7E+05

2.3.7.2 Analysis of Phenylthiohydantoin Amino Acids

The development of the CEC/TOAD method for analysis of PTH-AAs is a long-term effort by Dovichi's group. The previous accomplishments in this project include the 1) development of a micellar electrochromatography method to successfully resolve nineteen phenylthiohydantoin-amino acid derivatives produced by the Edman

degradation reaction [42-43]. 2) construction of a thermo-optical UV absorbance system and detection scheme adapted to on-column detection for capillary electrophoresis [44]. 3) design of various protein sequencing micro-reactors by using capillary and Teflon block with semi-automatic controlling programs [45-47].

The goals in using the CEC method for analyzing the PTH - amino acids was 1) to innovate a new capillary-scaled separation method for this group of compounds. 2) to provide more reproducible migration time and higher sensitivity. To make the problem less complicated, I first selected four of the amino acid derivatives as a test mixture: PTH - asparagine, PTH - tryptophan, PTH - leucine, and PTH - glutamic acid to stand for basic, neutral aromatic, neutral aliphatic, and acidic types of PTH amino acid derivatives. My strategy was to vary the types of buffer, buffer concentration, buffer pH, and organic solvent content in the mobile phase to tune the selectivity of the separation system. After a reasonable retention window had been found, the separation conditions were further optimized by separating the 19 PTH-AA standards. It is worthwhile to discuss some of the observations obtained from the optimization of the separation of 19 PTH - amino acid derivatives.

Compared to the class of polycyclic aromatic hydrocarbons analyzed previously, the PTH-AAs are less hydrophobic but fall in a large range of chemical properties because of the hydrophilic heterocyclic component in all of the molecules and the diversity of amino acid residues. Figure 2.18 shows the chromatograms of PTH-AAs and two other protein sequencing by-products, DMPTU, and DPTU, in 10 mM MES (pH 6.3) and 10 mM sodium acetate (pH 4.5) with 70%, 60%, and 55% ACN. Lower acetonitrile concentration in the buffer resulted in a longer retention window and better resolution.

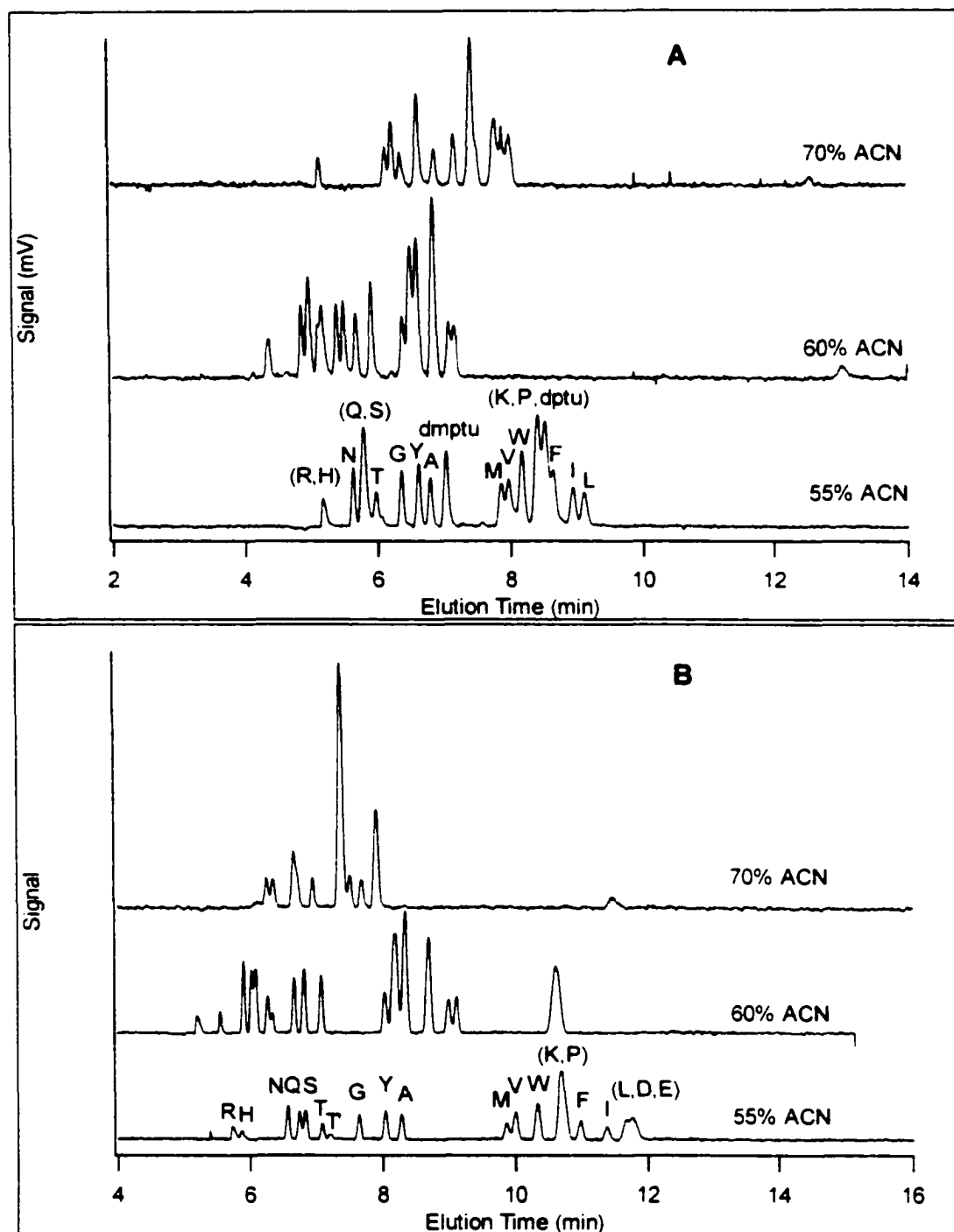


Figure 2.18 Electrochromatograms of phenylthiohydantoin amino acids by CEC. (A) Mobile phase, 10 mM MES, pH 6.3. Column, 22 cm/28 cm/34 cm. (B) Mobile phase, 10 mM NaAC/HAc, pH 4.5. column, 25 cm/30 cm/35 cm. The acetonitrile content (v/v) is as indicated. Packing, 3 μ m Spherosorb-ODS1.

The late-eluting peaks were not resolved for either buffer system. With MES having higher pH, reducing the acetonitrile concentration caused the two acidic amino acid derivatives, E and D, to have stronger reversed electrophoretic mobility and the compounds did not show up in the chromatograms.

In a sodium acetate / acetic acid buffer system, decreasing the acetonitrile concentration made the solvent system more acidic, which produced less dissociation for the two derivatives, therefore resulting in shorter retention times. The chromatograms from different buffer systems at the same organic concentration also show that the retention order and resolution for aliphatic and aromatic amino acid derivatives (G, Y, A, V, W, F, I, L) including T, M were less affected by the pH change.

From the trend of resolution improvement by reducing the concentration of acetonitrile, it was easy to think about lowering the acetonitrile concentration to the minimum which was still able to produce stable EOF. Figure 2.19 shows the chromatogram generated from mobile phase containing 50% acetonitrile. Unfortunately, the resolution between Y and A, V and W degraded. Fine tuning the retention factors was also adjusted by adding 5% to 10 % methanol as a modifier in the mobile phase, because methanol slows the EOF and can alter the solubility of the analytes in the mobile phase. Unfortunately, no improvement in the resolution was observed (data not shown).

As discussed previously, the pH of the buffer did not play a critical role in modifying the retention of most neutral PTH-AAs. The next strategy of optimization was to modify the buffer concentration in the mobile phase by using low pH buffer, a sodium acetate / acetic acid system, with pH of 4.5. Figure 2.20 shows the buffer concentration effect on the separation profile. For the neutral PTH compounds, buffer at higher

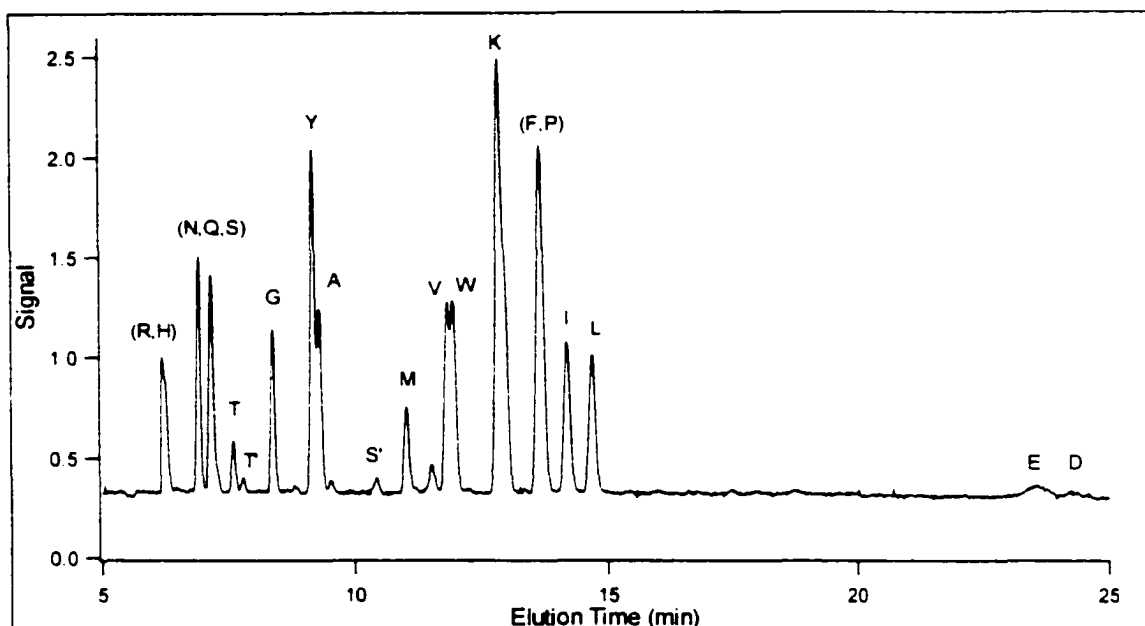


Figure 2.19 Electrochromatogram of 19 Phenylthiohydantoin amino acids. Mobile phase, 10 mM MES, pH 6.3, 50% acetonitrile. Column, 22 cm/28 cm/34 cm. Packing, 3 μ m Spherosorb-ODS1.

concentration produced a wider retention window that resulted in better resolution from 10 mM to 20 mM. However, the mobile phase with 30 mM buffer produced a high electrical current, 4 μ A. The Joule heating and risk of consequent bubble formation prohibited further increase of the buffer concentration. Figure 2.21 demonstrates the separation the 19 PTH-AAs by my optimizing procedure. Fifteen amino acid derivatives were separated within 16 min, only proline and lysine coeluted. Glutamic acid and aspartic acid coeluted at a retention time of 20 min. It was observed that the elution order of proline was susceptible to the buffer condition, and it could be coeluted with one of the three compounds with closest retention, lysine (K), phenylalanine (F), and isoleucine (I) under slightly different conditions. This sensitivity may be caused by the pK_b of the basic

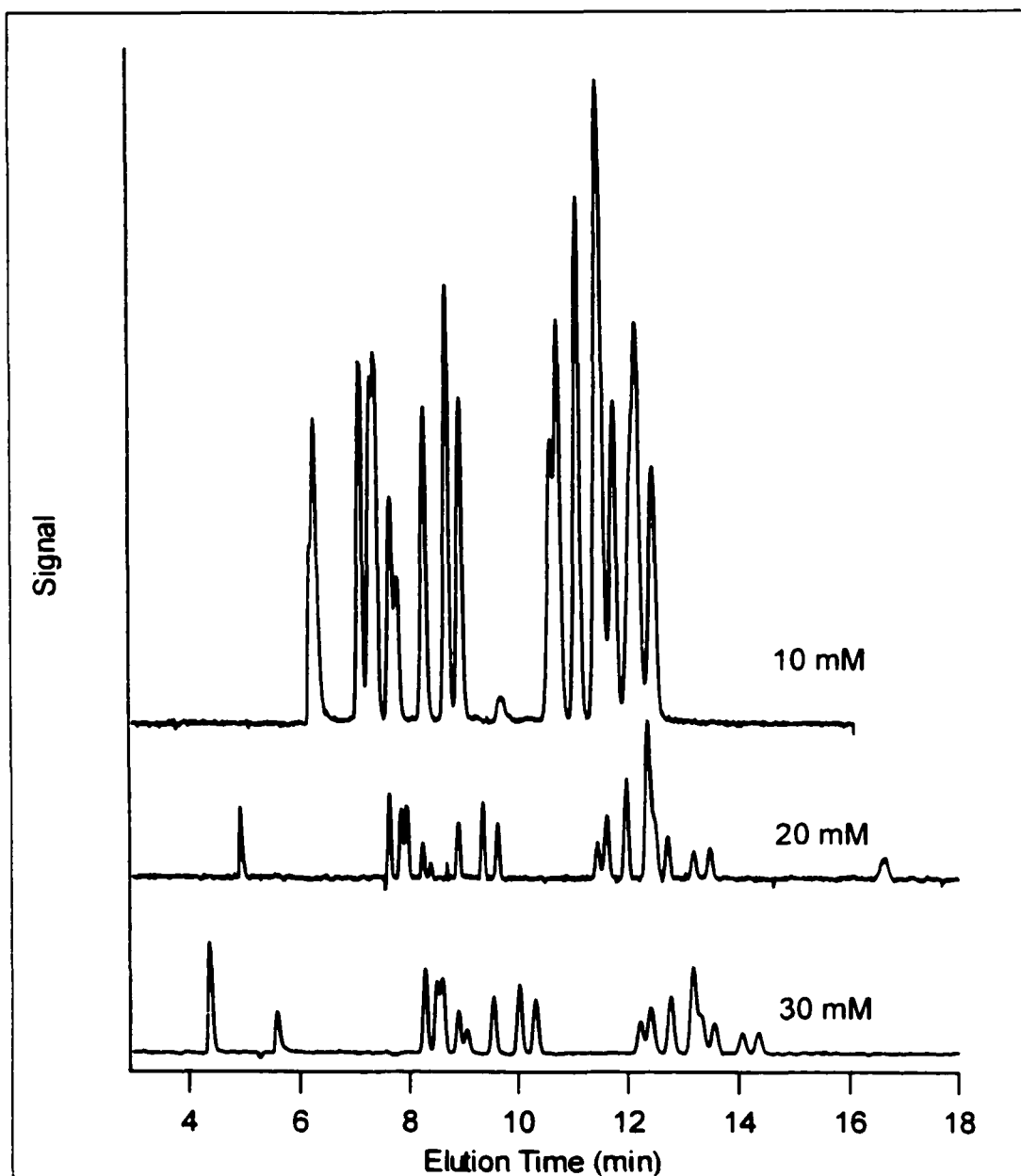


Figure 2.20 Electrochromatograms of 19 phenylthiohydantoin amino acids using buffers with different concentrations as indicated. Column, 25 cm/29 cm/34 cm. Packing: 3 μm Sphersorb-ODS1. Mobile phase: NaAc/HAc buffer system, pH 4.4, 55% acetonitrile.

functional group of proline, which falls within the pH range of the mobile phases. Although the optimized methodology is not sufficient for analysis of 19 PTH - amino acids with one sample injection, effective identification of PTH-K or PTH-P, and PTH-E or PTH-D could be done by use of another buffer pH.

The application of CEC in analysis of testosterone metabolites is described in Chapter 5.

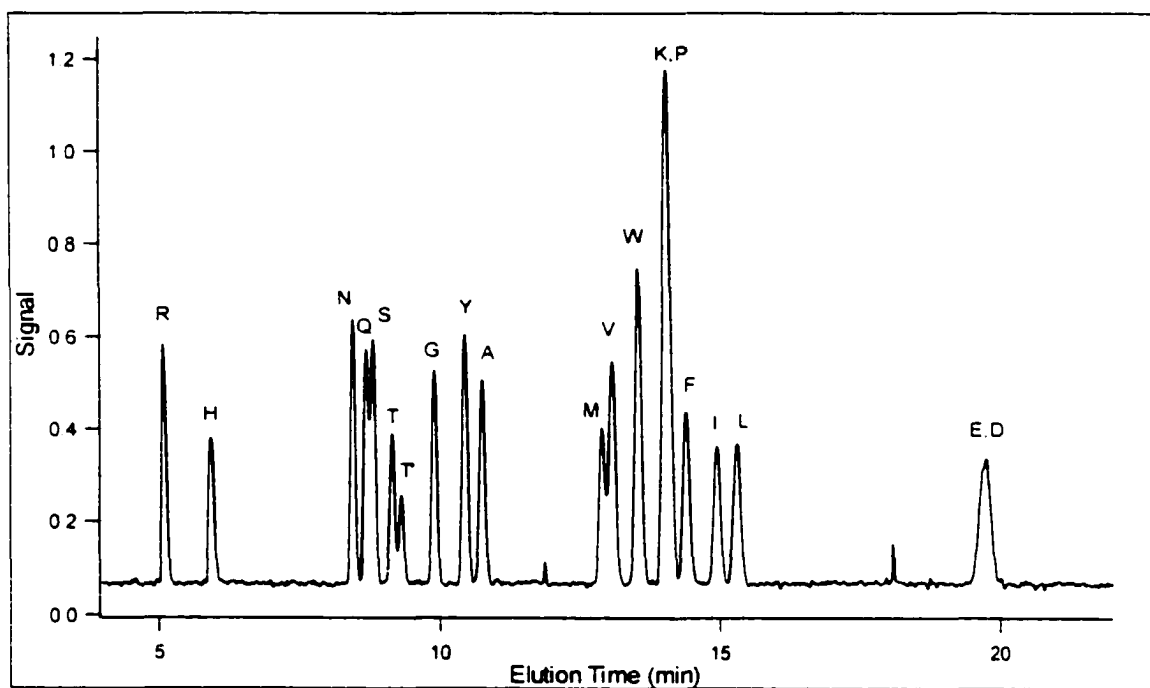


Figure 2.21 Electrochromatogram of 19 phenylthiohydantoin amino acids. Column, 27 cm/31 cm/36 cm. Packing, 3 μ m Spherisorb-ODS1. Electrokinetic injection at 15 kV for 10 sec. Mobile phase, 20 mM sodium acetate/acetic acid with pH 4.4, 55% acetonitrile.

2.3.8 Photothermal Absorbance Detection

Photothermal absorbance techniques are well-established methods for the determination of small absorbance values. In these methods, non-radiative relaxation following absorbance of a laser beam produces a temperature rise within a sample. This temperature rise is proportional to both laser power and absorbance and induces a refractive index change within the sample. If a chopped or pulsed excitation laser beam is used, then the periodic change in refractive index can be detected with high precision by use of a phase-sensitive detector.

Nolan *et al.* [48] developed a thermo-optical absorbance detector for micrometer capillaries. A modulated pump laser beam periodically illuminates the sample at a point near the exit of the capillary. Complicated deflection and diffraction effects occur at the capillary–solution interface. Perturbation of the refractive index at the interface changes the intensity of the probe beam, measured after the capillary with a small photodiode.

Dovich's group introduced the use of photothermal absorbance detection in the analysis of PTH - amino acids. Waldron and Dovich reported detection limits (3σ) for most amino acids ranged from 1 to 10 μM [42]. The sensitivity of the photothermal signal depends on the thermal-optical constants for the solvents. Aqueous solvents have poor sensitivity because of the low change in refractive index with temperature in water. Addition of organic solvents often improves detection limits in photothermal absorbance measurements.

The detection limits (3σ) for the 13 resolved PTH - amino acids are listed in Table 2.3. Detection limits ranged from 1.6 to 4.8×10^{-7} M, which are factors of 2 to 10 superior to the detection limits reported for micellar electrokinetic chromatography [42]. Most of this improvement in detection limit is due to the higher acetonitrile content of the

buffer compared to the aqueous buffer used in micelle electrokinetic separations. This enhanced sensitivity should be valuable in sequencing trace amounts of proteins.

Table 2.3 LODs of 13 resolved PTH - amino acids using CEC and MEKC with TOAD.

Amino Acid	CEC (μM)	MEKC^b (μM)
Alanine (A)	0.3	1.0
Asparagine (N)	0.3	1.0
Serine (S)	0.3	3
Glutamine (Q)	0.3	1.1
Glycine (G)	0.3	0.9
Isoleucine (I)	0.3	2
PTH α , ϵ -PTC lysine (K)	0.2	0.6
Leucine (L)	0.4	0.8
Methionine (M)	0.4	1.0
Threonine (T)	0.5	12
Tyrosine (Y)	0.3	0.7
Tryptophan (W)	0.2	0.5
Valine (V)	0.3	0.8

^b: Ref. 42

2.4 CONCLUSIONS

In Chapter 2, I describe a simplified slurry packing procedure to prepare 50 μm i.d., 180 μm o.d. CEC columns packed with 3 μm reversed-phase materials. By protecting the

outlet frit with a Teflon tube sleeve, the column rigidity and lifetime was greatly increased. Reproducible performance was obtained on the columns produced by the packing procedure. The influence of buffer concentration, pH, acetonitrile concentration on electroosmotic flow velocity, and selectivity of phenylthiohydantoin amino acids was studied. I also developed capillary electrochromatography for analysis of polycyclic aromatic hydrocarbons and phenylthiohydantoin amino acids by optimizing the separation conditions. The selectivity of polycyclic aromatic hydrocarbons by reversed-phase capillary columns shows an improvement compared to capillary electrophoresis. The on-column detection system of thermo-optic UV absorbance coupled to CEC shows up to 10-fold enhancement in limits of detection for PTH - amino acids compared to a previous separation by the micellar electrokinetic chromatography method.

REFERENCES

1. Dittmann, M. M.; Wienand, K.; Bek, F.; Rosing, G. P. *LC-GC* 1995, 13, 800.
2. Wen, E.; Asiaie, R.; Horváth, Cs. *J. Chromatogr. A* 1999, 855, 349.
3. Frame, L. A.; Robinson, M. L.; Lough, W. J. *J. Chromatogr. A* 1998, 798, 243.
4. Rebscher, H.; Pyell, U. *Chromatographia* 1996, 42, 171.
5. Behnke, B.; Grom, E.; Bayer, E. *J. Chromatogr. A*, 1995, 716, 207.
6. Smith, N. J.; Evans, M. B. *Chromatographia* 1994, 38, 694.
7. Yamamoto, H.; Baumann, J.; Erni, F. *J. Chromatogr.* 1992, 593, 313.
8. Takeuchi, T.; Ishii, D.; Nakanishi, A. *J. Chromatogr.* 1984, 285, 97.
9. Gluckman, J. C.; Hirose, A.; McGuffinn, V. L.; Novotny, M. *Chromatographia* 1983, 17, 303.
10. Yan, C. Electrokinetic Packing of Capillary Columns, *US Pat* 5453163, 1995.
11. Stol, R.; Mazereeuw, M.; Tjaden, U. R.; van der Greef, F. *J. Chromatogr. A* 2000, 873, 293.
12. Xin, B.; Lee, M. L. *Electrophoresis* 1999, 20, 67.
13. Robson, M. M.; Roulin, S.; Shariff, S. M.; Raynor, M.W.; Bartle, K. D.; Clifford, A. A.; Myers, P.; Euerby, M. R.; Johnson, C. M. *Chromatographia* 1996, 43, 313.
14. Koivisto, P.; Danielsson, R.; Markides, K. E. *J. Micro. Sep.* 1997, 9, 97.
15. Vissers, J. P. C.; Claessens, H. A.; Laven, J.; Cramers, C. A. *Anal. Chem.* 1995, 67, 2103.
16. Kennedy, R. T.; Jorgenson, J. M. *Anal. Chem.* 1989, 61, 1128.
17. Chen, J.; Dulay, M. T.; Zare, R.; Svec, F.; Peters, E. *Anal. Chem.* 2000, 72, 1224.
18. Boughtflower, R. J.; Underwood, T.; Paterson, C. J. *Chromatographia* 1994, 40,

- 329.
19. Dulay, M. T.; Yan, C.; Rakestraw, D. J.; Zare, R. N. *J. Chromatogr. A* 1996, 725, 361.
 20. Smith, N. J.; Evans, M. B. *Chromatographia* 1995, 41, 197.
 21. Euerby, M. R.; Johnson, C. M.; Bartle, K. R. *LC-GC* 1998, 16, 386.
 22. Angus, P. D. A.; Victorino, E.; Payne, K. M.; Demarest, C. W.; Catalano, T.; Stobaugh, J. F. *Electrophoresis* 1998, 19, 2073.
 23. Lurie, I. S.; Meyers, R. P.; Conner, T. S. *Anal. Chem.* 1998, 70, 3260.
 24. Sander, L. C.; Pursch, M.; Marker, B.; Wise, S. A. *Anal. Chem.* 1999, 71, 3477.
 25. Lim, J.; Zare, R. N.; Bailey, C. G.; Rakestraw, D. J.; Yan, C. *Electrophoresis* 2000, 21, 737.
 26. Thiam, S.; Shamsi, S. A.; Henry III, C. W.; Robinsin, J. W.; Warner, I. M. *Anal. Chem.* 2000, 72, 2541.
 27. Huber, C. G.; Choudhary, G.; Horváth, Cs. *Anal. Chem.* 1997, 69, 4429.
 28. Lottspeich, F. *J. Chromatogr.* 1985, 326, 321.
 29. Rebscher, H.; Pyell, U. *Chromatographia* 1994, 38, 737.
 30. Yang, F. J. *J. Chromatogr.* 1982, 236, 265.
 31. Hunter, R. J. in: *Zeta Potential in Colloid Science*, Academic Press, London, 1982, pp 61.
 32. Rathore, A. S.; Horváth, Cs. *J. Chromatogr. A* 1996, 743, 231.
 33. Knox, J. H.; Grant, I. *Chromatographia* 1991, 32, 317.
 34. Nyholm, L. in: High-Temperature Reverse-Phase Liquid Chromatography in Open Tubular Columns. *Comprehensive Summaries of Uppsala Dissertations from the*

Faculty of Science and Technology 230. Acta Univ. Ups 1996, pp 8.

35. Guzman, R. A. *Capillary Electrophoresis Technology*. Marcel Dekker. Inc. New York, 1993.
36. Furton, K. G.; Jolly, E.; Pentzke, G. Review, *J. Chromatogr. A* 1993, 642, 33.
37. Ren, H.; Li, X. F.; Qi, M.; Stathakis, C.; Dovichi, N.J. *J. Chromatogr. A* 1998, 817, 307.
38. Zlotorzynska, E. D.; Lai, E. P. C. *J. Cap. Elec.* 1996, 1, 31.
39. Yan, C.; Dadoo, R.; Zhao, H.; Zare, R. H.; Rakestraw, D. J. *J. Anal. Chem.* 1995, 67, 2026.
40. Yan, C.; Dadoo, R.; Zare, R. N.; Rakestraw, D. J.; Anex, D. *Capillary Electrochromatography for Environmental Analysis*. Presented at Pittcon'96, Chicago, IL, March 3-8, 1996.
41. Dadoo, R.; Yan, C.; Zare, R. N.; Anex, D. S.; Rakestraw, D. J.; Hux, G. A. *LC-GC* 1997, 15, 630.
42. Waldron, K. C.; Dovichi, N. J. *J. Anal. Chem.* 1992, 64, 1396.
43. Chen, M.; Waldron, K. C.; Zhao, Y. W.; Dovichi, N. J. *Electrophoresis* 1994, 15, 1290.
44. Dovichi, N. J. *Prog. Anal. Spectros.* 1988, 11, 179.
45. Waldron, K. C.; Li, X. F.; Chen, M.; Ireland, I.; Lewis, D.; Carpenter, M.; Dovichi, N. J. *Talanta* 1997, 44, 383.
46. Li, X. F.; Waldron, K. C.; Black, J.; Lewis, D.; Ireland, I.; Dovichi, N. J. *Talanta* 1994, 44, 401.
47. Li, X. F.; Ren, H. Qi, M.; Lewis, D.; Ireland, I.; Waldron, K. C.; Dovichi, N. J.

Tech. Prot. Chem. VIII 1997, 3.

48. Nolan, T. G.; Hart, B. K.; Dovichi, N. J. *Anal. Chem.* 1985, 57, 2703.

CHAPTER 3

SEPARATION OF TESTOSTERONE METABOLITES IN MICROSOMAL INCUBATES USING CAPILLARY ELECTROCHROMATOGRAPHY

3.1 INTRODUCTION

Cytochrome P450 isozymes (CYPs) play an important role in the oxidative biotransformation of numerous endogenous substrates and xenobiotics, the process mainly responsible for activation and detoxication of substrates in biological systems [1]. The enzymes were first discovered by Omura and Sato in 1962 [2]. Later it was recognized that cytochrome P450 isozymes were heme proteins containing noncovalently-bound iron protoporphyrine, a form of heme functional group [3]. These enzymes are widely found in liver and other tissues such as kidney, lung, intestine, and brain. These enzymes exhibit a broad spectrum of substrate specificity and a wide range of enzyme activity. The substrates of cytochrome P450's include steroid hormones, fatty acids, fat-soluble vitamins, prostaglandins, and leukotrienes, as well as drugs, chemical carcinogens, and environmental pollutants. Based on the encoding DNA sequence similarities, P450's have been classified into about forty different families. More than 200 different isozymes have already been discovered and characterized [4].

The metabolic pathway of testosterone by cytochrome P450's can be used to measure a number of different families of P450 isozymes [5]. For example, CYP2C11, a major isozyme in rat liver, accounts for about 40% of the total P450. CYP2C11 oxidizes testosterone and selectively produces 16α and 2α hydroxylated testosterone. 6β and 7α hydroxylation of testosterone are indicators of the activities of CYP3A1 and CYP2A1 respectively in rat liver. Studies also revealed that aging was associated with changes in the profiles of testosterone metabolism by liver cytochrome P450-related monooxygenases [6-7]. The accurate quantitation of testosterone metabolites is important in clinical and pharmacokinetic studies.

Due to the similarities of the isomers among testosterone metabolites, the measurement of an individual metabolite is challenging. HPLC with gradient elution and conventional UV absorbance detection, and GC/MS have been established as the most

powerful tools for quantitation and identification of unknown metabolites [8-13]. However, GC/MS often requires analyte derivatization. Capillary electrophoresis (CE) can also be used to determine the pathways of testosterone hydroxylation, but it still requires validation for quantitation [14]. GC/MS has been used for monitoring the level of steroids and metabolites in athletes due to the incidence of anabolic drug abuse in major sports. In order to prevent drug abuse and unfairness in sport competition, the approaches for this special purpose have matured with the development of modern analytical instrumentation. Recently, several groups have reported the analysis of anabolic steroids, testosterone hydroxy analogs, and testosterone conjugates using LC/MS and electrospray collision-induced dissociation (CID) [15-18]. For on-line mass spectrometric detection, the atmospheric pressure chemical ionization (APCI) interface with tandem mass spectrometry has proved a superior means for metabolite structure elucidation [19].

Capillary electrochromatography (CEC), as a micro separation method, has been promoted a great deal over the last five years due to its high separation efficiency and ability to analyze trace samples of biological importance. CEC has successfully resolved biological complexes of small molecules such as amino acid derivatives, nucleosides, saccharides, peptides, pharmaceuticals and large molecules such as protein digests [20-26]. In this Chapter, CEC with thermo-optic UV absorbance detection (TOAD) has been developed as a routine quantification tool for pharmacokinetic analyses of four monohydroxylated testosterone metabolites (2α , 6β , 7α , 16α). This is the first study to use CEC in testosterone metabolite analysis, to our knowledge.

3.2 EXPERIMENTAL

3.2.1 Materials and Instrumentation

Enzyme-grade 4-morpholinoethanesulfonic acid (MES), N-2-hydroxyethyl-piperazine-N'-2-ethanesulfonic acid (HEPES), reagent-grade sodium hydroxide (NaOH), and KCl were purchased from Fisher Scientific (Fair Lawn, NJ, USA). HPLC-grade acetonitrile (ACN) and methanol were purchased from EM Science (Gibbstown, NJ, USA). Thiourea, $MgCl_2$, NADPH were purchased from Sigma (Oakville, ON, Canada). The 3 μm C18 and C8 packing materials were a kind gift from by Dr. Henry Chen of Waters Corporation (Milford, MA, USA). Water for buffer preparation was treated using a Milli-Q purification system (Millipore, Bedford MA, USA). The CEC mobile phase was filtered through a 0.2 μm Millex PTFE filter (Millipore) prior to use. The capillaries used for packing CEC columns were 50 μm i.d. and 182 μm o.d. (Polymicro Technology, Phoenix, AZ, USA).

Testosterone, testosterone hydroxy metabolites, and cortexolone were purchased from Steraloids Inc. (Newport, RI, USA). The protein assay kit was from Bio-Rad Laboratories (Hercules, CA, USA). EDTA, glycerol, KH_2PO_4 and K_2HPO_4 were from BDH Inc. (Toronto, ON, Canada). Male Sprague-Dawley rats were from Biosciences Animal Services (University of Alberta, Edmonton, Canada).

A capillary electrophoresis instrument made in-house, was equipped with a laser-induced crossed-beam thermo-optical UV absorbance detector (TOAD), and was used for the analysis of testosterone and its metabolites. An UV excimer laser at a wavelength of 249 nm and a HeNe laser at 632 nm were used as pump and probe lasers respectively. The details of the instrument configuration were described previously [27-28].

3.2.2 Preparation of Standard Solutions

The stock solution of each metabolite and its parent drug were made by dissolving each compound in methanol to a concentration of 1 to 10 mg/mL. The mixture of standard solutions was diluted into the CEC mobile phase to give the following concentrations of 2 α : 5, 10, 20, 50, 80 ng/ μ L; of 6 β : 4.7, 9.4, 19, 47, 75 ng/ μ L; and of 7 α : 7, 14, 28, 70, 110 ng/ μ L monohydroxylated testosterone. Thiourea was added as an internal standard to each standard mixture and each microsomal incubate, with a final concentration of 50 μ M for correcting instrumental errors arising from laser power drift or shifting optical alignments.

3.2.3 Preparation of Testosterone Metabolites *in Vitro*

The testosterone metabolites were prepared by Ms. ZhongPing Mao in Professor Tam's research group in the Faculty of Pharmacy and Pharmaceutical Sciences. The procedures are briefly described as follow. Microsomes from livers of male Sprague-Dawley rats (200~250 g) were prepared as described in the literature [28] with slight modification. Testosterone (250 μ M) was incubated for 10 min at 37°C in a 1-mL total volume incubation mixture containing potassium phosphate buffer (100 mM, pH 7.4), MgCl₂ (3 mM), NADP (1 mM), glucose-6-phosphate (5 mM), glucose-6-phosphate dehydrogenase (1U), and 0.2 mg microsomal protein. The reaction was terminated by adding 6 mL of methylene chloride, after which 1 nmol of cortexolone was added as an internal standard. Cortexolone was used for calculating the extraction efficiency. The sample was vortexed on an IKA VIBRAX VXR vortex shaker (IKA, Wilmington, NC, USA) set at 1200 and then centrifuged at 1000g for 10 min. The methylene chloride layer was removed and dried under nitrogen at room temperature. The residues were reconstituted in the mobile phase used in the electrochromatography experiments.

3.2.4 CEC Conditions

The CEC mobile phases were prepared as follows: 100 mM of aqueous MES or HEPES was titrated with 2M NaOH to a pH of 6.3 or 7.4, respectively. Then the aqueous buffer was mixed with acetonitrile to the desired concentration. The pH of the mobile phase was estimated as the pH of the aqueous buffer before mixing. The manufacturing of the CEC column was reported in Chapter 2. Quantification was carried out with CEC columns made in-house, of 50 μm i.d., 180 μm o.d., packed with 3 μm C18 reverse phase particles. The column had a 22 cm packed length and 33 cm total length, with a detection window 6 cm from the outlet of the column. The dimensions of the C8 column was 27 cm packed length and 37 cm total length. The sample was introduced by electrokinetic injection for 10 s at 5 kV. The voltage applied for separation was 20 kV. The optimized running buffer consisted of 10 mM HEPES at pH 7.4 in 70% ACN.

3.3 RESULTS AND DISCUSSION

3.3.1 CEC Method Development

Testosterone metabolism by rat liver microsomal isozymes is via monohydroxylation. The sites where transformations occur are shown in Figure 3.1. Thus, routine LC/MS is not a suitable method since all the metabolites have an equal mass. I developed a highly efficient CEC method that only needs 1 μL of each sample for analysis. The separation of four metabolites and parent drug was optimized by manipulating several chromatographic parameters such as the composition of the mobile phase, types of zwitterion buffer, and the carbon chain length of the stationary phase. Figure 3.2 shows the separation profile of standards using 10 mM MES buffers at pH 6.3

with 50 - 80% acetonitrile. The faster separation at higher organic modifier concentration was due to both the higher flow rate of electroosmosis and larger capacity factors in the mobile phase system. The 70% acetonitrile buffer provides a baseline-resolved profile, with slight tailing of the 2α and 16α metabolites. This tailing is presumably caused by the strong adsorption of the analytes on the stationary phase. Following the above experiment, 10 mM HEPES, pH 7.4 and 70% acetonitrile was used as the mobile phase on the same C18 column. A comparison of the separations is shown in Figure 3.3. The top trace obtained from HEPES buffer shows a faster separation and less tailing than the bottom trace from MES buffer, which was mostly caused by higher electroosmotic flow rate using a higher pH buffer. The sample mixture contained an EOF marker, thiourea, and no 16α metabolite because of a shortage of the standard during the experiment. A different type of packing material with the same size particles but a shorter carbon chain, C8, was also investigated. Figure 3.4 depicts the separation profiles for both packing materials under the same conditions of electric field strength and buffer. The EOF velocity was 5.1 cm/min. and 5.3 cm/min. for C8 and C18 columns, respectively, which indicated the densities of uncapped silanol groups were similar for both materials as expected. The number of theoretical plates generated for C18 was slightly higher than that on C8. So for these hydrophobic compounds, the C18 column was a better choice for the analysis.

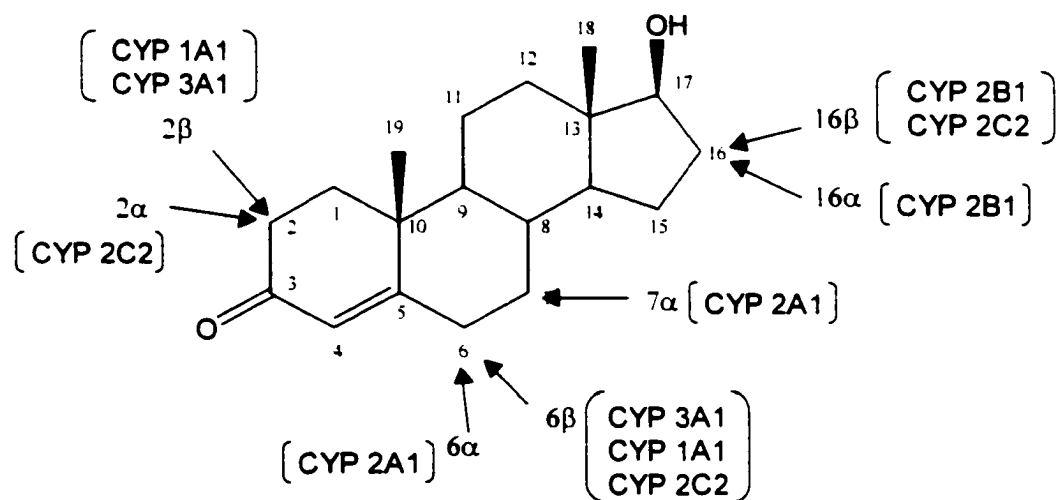


Figure 3.1 Structure of testosterone with possible monohydroxylation sites by CYPs.

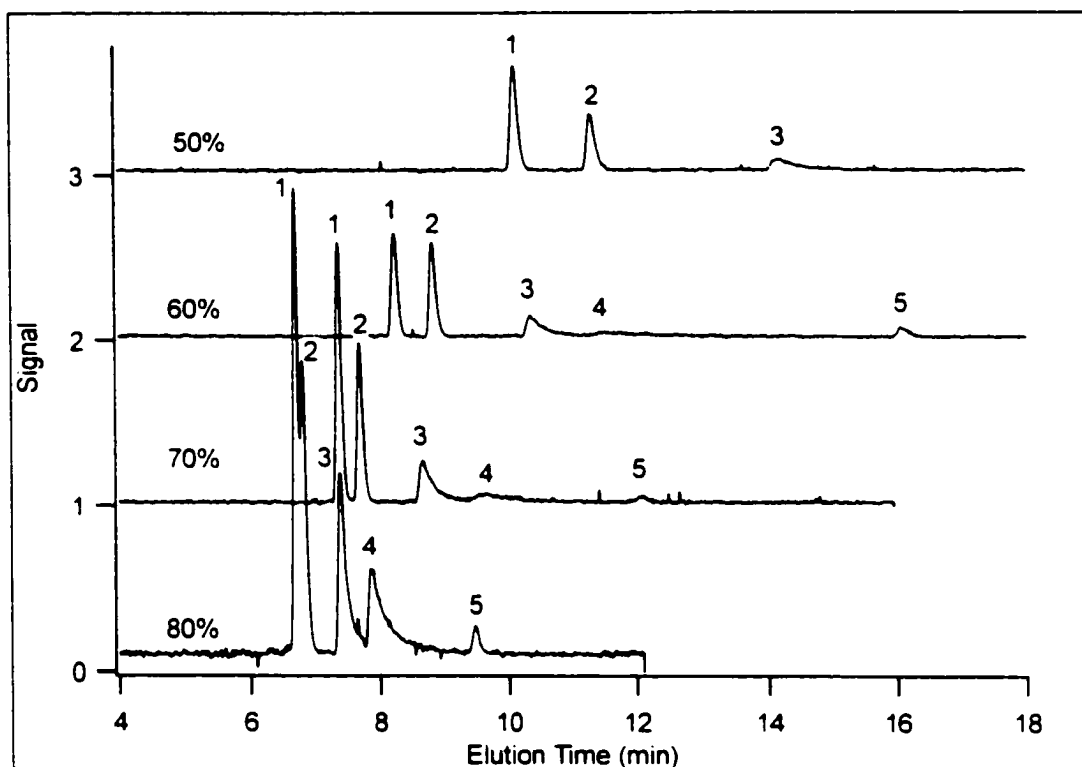


Figure 3.2 Chromatograms of standard mixture of 7α , 6β , 2α , 16α - hydroxytestosterone and testosterone by using 10 mM MES with 50 to 80% acetonitrile. 1: 7α , 2: 6β , 3: 2α , 4: 16α -hydroxytestosterone, and 5: testosterone. Chromatographic conditions are as described in the text.

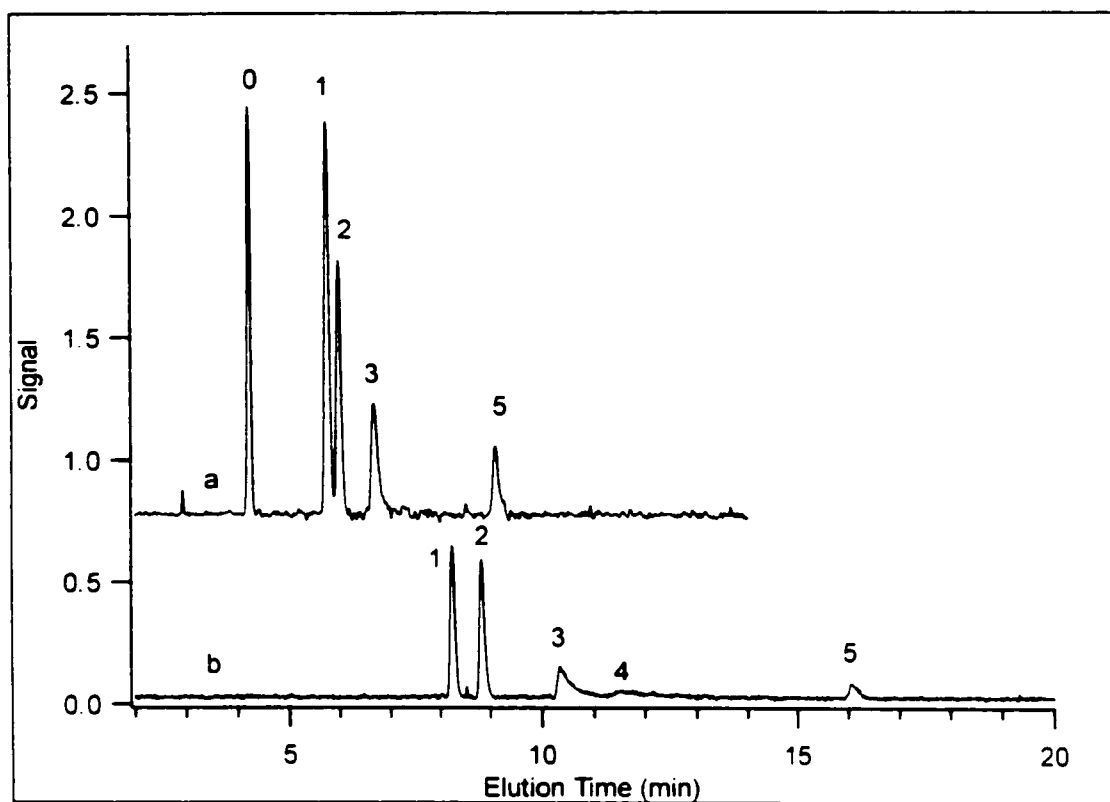


Figure 3.3 Chromatograms of a standard mixture by using a: 10 mM HEPES, pH 7.4, 70% ACN, b: 10 mM MES, pH 6.3, 70% ACN. 0: thiourea. 1: 7 α . 2: 6 β . 3: 2 α . 4: 16 α -hydroxytestosterone. 5: testosterone.

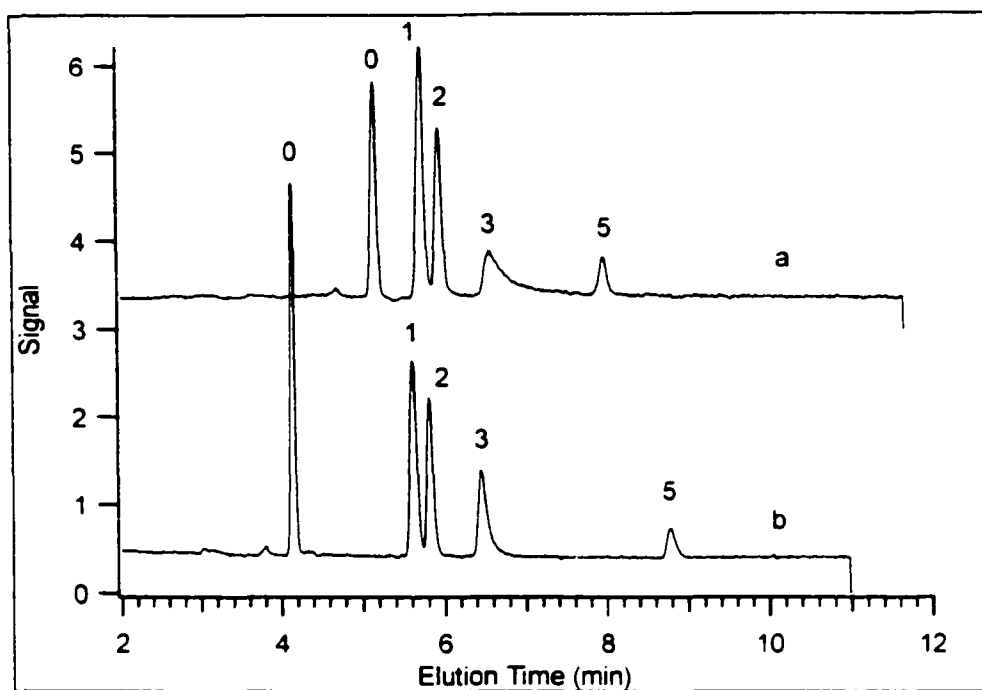


Figure 3.4. Chromatograms of standard mixture separated by a: C8 stationary phase, column dimension 27 cm/31 cm/37 cm. b: C18 stationary phase, column dimension, 22 cm/27 cm/33 cm. Chromatographic conditions are as described in Figure 3.2.

3.3.2 Calibration and Quantification

The optimized conditions for 10 mM HEPES and 70% acetonitrile buffer were employed to quantify testosterone metabolites. All the standard solutions were diluted in the mobile phase used for separation. Linear calibration curves were constructed by plotting peak height and area versus concentration for each metabolite within the ranges of 10 to 50 ng/ μ L for 2 α -, 4.7 to 47 ng/ μ L for 6 β -, and 7 to 70 ng/ μ L for 7 α -monohydroxylated testosterone. Each curve had a linear regression coefficient of 1.00. The data for the calibration curves are summarized in Table 3.1. If the highest concentration data point was included for curve fitting, I found the linear regression coefficient degraded into a range of 0.95 to 0.98. The signal intensities for all the

metabolites at the highest concentrations were below the linear calibration line, which might be due to the limited linear dynamic range of the photodiode used for determination of the signal. Concentration limits of detection (LOD) for the above metabolites were computed using 3 times the background noise (3σ). They were 5.5, 3.1, 0.77 ng/ μ L for metabolites 2 α , 6 β and 7 α respectively. The relatively lower sensitivity for 2 α metabolite is caused by its low absorption at the excitation wavelength of the pump laser.

Table 3.1 Calibration curve data for the quantitation of testosterone metabolites (2 α , 6 β , 7 α hydroxylates)

Analyte	Linear Range (ng/ μ L)	Calibration Curve (r^2) (n=4)	LOD(3σ) (ng/ μ L)
2 α	10-50	y(height) = -0.022 + 0.0068x (1.00)	5.5
		y(area) = -0.040 + 0.016x (1.00)	-
6 β	4.7-47	y(height) = -0.031 + 0.016x (1.00)	3.1
		y(area) = -0.038 + 0.022x (1.00)	-
7 α	7-70	y(height) = 0.0064 + 0.012x (1.00)	0.77
		y(area) = -0.011 + 1.019x (1.00)	-

The analysis of *in vitro* testosterone metabolites by rat hepatic microsomes is shown in Figure 3.5. It was observed that 6 β hydroxylation of testosterone was the main metabolic pathway. The most intense peak was due to the internal standard, cortexolone, introduced in order to calculate the extraction efficiency during the sample preparation. The total chromatographic time was only 10 minutes, which is much faster than the current HPLC method. From the calibration curve and extraction efficiency, the amount of 6 β hydroxylated testosterone was 22 ng/ μ L. Unfortunately, the metabolite

corresponding to the peak adjacent to testosterone could not be identified by matching its elution time to a standard. Before being used for routine screening, the above CEC thermo-optical absorbance technique will need further validation.

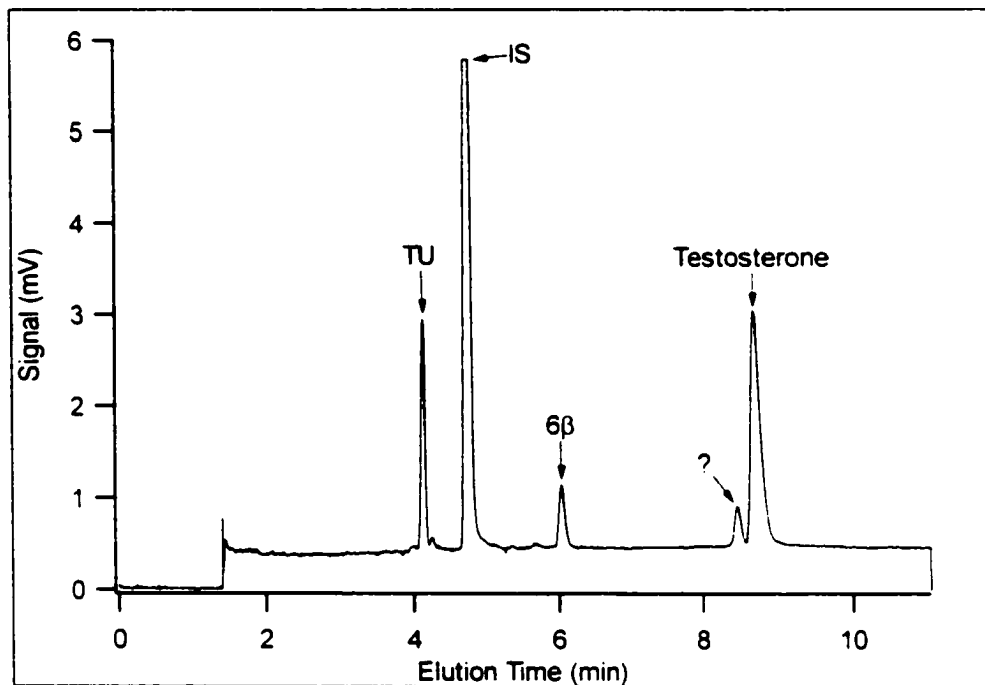


Figure 3.5 Separation of *in vitro* testosterone metabolites from rat hepatic microsomes. TU: thiourea, IS: cortexolone.

3.4 CONCLUSIONS

These preliminary studies have demonstrated that capillary electrochromatography can be used for fast screening of testosterone metabolism by liver microsomes for pharmacokinetic and clinical studies. This method is accurate and reproducible, and cost effective as a quantitation tool.

REFERENCES

1. Belpaire, F. M.; Bogaert, M. G. *Acta Clinica Belgica* 1996, 51, 254.
2. Omura, T.; Sato, R. *J. Biol. Chem.* 1964, 237, 1375.
3. Omura, T.; Sato, R. *J. Biol. Chem.* 1964, 239, 2370.
4. Nelson, D. R.; Kamataki, T.; Waxman, D. J.; Guengerich, F. P.; Estabrook, R. W.; Feyereisen, R.; Gonzalez, F. J.; Coon, M. J.; Gunsalus, I. C.; Gotoh, O. *DNA Cell Biol.* 1993, 12, 1.
5. Nebert, D. W.; Hegishi, M. *Biochem. Pharmacol.* 1982, 31, 2311.
6. Galinsky, R. E.; Johnson, D. H.; Kane, R. E.; Flanklin, M. R. *J. Pharmacol. Exp. Ther.* 1990, 255, 577.
7. Leakey, J. E.; Cunny, H. C.; Bazare Jr. J.; Webb, P. J.; Feuers, R. J.; Duffy, P. H.; Hart, R. W. *Mech. Aging Dev.* 1989, 48, 145.
8. Sonderfan, A. J.; Arlotto, M. P.; Duttonand, D. R.; McMillen, S. K. *Arch Biochem Biophys.* 1987, 255, 27.
9. Arlotto, M. P.; Trant, J. M.; Estabrook, R. W. *Methods Enzymol.* 1991, 206, 454.
10. Wolthers, B. G.; Kraan, G. P. *J. Chromatogr. A* 1999, 843, 247.
11. Munoz-Guerra, J.; Carreras, D.; Soriano, C.; Rodriguez, C.; Rodriguez, A. F. *J. Chromatogr. B, Biomed Sci Appl.* 1997, 704, 129.
12. Purdon, M. P.; Lehman-McKeeman, L. D. *J. Pharmacological & Toxicological Methods.* 1997, 37, 67.
13. Swales, N. J.; Johnson, T.; Caldwell, J. *Drug Metab Dispos.* 1996, 24, 1224.
14. Fernandez, C.; Egginger, G.; Wainer, I. W.; Lloyd, D. K. *J. Chromatogr. B* 1996, 677, 363.
15. Joos, P. E.; Ryckeghem, M. V. *Anal. Chem.* 1999, 71, 4701.
16. Williams, T. M.; Kind, A. J.; Houghton, E.; Hill, D. W. *J. Mass Spectrom.* 1999, 34, 206.
17. Borts, D. J.; Bowers, L. D. *J. Mass Spectrom.* 2000, 35, 50.

18. Chu, I.; Favreau, L.; Soares, T.; Lin, C.; Nomeir, A. A. *Rapid Commun. Mass Spectrom.* 2000, 14, 207.
19. Singh, G.; Arora, V.; Fenn, P. T.; Mets, B.; Blair, I. A. *Anal. Chem.* 1999, 71, 2021-2027.
20. Huber, C. G.; Choudhary, G.; Hováth, C. *Anal. Chem.* 1997, 69, 4429.
21. Hjerten, S.; Vegvari, A.; Srichaiyo, T.; Zhang, H. X.; Ericson, C.; Eaker, D. J. *Capillary Electrophor.* 1998, 5, 13.
21. Yang, C.; El Rassi, Z. *Electrophoresis* 1998, 19, 2061.
22. Huang, P.; Jin, X.; Chen, Y.; Srinivasan, J. R.; Lubman, D. M. *Anal. Chem.* 1999, 71, 1786.
23. Krause, K.; Girod, M.; Chankvetadze, B.; Blaschke, G. *J. Chromatogr. A* 1999, 837, 51.
24. Euerby, M. R.; Johnson, C. M.; Smyth, S. F.; Gillott, N.; Barrett, D. A.; Shaw, P. N. *J. Microcolumn Sep.* 1999, 11, 305.
25. Huang, P.; Wu, J. T.; Lubman, D. M. *Anal. Chem.* 1998, 70, 3003.
26. Waldron, K. C.; Dovichi, N. J. *Anal. Chem.* 1992, 64, 1396.
27. Li, X. F.; Waldron, K. C.; Black, J.; Lewis, D.; Ireland, I.; Carpenter, M.; Dovichi, N. J. *Talanta* 1997, 44, 401.
28. Guengerich, F. P. in: Hayes, A. W. (Ed.) *Principles and Methods of Toxicology*, 2nd Ed. NY: Raven Press, Ltd. 1989, pp 777-814.

CHAPTER 4

DEVELOPMENT OF NON-AQUEOUS CE/MS METHOD FOR ANALYSIS OF ALKALOIDS FROM *FRITILLARIA*

4.1 INTRODUCTION

New drug discovery from natural products is one of the major tasks in the current pharmaceutical industry. Herbal medicines, known in ancient healing arts, have been used for many centuries. The active components for their claimed actions are still being systematically investigated by modern drug screening processes, which involves pharmacological, toxicity and biochemical testing. Verticine, verticinone, and imperialine are the three major ingredients in Chinese herbal medicine of *Bulbus Fritillaria*. (Chinese name Beimu) which possesses antitussive and expectorant activities and has been used for more than two thousand years [1]. Pharmacological studies indicated that the therapeutic activities and toxicities depend on the geographic origin of the plants, which was explained by the variation of the contents and types of above constituents in Beimu species growing in different provinces in China [2]. Much evidence already showed that isomerization of natural product molecules plays a significant role in bioactivity and toxicity. Some of the geometric components may only exist in trace amount but have strong bioactivity [3]. Therefore, the quality control of these herbal medicines requires an efficient, highly sensitive and robust analytical technique to provide a thorough and informative description of the drug identities.

The major constituents in *Fritillaria* plants are isosteroidal alkaloids listed in Figure 4.1. Due to the similarities of these molecular structures and the presence of geometric isomers among some of these compounds, analysis of these molecules needs highly efficient, specific analytical techniques. High performance liquid chromatography detection (GC/FID), and thin layer chromatography (TLC) are the only methods reported

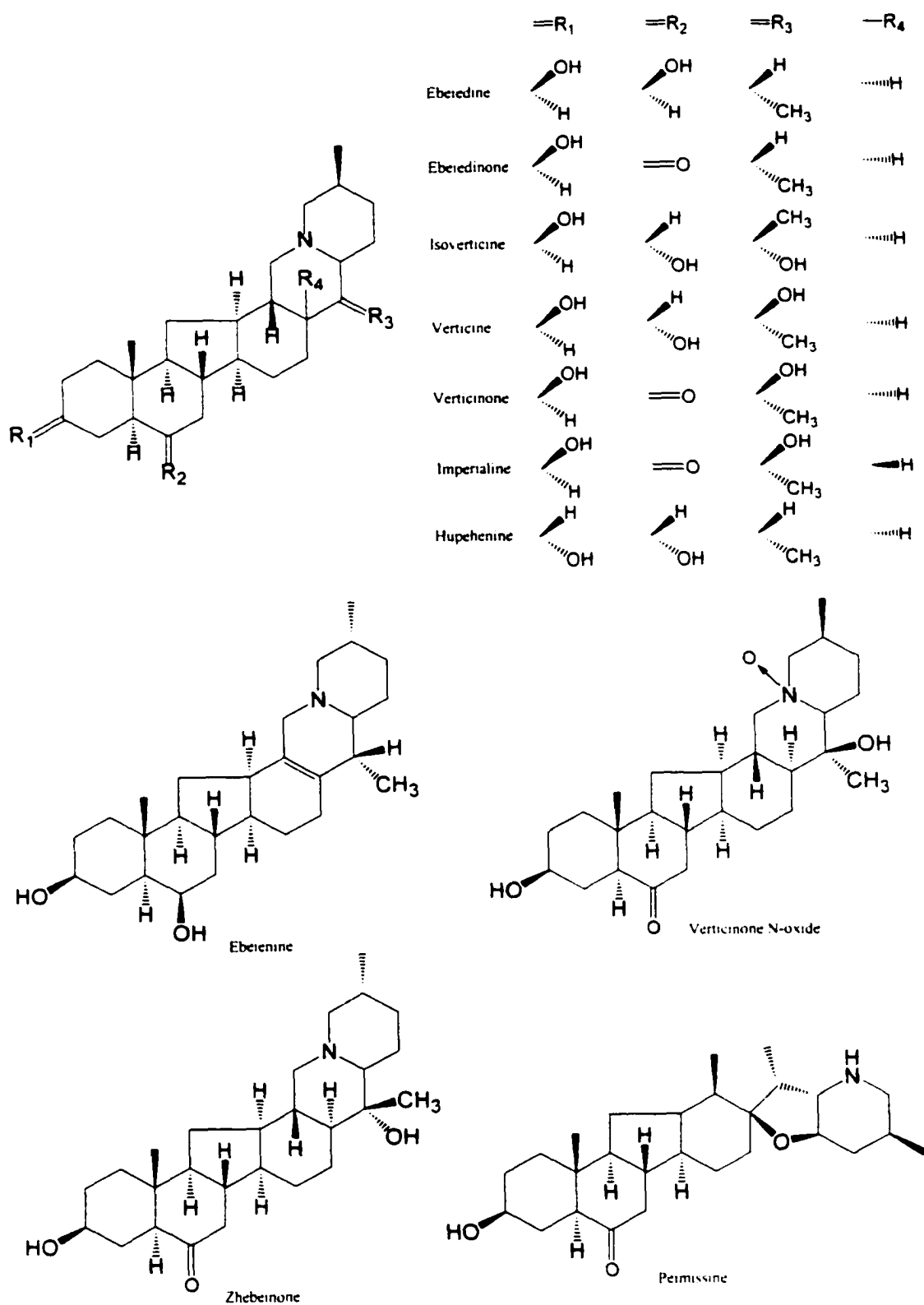


Figure 4.1 Structure of *Fritillaria* alkaloids

in the literature for quantification of the alkaloids in Beimu plants [2, 3]. Since these molecules have low UV absorption, high polarity, and are non-volatile, both LC/UV and GC/FID require pre-column derivatization. Detection at short UV wavelength without derivatization could only be applied to compounds that possess double bonds, however, which suffer interference from solvents and other chemicals present in the herbal extract. Derivatization processes generate a complex background in the chromatogram due to the sample matrix. In each case modern techniques such as HPLC/MS and GC/MS have been employed to characterize the derivatized alkaloids [2, 3].

Non-aqueous capillary electrophoresis (NACE) has been established as a very efficient separation method for both hydrophobic and hydrophilic molecules [4-6]. Nonaqueous separation buffers consist of electrolyte and one organic solvent or a mixture of solvents. Compared to an aqueous buffer, nonaqueous media generate low Joule heating due to low conductivity of the organic solvents, which minimizes band broadening and allows use of a high electrolyte concentration and high separation voltage. Organic solvents also improve the solubility of hydrophobic compounds and thus reduce capillary wall adsorption and peak tailing that occurs using aqueous buffers. When coupled to online electrospray ionization mass spectrometric detection, the organic solvents assist electrospray ionization efficiency and enhance detection sensitivity.

The most of alkaloids of interest in this study consist of a steroidal ring structure and a tertiary amine group. They possess both hydrophobic and hydrophilic properties. The soft ionization process of electrospray is ideal for producing positive ions by protonating the amine groups. To my knowledge, this was the first use of NACE/MS for analyzing the alkaloids in *Fritillaria* plants.

4.2 EXPERIMENTAL

4.2.1 Chemicals and Materials

Pure compounds of verticine, verticinone, imperialine and aqueous crude extract from Zhebei, (one of the Beimu species grown in Zhejiang province in China) and the active fraction of the extract, were kindly supplied by Dr. Lin Ge's group in the Department of Pharmacology at Hong Kong University. The procedures for preparation of active extract and aqueous crude extract were described elsewhere [7-9]. Amitriptyline (AMI) used as an internal standard in NACE/MS was obtained from Sigma (St. Louis, MO). Ammonium acetate (NH₄Ac) was purchased from Anachemia (Montreal, PQ, Canada). HPLC grade methanol (MeOH) and acetonitrile (ACN) were purchased from BDH (Toronto, Ontario, Canada). Deionized water was produced by a Milli-Q water purification system (Millipore, Bedford, MA). Fused-silica capillaries used in all experiments with dimensions of 20 µm i.d., 148 µm o.d. were purchased from Polymicro Technologies (Phoenix, AZ, USA).

4.2.2 Instrumentation

All MS analyses were performed on a Perkin Elmer Sciex API 100 single quadrupole mass spectrometer equipped with sheathless MicroIonSpray and IonSpray interfaces (PE Sciex, Concord, Ontario, Canada). The MicroIonSpray interface was used in flow injection analysis while the IonSpray interface was utilized to couple nonaqueous

CE to the mass spectrometer. The positive ion mode was used for all mass spectrometric detection. The data were collected by a Macintosh desktop computer using LCTune software and processed using Multiview 1.2 software supplied by PE Sciex.

4.2.3 Flow Injection Analysis (FIA)

Flow injection analysis (FIA) via a MicroIonSpray interface was utilized to study the influence of spray parameters including electrospray voltage (IS), orifice voltage (OR) and ring voltage (RING) on electrospray mass spectra of the alkaloids. FIA was selected at the early stage of this study. Verticine (MH^+ 432 amu) was chosen as a model compound for the investigation. The solution to be tested contained 20 μ M verticine, which was dissolved in acetonitrile / water (7/3 v/v). The flow rate was 0.2 μ L/min., pumped with a syringe infusion pump (Harvard Apparatus, South Natick, MA, USA). A full mass range scanning mode from 50 to 800 amu was applied to acquire the mass spectra with a dwell time of 1.5 ms, step size of 1.0 amu and scan speed of 1.13 s. The curtain gas (CUR) and nebulizer gas (NEB) were optimized at 0.95 L/min and 0.03 L/min, respectively.

4.2.4 NACE/MS

The NACE separation was conducted on a capillary electrophoresis instrument constructed in-house. The maximum voltage of the power supply for CE separations was 30 kV. An IonSpray interface with coaxial sheath liquid make-up and nebulizer gas was

used to couple CE separations to the mass spectrometer. The CE column was directly fed into the interface. The nebulizer gas and curtain gas both were purified nitrogen. The sheath liquid was 100% MeOH delivered at 2 $\mu\text{L}/\text{min}$. by a syringe infusion pump (Harvard Apparatus). A 60 cm long fused-silica capillary was used for separations. The buffer for separations consisted of up to 100 mM ammonium acetate in methanol/acetonitrile mixtures. The sample was introduced into the CE column by electrokinetic injection at 5 kV for 10 s. CE separations were conducted at 20 to 25 kV. A full scan mode was applied at conditions used in FIA, except for quantitation analysis, where the mass range was selected from 250 to 450 amu.

4.2.4.1 Optimization

The NACE separation conditions were optimized by examining the effect of a variety of experimental conditions on both sensitivity and separation efficiency, including ion competition from electrolyte, electrolyte concentration of the separation buffer and sample matrix, and fraction of nonaqueous organic solvents in the separation buffer. The ion suppression effect by ammonium ion contained in the separation buffer was investigated by the process of electrokinetic infusion of a sample that contained a constant concentration of verticine (20 μM) with varied concentrations of ammonium acetate from 0.01 mM to 100 mM. The total ion current (TIC) and extracted ion current (EIC) of the protonated species of verticine (MH^+ 432 amu) were monitored. The effect of electrolyte concentration on separation efficiency was examined for a range of 10^{-7} M to 0.1 M of ammonium acetate in MeOH/ACN. The stacking effect of sample matrix was

examined for a sample matrix without electrolyte, and up to 10 mM of ammonium acetate in MeOH/ACN (7/3 v/v), while the separation buffer consisted of 50 mM NH₄Ac in the same nonaqueous solvent system. The influence of the composition of organic solvents was examined by varying the volume percentage of MeOH from 50% to 100%.

4.2.4.2 Calibration Curve

The stock solutions of verticine, verticinone, and imperialine were prepared by dissolving each compound in methanol to a concentration of 2 mM. The standard solutions for constructing calibration curves were made by serial dilution with methanol to concentrations of 1.0×10^{-7} M, 2.5×10^{-7} M, 5.0×10^{-7} M, 1.0×10^{-6} M, 2.5×10^{-6} M, 5.0×10^{-6} M, 1.0×10^{-5} M, 2.5×10^{-5} M, 5.0×10^{-5} M, and 1.0×10^{-4} M. Each standard solution contained 20 μ M AMI as internal standard. Triplicate analyses were conducted for each standard solution.

4.2.4.3 Analysis of Active Extract and Crude Extracts from *Fritillaria* Species

Stock solutions of crude extract and active extract were prepared at concentrations of 1.17 mg/mL and 2.25 g/mL by dissolving extract powder into MeOH. The sample was further diluted by a factor of 10 to 100 in methanol so that each sample contained 20 μ M AMI. The crude extract powder was not completely dissolved in MeOH or MeOH/ACN mixtures due to a wide range of constituents in the plant extract. Residual particles were

filtered by a 0.2 μm Millex PTFE filter (Millipore, Bedford, MA, USA) prior to sample injection.

4.3 RESULTS AND DISCUSSION

4.3.1 Influence of Spray Parameters on Mass Spectra of Verticine

Figure 4.2A shows that both total ion current and the extracted ion current of molecular species of verticine varies with electrospray voltage (IS) in FIA. Both signals present a similar pattern, intensities increase at high electrospray voltage. The abundance of molecular ion increased two-fold at the highest voltage (5500 V) compared to the lowest voltage (2800 V). It was found that the electrospray stability was poor at low IS voltage with RSD (n=10) of 6% which was presumably due to incomplete ionization. To avoid possible discharge at high voltage and maintain the high sensitivity, the optimized IS voltage was chosen at 5000 V for FIA analysis, which achieved 95% of the intensity compared to the maximum intensity obtained at 5500 V.

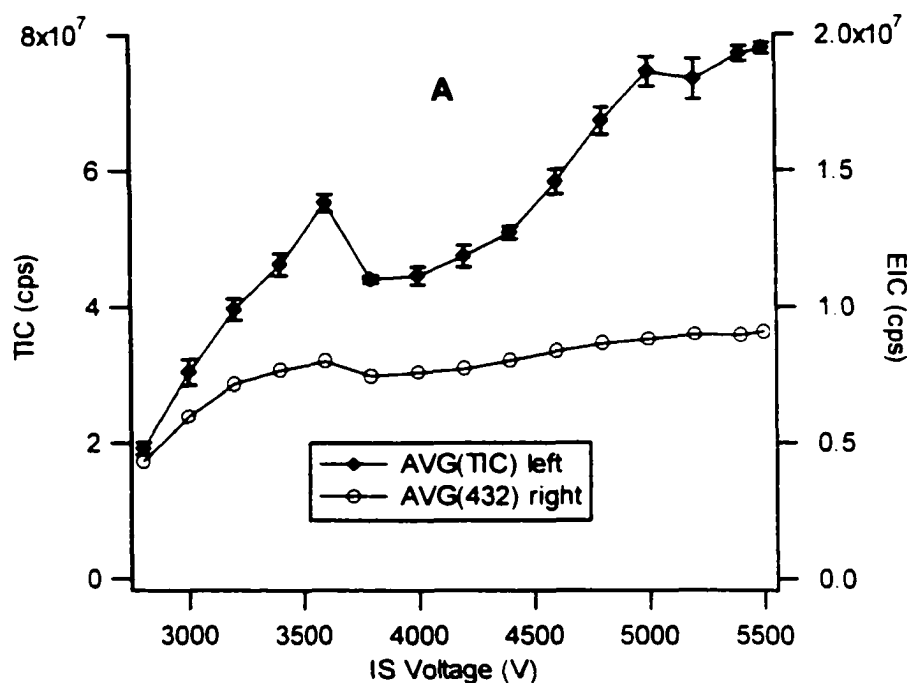


Figure 4.2 A: Influence of ionspray voltage (IS) on the total ion current and the extracted ion current of molecular species of verticine (MH^+ 432) during infusion of verticine solution. Flow injection conditions were as described in the Experimental Section.

The effect of orifice voltage (OR) on in-source fragmentation of verticine is shown in Figure 4.2B. In addition to the molecular ion MH^+ at 432 amu, only one fragment ion with m/z of 414 amu was observed, which was caused by loss of water from verticine. At low orifice voltage between 10 to 60 V, the molecular ion was the dominant species in spectra. The molecular ion signal decreased dramatically when the OR was larger than 80 V. The fragment ion reached its maximum at OR of 140 V. No other daughter ions were observed by further increasing the OR, which indicated that the steroidal structure with a tertiary amine was rigid and hard to break down. At the highest voltage of OR, the sensitivities decreased 40-fold for the molecular ion and 8-fold for the

fragment ion relative to the maximum signal level of each ion. To obtain high sensitivity with the molecular species, OR was optimized at 35 V.

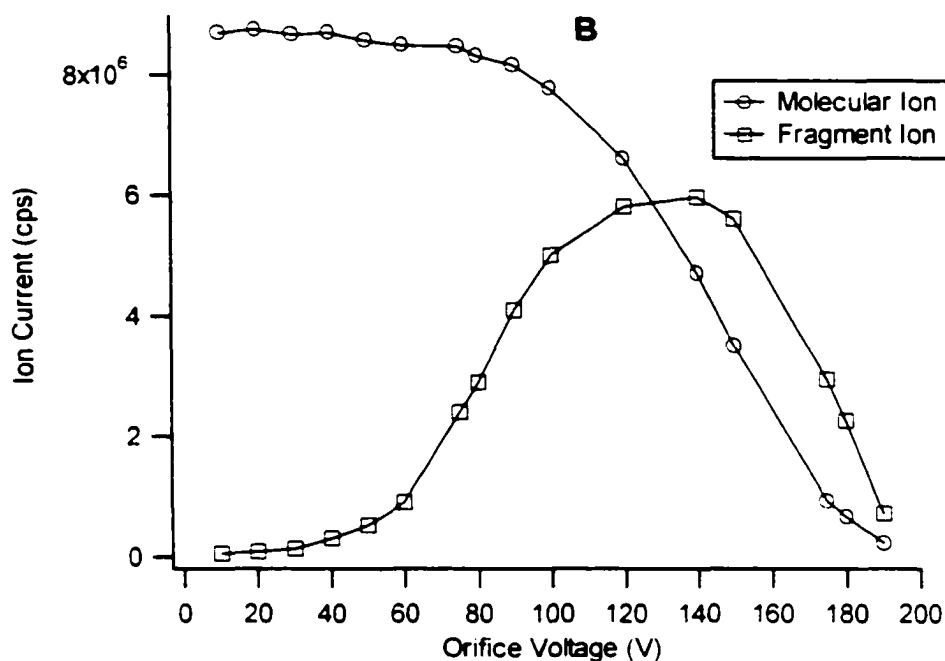


Figure 4.2 B: Influence of orifice voltage (OR) on the extracted ion current of molecular species of verticine (MH^+ 432) and of its fragment ion (414).

After optimizing the IS and OR voltages, the effect of ring voltage on the sensitivity was also investigated. When ring voltage changed from 200 to 350 V, the molecular ion was only increased 4%, while the fragment ion increased 4.5 fold.

The effect of infusion flow rate on the signal sensitivity and electrospray stability was examined. It was found that by using the MicroIonSpray interface, stable electrospray could be achieved at the flow rates between 0.05 to 0.4 $\mu\text{L}/\text{min}$. To maintain the stable electrospray at low flow rate, the electrospray voltage (IS) was adjusted. For

example, at 0.05 $\mu\text{L}/\text{min}$, the IS was set at 3600 V compared to 5000 V at the flow rate of 0.2 $\mu\text{L}/\text{min}$. The MicroIonSpray interface performed best when flow rate was within 0.1 to 0.2 $\mu\text{L}/\text{min}$ when both transfer and spray capillaries with 20 μm I.D. were used.

4.3.2 Ion Suppression

CE separations require electrolytes in the buffer. However, the electrolyte also creates high background and suppresses the analyte signal due to ion competition in mass spectrometric detection. Thus volatile electrolytes such as ammonium acetate, formic acid, ammonium bicarbonate, and ammonium hydroxide are commonly required in on-line CE/MS. Inorganic electrolytes are avoided in order to diminish the danger of ion source contamination. To achieve the best sensitivity and reasonable separation efficiencies, the extent of ion suppression from the ammonium ion was studied. Figure 4.3 shows the sensitivity of the molecular ion in the presence of different concentrations of ammonium acetate. When NH_4AC was below 10^{-4} M, the analyte signals were not significantly affected by the presence of ammonium ion. When the concentration increased 3 orders of magnitude from 10^{-4} to 10^{-1} M, only 15 to 20 % of the maximum signal remained. This result indicated that even using volatile buffer like NH_4Ac , ion suppression was inevitable at high buffer concentrations.

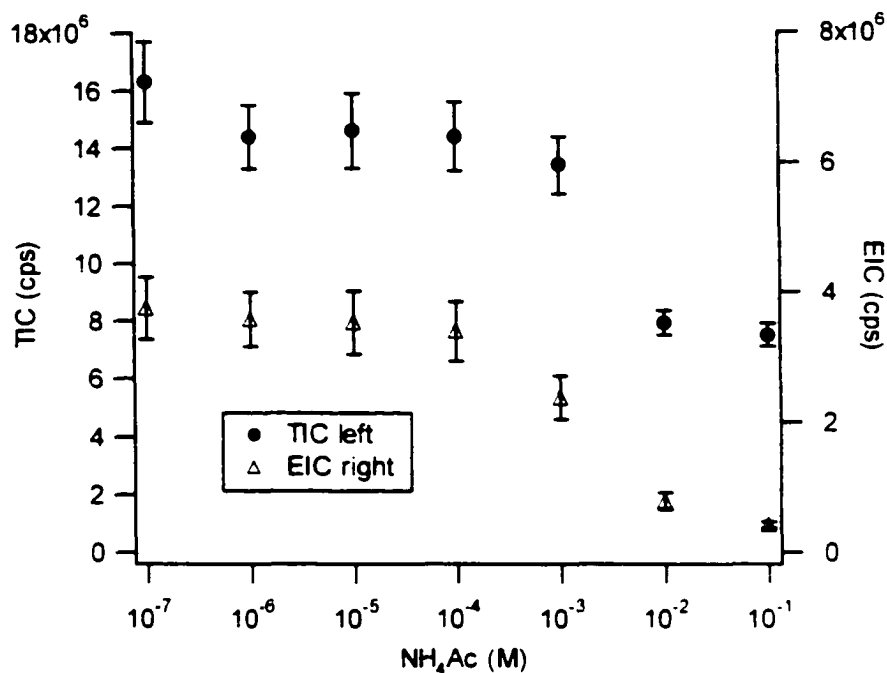


Figure 4.3 Matrix ion competition of NH_4^+ on signal level of the total ion current and extracted ion current of molecular species of verticine (MH^+ 432) in electrokinetic infusion using NACE/ESI/MS. Electrokinetic infusion voltage was 20kV. The current variation of each data point was calculated from 10 consecutive acquisitions ($n=10$).

4.3.3 NACE/MS Condition Optimization

Ionic Strength. The ionic strength in the separation buffer caused the most profound effect on separation efficiencies compared to the other experimental conditions studied. When the separation buffer contained less than 1 mM of NH_4Ac , the sample plug was extensively dispersed and no separation was achieved. Figure 4.4 shows electropherograms of three major alkaloids at electrolyte concentrations from 10 mM to

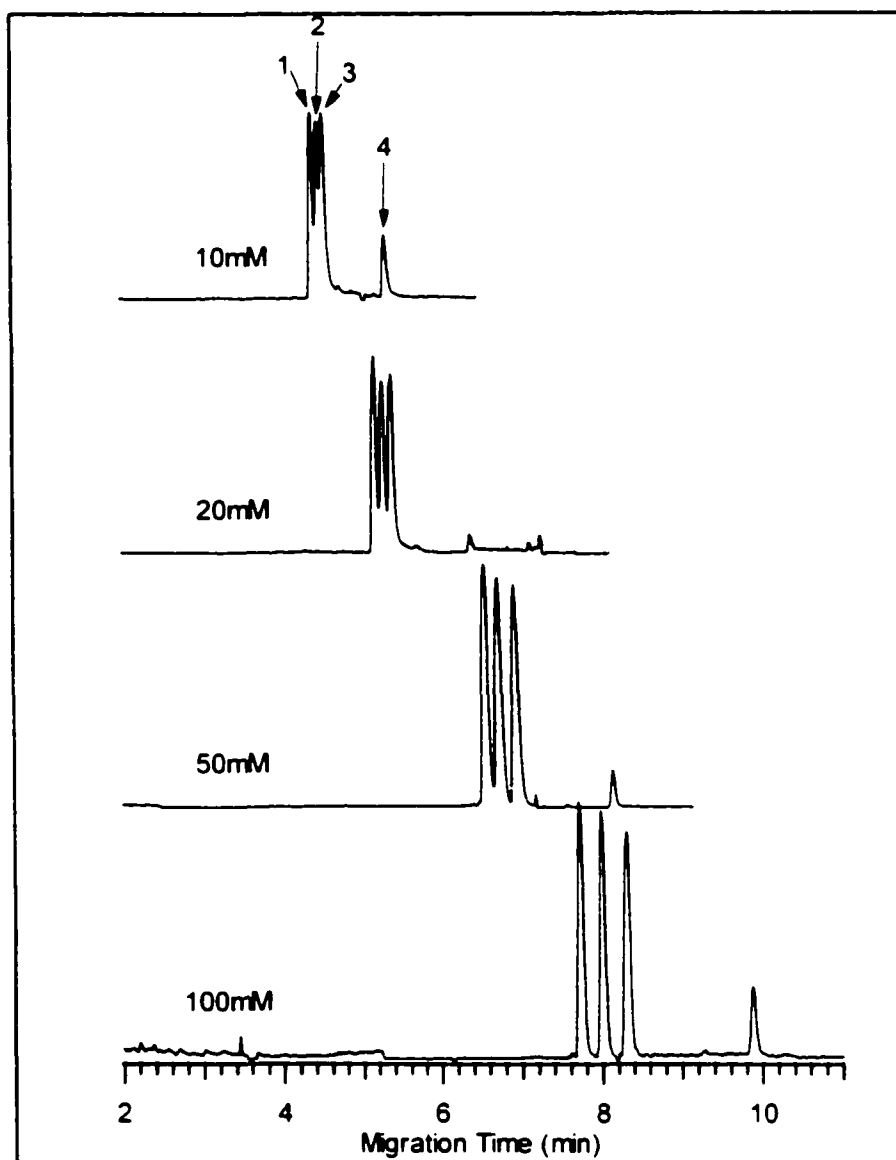


Figure 4.4 Effect of ionic strength on separation selectivity. Separation buffer: NH₄Ac in MeOH/ACN (7/3 v/v). Concentration of NH₄Ac in each analysis was as described in the figure. Sample mixture contained 2×10^{-5} M of each alkaloid and IS in MeOH. Peak assignment: 1: imperialine, 2: verticinone, 3: verticine, 4: amitriptyline.

100 mM. As the buffer concentration increased, better resolution was obtained at the expense of longer analysis times. The increased separation time was caused by lower electroosmotic flow (EOF) velocity at higher ionic strength, because EOF mobility was inversely proportional to the square root of electrolyte concentration [10]. Under the separation condition (apparent pH 6.8), the tertiary amine groups ($pK_a > 8$) of the analytes are mostly present as cationic species. The molecules migrate at a rate combining electroosmosis and electrophoresis. Two of the analytes are geometric isomers, the third analyte only differs in 2 mass units in molecular weight from the first two geometric isomers. Only when the EOF velocity was low enough, so that the difference in electrophoretic mobility is the dominant factor in this separation, will these similar species be resolved. Considering the high resolution and possible ion competition effect, the optimal concentration of NH_4Ac was 100 mM. The specificity of MS detection was inadequate in this case to identify the isomers, because of identical molecular ions and fragment ions for both species. The identification of imperialine and verticinone was accomplished by spiking authentic compound in the standard mixture and comparing the peak intensities between spiked sample and unspiked sample.

Stacking Effect. Stacking is a widely used phenomenon in capillary zone electrophoresis (CZE) for on-column preconcentration [11-12]. In this study, stacking was mainly employed to enhance the detection sensitivity. Varied NH_4Ac concentrations in the sample matrix were examined in conjunction with 20 μM of each alkaloid, in MeOH/ACN (7/3 v/v), while the separation buffer for all samples was 50 mM NH_4Ac in MeOH/ACN (7/3 v/v). Figure 4.5 shows the electropherograms of the same standards in different ionic strength matrixes. The electrolyte concentration in the sample matrixes can

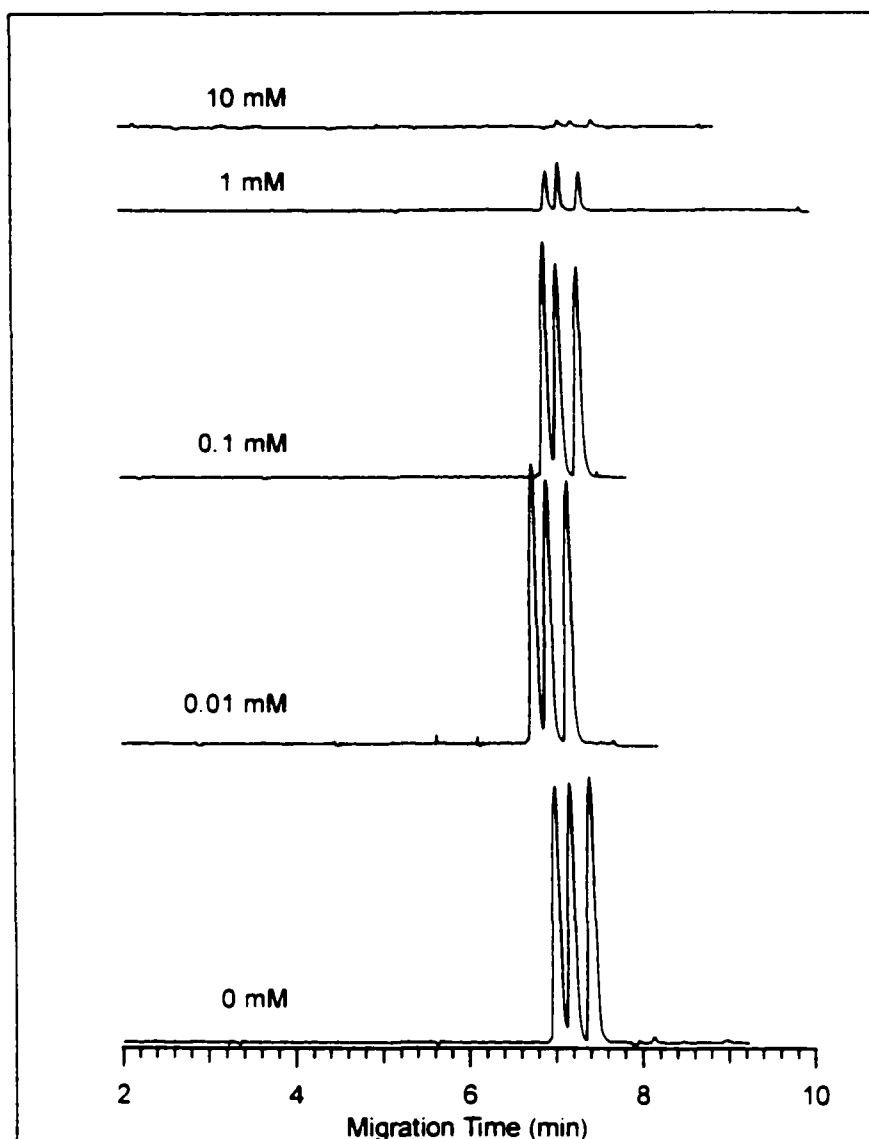


Figure 4.5 Effect of alkaloids stacking. Sample matrix consisted of NH_4Ac and MeOH/ACN (7/3 v/v). The concentrations of NH_4Ac were shown on the figure. Separation buffer was 50 mM NH_4Ac in MeOH/ACN (7/3 v/v).

be used to manipulate the relative fields in the sample matrix and separation buffer and therefore, the velocity of the components in these zones [13]. When the sample matrix has lower conductivity than the separation buffer, the constituents in the sample matrix

experience an enhanced field upon application of the separation voltage. Thus, the injected analytes accelerate to form a narrower zone at the boundary of the sample matrix and separation buffer. If the sample is introduced into the column by electrokinetic injection, there is an additional benefit for improving sensitivity. The stacking process is accomplished during both sample injection and application of the separation voltage. In this study, both the alkaloids and electrolyte were positively-charged species in the sample matrix, they competed during electrophoresis into the column. From Figure 4.5, a dramatic signal enhancement (S/N enhanced a factor of 33) was observed from where the sample matrix was changed 10 mM NH₄Ac to 10 μM NH₄Ac. For high sensitivity, stacking is an attractive approach.

Nonaqueous Solvent Compositions. In order to achieve an appropriate electrophoretic resolution, organic solvents are added to the separation buffer to modify certain physicochemical properties of the analytes, such as the effective mobility and pK values [14]. Organic solvents also could modify the surface of the capillary wall leading to different EOF values. The separation of the analytes was examined by using a mixed solvent of methanol (MeOH) and acetonitrile (ACN), as MeOH varied from 50% to 100% (v/v). The result is shown in Figure 4.6. Resolution of the three alkaloids was slightly affected by the solvent compositions. Higher ACN provided better resolution for the isomers imperialine and verticinone, while more MeOH resolved verticinone and verticine better. The differentiation in electrophoretic mobilities among these compounds arises from changes of molecular size and shape in the solvent system. The increasing migration time for high MeOH solvents can be explained as the reduced EOF because EOF is proportional to the ratio of dielectric constant to viscosity, ϵ/η . (The ϵ/η for ACN

is 105.5 (cP)^{-1} , for MeOH is 60.06 (cP)^{-1} [14]). From the electropherograms, the 70% MeOH solvent system was considered as a best approach to high resolution for the three compounds of interest.

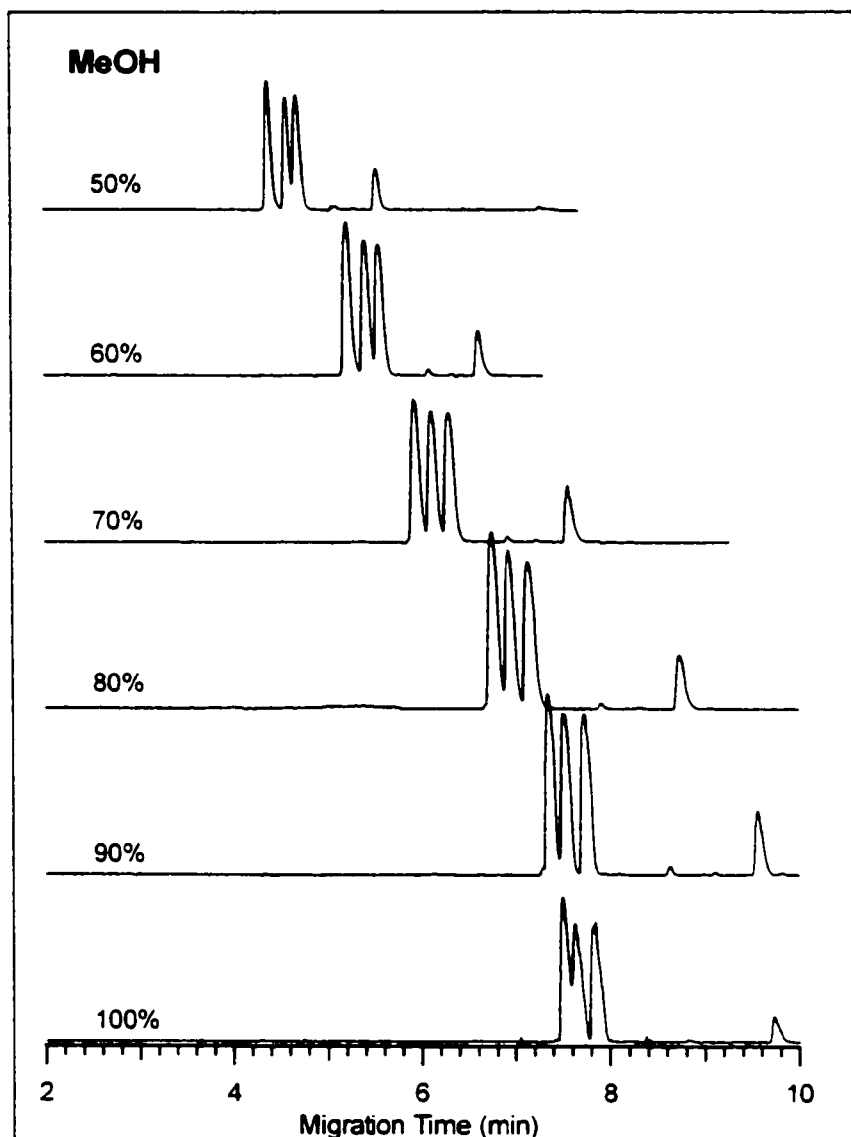


Figure 4.6 Effect of composition of MeOH and ACN on separation efficiency. Sample matrix was MeOH. The concentration of NH_4Ac in each buffer was 50 mM. The volume percentage of MeOH was depicted in the figure.

Figure 4.7 shows the electropherogram of three alkaloids and amitriptyline under the optimized conditions, and includes the mass spectrum corresponding to each individual chromatographic peak. The separation buffer was 100 mM NH₄Ac in MeOH/ACN (7/3 v/v). MeOH was chosen as the sample matrix without adding any other electrolyte to maximize the stacking effect. To retain the original separation peak shape, a fast scan rate was preferred, by reducing the mass scan range from 750 amu (scan rate 1.1 s) to 200 amu (scan rate 0.3 s). The three major alkaloids and the internal standard were baseline resolved in 10 minutes. The average number of theoretical plates for these peaks was 5.3×10^4 plates. A much higher number of theoretical plates was observed for smaller sample injection volumes. High resolution was required for further quantitative experiments since extremely similar compounds were dealt with in this case.

4.3.4 Calibration, LOD, Precision and Assays

Linear calibration curves were established for the three alkaloids. The data are summarized in Table 4.1.

Table 4. 1 Calibration data for quantitation. Linear concentration range for all the analytes was from 1×10^{-7} M to 5×10^{-6} M.

Analyte	t_m (min)	Calibration Curve (r^2)	Mean %RSD	LOD(3σ) (M)
imperialine	7.36	$Y = -0.0052 + 2.7e5x$ (0.99)	26	9×10^{-8}
verticinone	7.62	$Y = -0.0055 + 2.5e5x$ (0.99)	24	7×10^{-8}
verticine	7.88	$Y = 0.011 + 2.7e5x$ (0.99)	19	7×10^{-8}

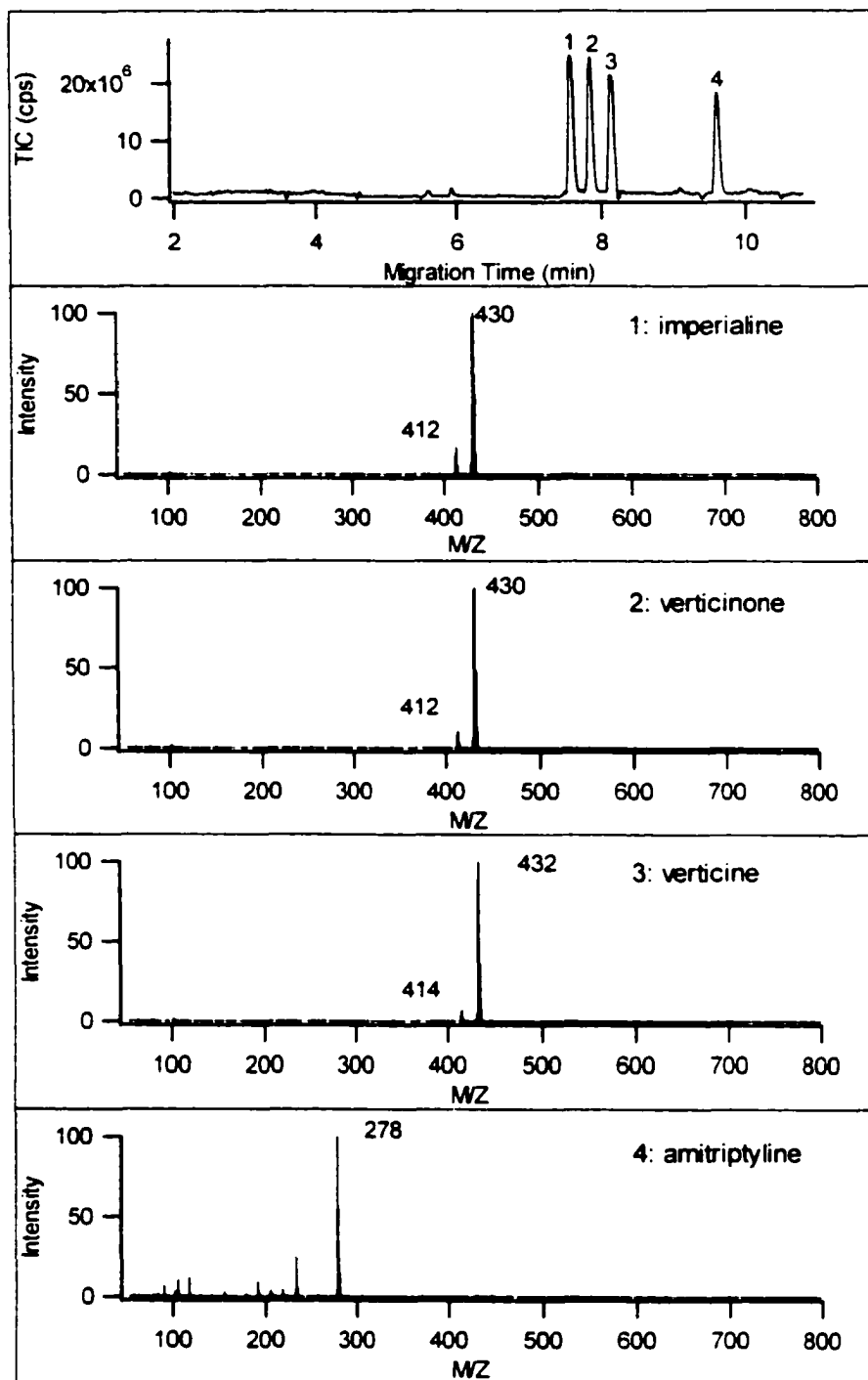


Figure 4.7 Separation of three major alkaloids and mass spectrum corresponding to each peak. Sample mixture contained 2×10^{-5} M of each alkaloid and IS in MeOH. Separation buffer was 100 mM NH_4Ac in MeOH/ACN (7/3, v/v).

The limits of detection (LOD) for all the compounds were estimated as concentrations that could generate a peak height corresponding to 3 times the signal standard deviation from a blank sample (3σ). The data points at the three lowest concentrations were used to plot peak height as a function of concentration and extrapolated to determine LOD. The concentration LOD's for imperialine, verticinone, verticine were on the order of 10^{-8} M as shown in Table 4.1.

The reproducibility of migration time within a day ($n=5$) was less than 1%. However, the RSD for peak height and peak area was between 15% to 30%. The mass signal variation was due to the intrinsic properties of the electrospray and capillary electrophoresis process. An internal standard was introduced to correct spray variations from run to run. According to Choi *et al.*'s report [15], the use of an analogue compound or an isotope analogue as an internal standard could provide better correction for variation of spray efficiency during the run. Another source of large variation might be attributed to the electrokinetic injection process. The biased sample injection arising from the competition between analyte and internal standard was corrected by using the internal standard method.

The developed method was applied to analyze the active fraction of extract and aqueous crude extract from Zhebei, one of the Beimu species grown in Zhejiang province. Figure 4.8 shows the TIC electropherogram of the active fraction of extract and the mass spectrum corresponding to each peak. The electropherogram indicates the presence of 10 compounds in the extract. The identification of each compound listed in Table 4.2 was based on the mass spectrum and further comparison with authentic standards. The profile of the active alkaloid composition provides pharmacologists strong

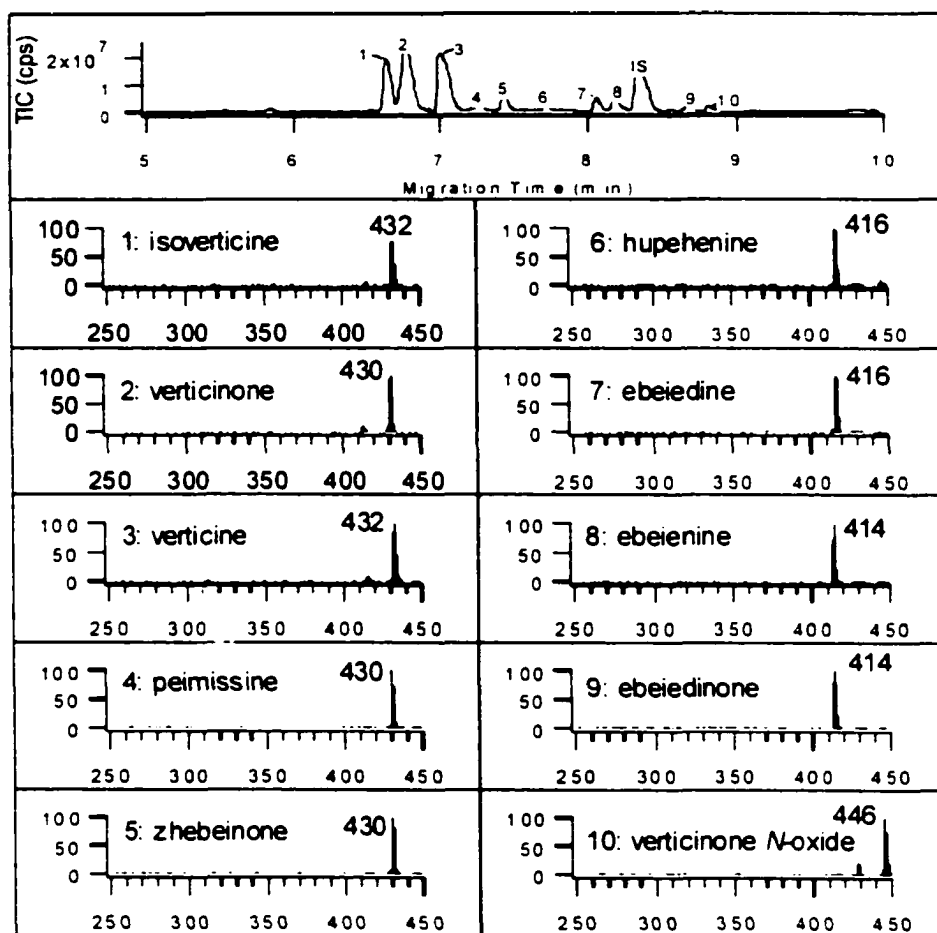


Figure 4.8 Analysis of extract of active fraction of Zhebei herb.

evidence to explain the toxicity of the active fraction extract from Beimu plants. It suggests that some unexpected toxicity of herbal medicine might be caused by different geometric isomers unidentified by traditional methods. The three major compounds were isoverticine, verticinone and verticine. All the minor isomeric components were baseline resolved and could be quantified using the same method. The previous two published HPLC/UV and GC/MS methods were unable to analyze the pairs of isomers of peimissine and zhebeinone (MH^+ 430), hepehenine and ebeiendine (MH^+ 416), ebeienine

and ebeiedinone (MH^+ 414) simultaneously due to the limited sensitivity and selectivity. Also, the chromophore labeling reaction in the LC/UV method might obviate the structural distinction between geometric isomers and result in insufficient separation efficiency of the methods. The amount of verticinone and verticine were determined as 10% and 11% in the active fraction of extract, respectively. The total active component level of verticinone and verticine combined was 21% compared to 37.5% obtained by the previous LC/UV method [2].

Table 4.2 Identification of alkaloids in active fraction extract.

Peak	Alkaloid	Migration Time (min)	Mass (MH^+)
1	isovorticine	6.63	432
2	verticinone	6.77	430
3	verticine	7.00	432
4	peimissine	7.27	430
5	zhebeinone	7.43	430
6	hupehenine	7.72	416
7	ebeiendine	8.06	416
8	ebeienine	8.18	414
9	ebeiedinone	8.67	414
10	verticine N-oxide	8.80	446

The analysis of crude extract by NACE/ESI/MS is shown in Figure 4.9. The verticinone and verticine present in crude extract was determined as 0.04% and 1.1%, which was lower than the result from the previous method. It might be due to interference

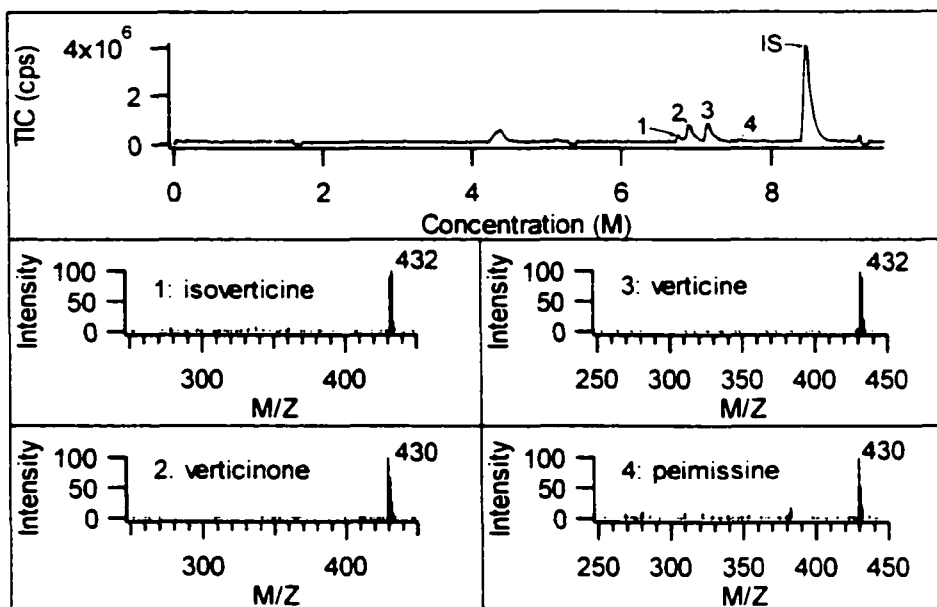


Figure 4.9 Analysis of crude extract of Zhebei herb.

of the complex matrix in the crude extract or incomplete dissolution of the crude extract in the nonaqueous solvent.

4.4 CONCLUSIONS

The present investigation demonstrated that NACE/ESI/MS may be a useful method for analysis of alkaloids presented in Beimu herbs. The developed methods determined ten geometric steroidal alkaloids. This method could be used for quality control of the Beimu plants. Due to its high sensitivity, the method could be considered as a potential analytical tool for studying metabolism of the Beimu alkaloids. However, for direct analysis of crude extract, the developed method can only provide partial

information of the alkaloid compounds dissolved in methanol. The accuracy and precision of the method still needs further improvement.

REFERENCES

1. Xu, D. M.; Xu, Y. J. *Zhong Cao Yao* 1991, 8, 132.
2. Ding, K.; Lin, G.; Ho, Y. P.; Cheng, T. Y.; Li, P. *J. Pharm. Sci.* 1996, 85, 1174.
3. Li, S. L.; Chan, S. W.; Li, P.; Lin, G.; Zhou, G. H.; Ren, Y. J.; Chiu, F. C. K. *J. Chromagr. A* 1999, 859, 183.
4. Liu, C. S.; Li, X. F.; Pinto, D.; Hansen Jr., E. B.; Cerniglia, C. E.; Dovichi, N. J. *Electrophoresis* 1998, 19, 3183.
5. Karbaum, A.; Jira, T. *Electrophoresis* 1999, 20, 3396.
6. Yang, Q.; Benson, L. M.; Jonson, K. L.; Nalor, S. *J. Biochem. Biophys. Methods* 1999, 38, 103.
7. Li, P.; Li, X. G.; Kaneko, K. *J. China Pharm. Uni.* 1990, 21, 198.
8. Li, P.; Xu, G. J.; Jin, R. L.; Xu, L. S. *J. China Pharm. Univ.* 1990, 21, 319.
9. Li, P.; Wang, Y. X.; Xu, G. *J. Phytother. Res.* 1995, 9, 460.
10. Hunter, R. J. in: *Zeta Potential in Colloidal Science*, Academic Press, London, 1981, pp 61.
11. Hjertèn, S. *Biochim. Biophys. Acta* 1959, 32, 531.
12. Chien, R. L.; Burgi, D. S. *J. Chromatogr.* 1991, 559, 141.
13. Palmer, J.; Munro, N. J.; Landers, J. P. *Anal. Chem.* 1999, 71, 1679.
14. Kenndler, E. "Organic Solvent in Capillary Electrophoresis" in: *Capillary Electrophoresis*, Ed. Guzman, N. A., Marcel Dekker, Inc. 1993, pp 161.
15. Choi, B. K.; Gusev, A. I.; Hercules, D. M. *Anal Chem.* 1999, 71, 4107.

CHAPTER 5

CAPILLARY ELECTROPHORETIC SEPARATION OF POLYCYCLIC AROMATIC HYDROCARBONS USING SODIUM CHOLATE IN MIXED AQUEOUS-ORGANIC BUFFERS*

* A version of this chapter has been published. *J. Chromatogr. A* **1998**, **817**, 307-311.

5.1 INTRODUCTION

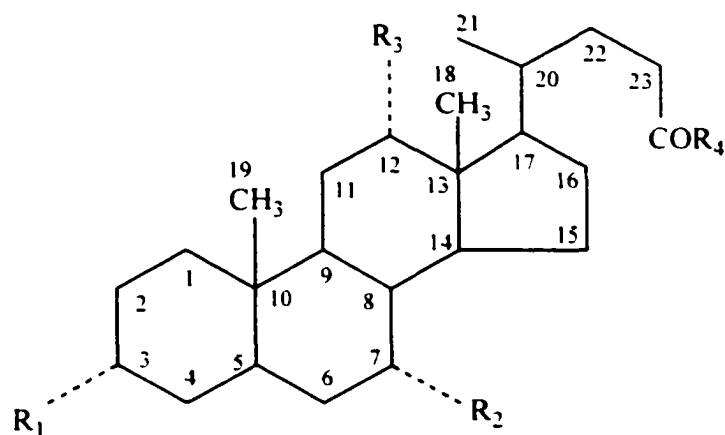
Polycyclic aromatic hydrocarbons (PAHs) are environmentally and biologically important species due to their mutagenic and carcinogenic properties [1]. PAHs are produced during burning of organic matter. Human exposure might occur through diet, smoking, or polluted air. PAHs are highly hydrophobic compounds and dissolve in fat as well as in aromatic solvents. Traditional methods for analyzing these pollutants include gas chromatography and high-performance liquid chromatography [2,3].

Capillary electrophoresis (CE) is an attractive method for analyzing ionic species. The use of surfactants included in the buffers enables the electrophoresis of neutral analytes such as polychlorinated biphenyl or polyaromatic hydrocarbons [4-8]. A number of difficulties are encountered in the analysis of these highly hydrophobic analytes, including long migration times, low efficiencies and poor resolution. The poor selectivity is due to the complete inclusion of highly hydrophobic analytes by the micellar phase formed from the surfactants. The separation can be improved by use of organic additives [9,10]. Cyclodextrins (CyDs) have also been used alone [11] or in the presence of micelles [5,8] to reduce analysis times and improve resolution. A series of eight PAHs has been separated using γ -CyD and sodium dodecyl sulphate (SDS), with urea as a modifier [5]. The limitations of CyDs include poor water solubility for some CyDs and their relatively high cost.

More recently, bile salts, synthesized by liver, have been used instead of long-chain surfactants for separating a range of neutral analytes, as well as for chiral separation, owing to their detergent-like characteristics [12-16]. Bile salts such as cholate, deoxycholate or taurodeoxylate, are composed of a cholesterol skeleton with two to

three hydroxyl groups in different positions (3,7,12) and with α orientations as shown in Figure 5.1. All the polar hydroxyl groups are nearly perpendicular to the cholesterol frame, forming the hydrophilic phase of the bile salts. The cholesterol skeleton, the opposite hydrophobic phase, can form small helical aggregates with aggregation number from 2 to 20, with a conformation that exposes hydroxyl and charged functional groups to the aqueous solution [13]. The smaller size of the aggregates and different hydrophilicity/hydrophobicity ratios allow bile salts to interact with analyte species to a different extent compared to long-chain surfactant aggregates. In the case of highly hydrophobic analyte, bile salts could reduce partitioning and thus lead to faster and more efficient separations. In addition, the manner of analyte interaction with bile salts is different from the long chain surfactant aggregates, therefore different selectivities may be possible. Bile salts have been applied to the CE separation of some particular PAHs under a limited range of experiment conditions. Cole *et al.* showed a CE separation of anthracene, pyrene and benzo[a]pyrene in 50 mM/L sodium cholate plus 0-20% methanol using laser induced fluorescence detection [13]. Dabek-Zlotorzynska and Lai showed the effect of 0-30% (v/v) acetone in 50 mM/L sodium taurodeoxylate on the CE separation of 16 PAHs using UV detection at 214 nm [16].

In this chapter the analysis of 16 PAHs is described using CE with sodium cholate (20-60 mM) in the presence of methanol and acetonitrile at a total concentration of up to 70% (v/v), ethanol (30-50%), urea (3.2-6.8 mM) or methylene chloride (1%). Parameters that were examined as a function of buffer composition included analyte migration times, resolution and efficiency.



Bile Salts	R ₁	R ₂	R ₃	R ₄
sodium cholate	OH	OH	OH	ONa
sodium deoxycholate	OH	H	OH	ONa
sodium taurodeoxycholate	OH	H	OH	NHCH ₂ CH ₂ SO ₃ Na

Figure 5.1 Structure of bile salts

5.2 EXPERIMENTAL

5.2.1 Reagents and Materials

Sixteen PAHs were purchased from Aldrich (Milwaukee, WI, USA). Listed in the order of increasing molecular mass and hydrophobicity are 1) naphthalene. 2) acenaphthylene. 3) acenaphthene. 4) fluorene. 5) phenanthrene. 6) anthracene. 7)

fluoranthene, 8) pyrene, 9) benzo[a]anthracene, 10) chrysene, 11) benzo[b]fluoranthene, 12) benzo(k)fluoranthrene, 13) benzo(a)pyrene, 14) dibenzo[a,h]anthracene, 15) benzo[g,h,i]perylene and 16) indeno[1,2,3-cd]pyrene. The stock solutions of individual PAHs were prepared to 100 ppm in dichloromethane / methanol (1/1, v/v). The mixture standards of 16 PAHs were obtained from Supelco and diluted to 50 ppm with dichloromethane / methanol (1/1, v/v). Sodium cholate, deoxycholate, and tautodeoxycholate were purchased from Sigma (St. Louis, MO, USA) and prepared to 0.2 M with nanopure deionized water. Methanol and acetonitrile were HPLC grade and were obtained from BDH (Toronto, Canada). Buffer solutions were prepared by mixing different initial volumes of methanol, acetonitrile, and stock inorganic buffer solution (10.7 mM NaH₂PO₄ - 18 mM Na₂B₄O₇), sodium cholate and water.

The capillaries with 50 µm inner diameter and 182 µm outer diameter were purchased from Polymicro Technologies (Phoenix, AZ, USA).

5.2.2 Instrumentation

A CE instrument constructed in-house with a thermo-optical UV absorbance detection system was used in all experiments. The details of the instrument configuration were described in Chapter 1 of this thesis.

The capillary columns were 60 cm long and the detection window was located 55 cm from the injection end. Sample injections were conducted by hydrostatic injection for 15 sec. over a height of 4 cm. The electrophoresis was performed under positive mode with high potential applied at the inlet vial and ground potential at the outlet vial.

5.2.3 Calculations

Analyte migration mobilities (μ_{mig}) were calculated from:

$$\mu_{eo} = \frac{Ll}{Vt_{eo}} \quad (\text{Eq. 5.1})$$

where L is capillary length (cm), l is the capillary length to the detection window, V is voltage for electrophoresis (V), and t is analyte migration time (s).

Electroosmotic mobilities (μ_{eo}) were calculated from above equation using the migration time (t_{eo}) of methanol (neutral marker).

Since the net migration mobility (μ_{mig}) of an individual PAH depends the difference between the electroosmotic flow mobility (μ_{eo}) and electrophoretic mobility (μ_{ep}), the μ_{ep} is:

$$\mu_{ep} = \mu_{eo} - \mu_{\text{mig}} \quad (\text{Eq.5.2})$$

5.3 RESULTS AND DISCUSSION

5.3.1 Effect of Bile Salt Type and Concentration

The effect of sodium cholate concentration in mixed 20% methanol, 20% acetonitrile solvent on analyte migration time is shown in Figure 5.2 The critical micelle concentration (CMC) of sodium cholate is 12.5 mM [17]. The presence of methanol at this concentration was not expected to influence the cholate CMC, which has been shown to be approximately constant over 0-30% (v/v) methanol [13]. As Figure 5.2 indicates,

the migration times increased 54% for naphthalene and 104% for benzo[g,h,i]perylene with increasing cholate concentration over the range of 20-60 mM, except at 40 mM, indicating a low selectivity. The migration window at 60 mM was about 20 min., three times that at 20 mM. The longer migration times at high concentration of sodium cholate were mostly caused by the slower μ_{e0} and enhanced analyte interaction. The migration time of electroosmotic flow (EOF) marker increased 45% over the range of 20-60 mM sodium cholate. The trend of EOF mobility as a function of cholate concentration is similar to the one previously reported for deoxycholate [12], caused by reduced thickness of the electrical double layer in the presence of high concentrations of cholate. Since the cholesterol skeletons from bile salts are negatively charged, contributions of wall adsorption toward decreasing EOF is minimal, as previous studies with SDS have indicated.

Resolution and efficiency improved at cholate concentrations greater than 40 mM. The working concentration of cholate was chosen to be 60 mM as an upper limit, since increased background noise, presumably due to light scattering, was observed at higher cholate concentrations.

The effect of long-chain alkyl surfactant concentrations on μ_{ep} of PAHs was reported by Shi and Fritz [18]. They found a trend of continuously increasing μ_{ep} with increasing sodium dioctyl sulfosuccinate (DOSS) concentration within a range of 10 mM to 80 mM. This result could be caused by more complete association of PAH with the DOSS phase as the micelle concentration grows. Unlike traditional surfactants, with limited variation in CMC and micelle structure, bile salts aggregate over a broad range of concentrations, with a progressive increase in the micellar size and modification of

micellar structure [13]. Figure 5.3 shows the effect of sodium cholate concentration on the μ_{ep} . The μ_{ep} of all analytes produce a zigzag plot with increasing surfactant concentration. The shape is hard to interpret but suggests that mixed micelles may form, with varied inclusion characteristics with analytes. Furthermore, the large mass PAHs, having higher hydrophobicities, tend to be effected to a greater extent than molecules with low hydrophobicity. Although the mechanism of partition of hydrophobic compounds into bile salt micelles was not the major purpose of this study, the observed phenomenon obviously raised an interesting question for future investigation.

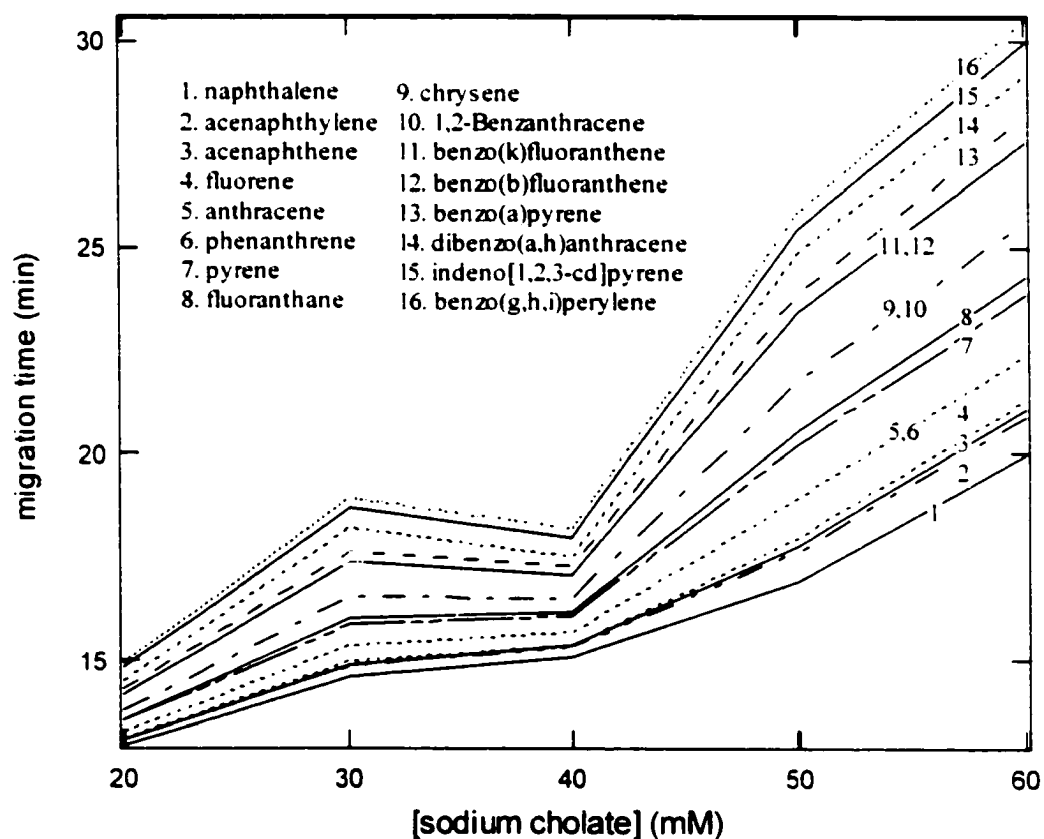


Figure 5.2 Plot of migration times vs. sodium cholate concentration (20-60 mM). Buffer composition: 20% (v/v) methanol and 20% (v/v) acetonitrile in 10.7 mM NaH_2PO_4 - 1.8 mM $\text{Na}_2\text{B}_4\text{O}_7$. The electric field was 250 V/cm.

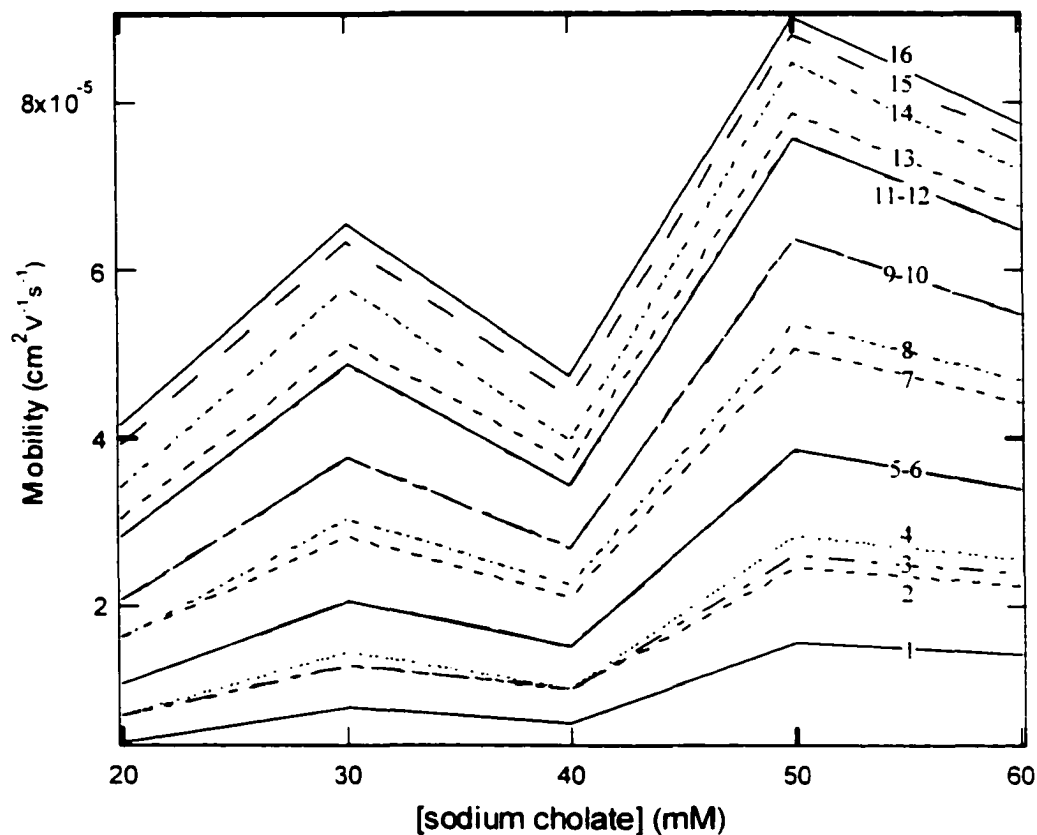


Figure 5.3 Plot of electrophoretic mobility vs. sodium cholate concentration (20-60 mM). Buffer composition: 20% (v/v) methanol and 20% (v/v) acetonitrile in 10.7 mM NaH_2PO_4 -1.8 mM $\text{Na}_2\text{B}_4\text{O}_7$. The electric field was 250 V/cm. The label of analytes is as same as indicated in Figure 5.2.

5.3.2 Effect of Organic Modifiers

Organic additives such as methanol, acetonitrile, and urea have been used in MEKC to widen the elution window and manipulate selectivity and resolution [9, 19-21]. Increasing the concentration of methanol or acetonitrile leads to higher solvent strength

and reduced aggregation numbers, which moderates interactions between the hydrophobic analyte and the surfactant.

The influence of methanol concentration on PAH electrophoretic mobilities is shown in Figure 5.4. It shows that the electrophoretic mobilities of all analytes decrease as the volume ratio of methanol increases in the buffer. Similar behavior was also found in CZE [22] and MEKC [18] with organic additives in the buffer. It was mainly attributed to three factors including 1) the concomitant increase in viscosity, 2) stronger solvation of analytes into mixed aqueous-organic phase, 3) less association of analytes with micelles. It is found in the literature for methanol concentrations higher than 30% in the buffer, the CMC for sodium cholate increases, leading to reduced micellar concentrations for partitioning [13]. This phenomenon might be applied to this experiment, because under 70% methanol, the concentration of sodium cholate was 12 mM, lower than the CMC in water. It was also found that lower methanol concentrations were more favored for resolving the low mass PAHs (analytes 1-4), while creating strong tailing peaks for higher mass PAHs. The condition of 30% methanol produced best separation for higher mass PAHs (analytes 11-16).

In the case of acetonitrile, similar profiles of μ_{ep} versus concentration of acetonitrile (10-50%, v/v) were observed, shown in Figure 5.5. It can be explained as the same effect due to methanol. A notable difference between Figures 5.4 and 5.5 are the considerably higher μ_{ep} observed with acetonitrile, due to its lower viscosity than methanol. ($\eta_{\text{MEOH}}=0.5445$, $\eta_{\text{ACN}}=0.3409$). More than 10% methanol was required for sufficient dissolution of PAHs, otherwise the peaks were broad and showed tailing.

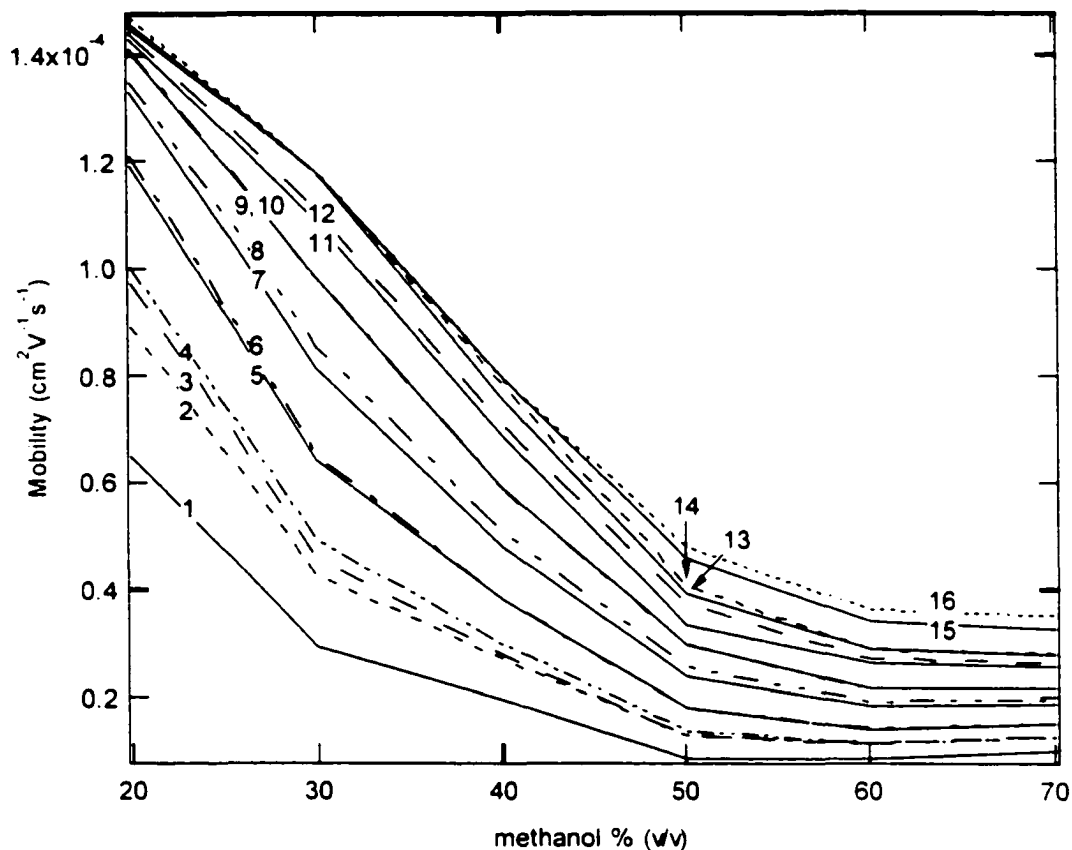


Figure 5.4 Plot of analyte electrophoretic mobility vs. percent of methanol (v/v) in separation buffer (20-70%). Buffer composition: 40 mM sodium cholate - 10.7 mM NaH_2PO_4 - 1.8 mM $\text{Na}_2\text{B}_4\text{O}_7$. Electric field was 250 V/cm. Compounds are numbered as in Figure 5.2.

Two different buffer compositions gave reasonably good separations on 16 PAHs. A 60 mM sodium cholate - 20% acetonitrile buffer produced a fast separation of the mixture (Figure 5.6A), which was better for resolving low molecular weight PAHs. On the other hand, 50 mM sodium cholate - 60% methanol produced a better separation for higher mass PAHs, but took twice as long (Figure 5.6B). Separation efficiencies under these conditions were found to be 1.05×10^5 plates for indeno[1.2.3-cd]pyrene. Some of

the peak orders were reversed in the above two buffer systems due to the effect of organic solvent properties on bile salt micelle characteristics.

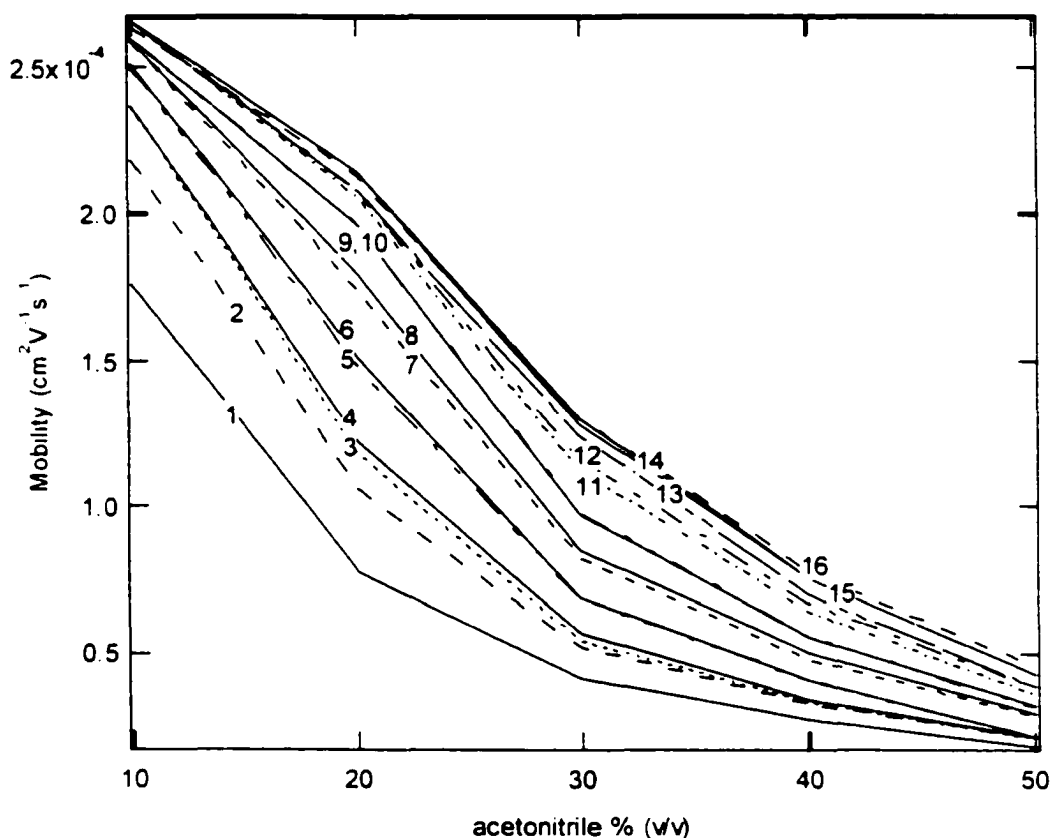


Figure 5.5 Plot of analyte electrophoretic mobility vs. percent of acetonitrile (v/v) in separation buffer (10-50%). Buffer composition: 50 mM sodium cholate- 10.7 mM NaH_2PO_4 -1.8mM $\text{Na}_2\text{B}_4\text{O}_7$. Electric field was 250 V/cm. Compounds are numbered as in Figure 5.2.

A number of experiments were performed to evaluate the effects of ethanol (3%-50%, v/v), urea (3.2-6.8M) and methylene chloride (1%) on the PAH separation (data not shown). Ethanol (50%) was effective in resolving as many as 14 PAHs at the expense of long separation times, >80 min. These excessive analysis times were most likely due to

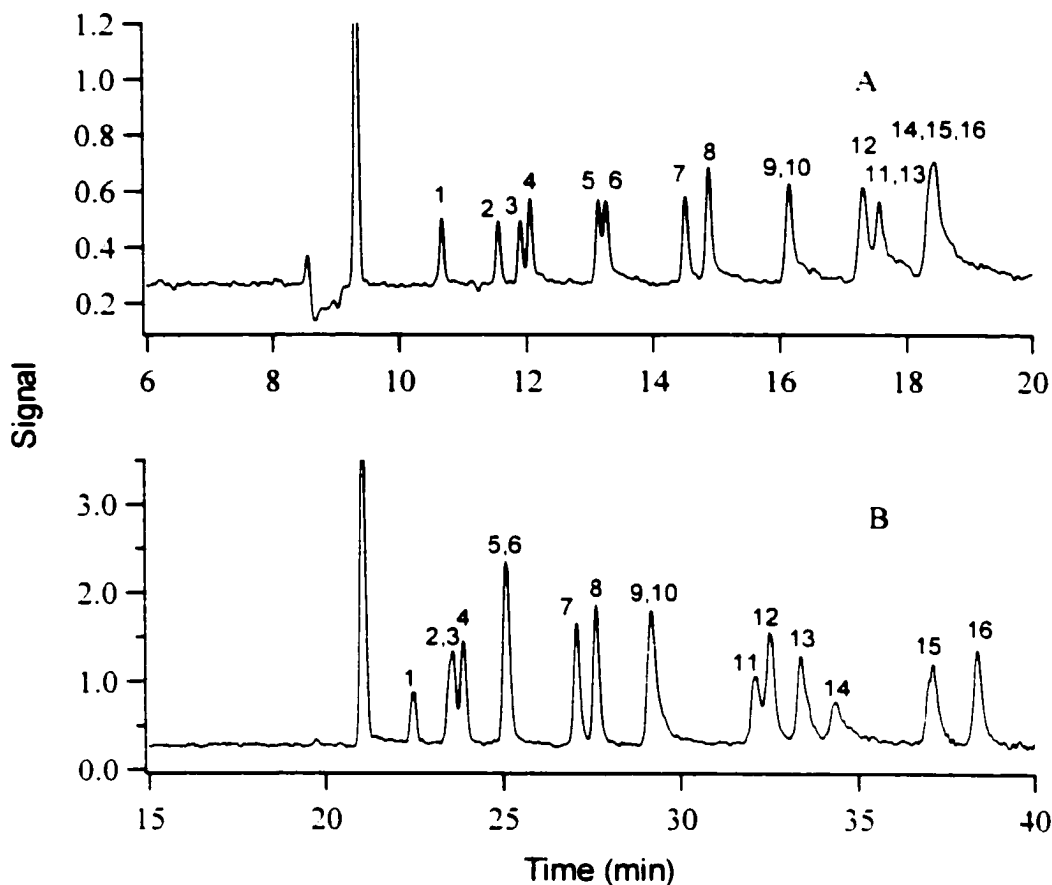


Figure 5.6 Electropherograms of 50 ppm PAHs at an electric field of 300 V/cm using A: 60mM sodium cholate - 20% acetonitrile. B: 50mM sodium cholate - 60% methanol. Peak identification: 1= naphthalene, 2= acenaphthylene, 3= acenaphthene, 4= fluorene, 5= phenanthrene, 6= anthracene, 7= pyrene, 8= fluoranthene, 9= benzo[a]anthracene, 10= chrysene, 11= benzo[k]pyrene, 12= benzo(b)fluoranthrene, 13= benzo(a)Pyrene, 14= dibenzo[a,h]anthracene, 15= indeno[1.2.3-cd]pyrene, and 16= Benzo[g,h,i]perylene

the exceedingly low electroosmotic flow rates associated with ethanol in comparison to both methanol and acetonitrile at equimolar concentration.

Urea has been used in MEKC to increase the aqueous solubility of sparingly soluble analytes and/or additives [8,10]. In this study, urea concentrations lower than 6.8 M improved resolution, particularly for the higher-molecular mass PAHs. A total of 13 peaks were observed without compromising analysis time (about 12 min). Above 6.8 M, poor resolution was observed for most analyte species and broad peaks for higher molecular mass PAHs. Excess urea was effective in solubilizing the PAHs in the aqueous phase, thus diminishing their interactions with the bile salt aggregates. When 1% (v/v) methylene chloride was used to aid PAH solubility in the buffer, precipitation of electrolytes was observed.

5.3.3 Effect of Buffer Concentration and pH

Buffer concentrations of 10.7-21.4 mM of NaH_2PO_4 and 1.8-3.6 mM $\text{Na}_2\text{B}_4\text{O}_7$ in the presence of 60 mM sodium cholate plus 20% methanol and 20% acetonitrile showed no selectivity differences, although resolution improved at lower buffer concentrations (data not shown). Such resolution improvements at lower buffer concentrations were probably due to an aggregation size decrease at lower ionic strengths [23] because of less charge shielding and thus greater repulsion between cholate monomers. The smaller aggregate size probably allows for greater analyte differentiation and thus improved resolution.

Changes in pH over the range 6.8-9.2 had little effect on analyte migration times and resolution (data not shown). Cholic acid has a $\text{p}K_a$ ($\text{p}K_a$, 6) that is outside that range:

the pH of the buffer is not expected to influence aggregate properties or pseudo-stationary phase rate and direction of migration [24].

5.4 CONCLUSION

Capillary electrophoresis with bile salts in mixed organic modifier media is a cost-effective and efficient analytical method for separation of polyaromatic hydrocarbons. The formation of the multi-conformational bile aggregates induced by concentration of sodium cholate results in a partition variation for polyaromatic hydrocarbons. Choice of methanol, acetonitrile, and their concentrations in the separation buffer allows resolution of low or high molecular weight polyaromatic hydrocarbons at different conditions. The ability to sustain bile aggregate formation in the presence of a relatively large concentration (70% v/v) of organic solvents, and to therefore moderate the hydrophobic partition of PAHs, offers a promising approach for separation of a wide range of hydrophobic species. Further studies should address the mechanism of analyte interaction with bile salt micelles.

REFERENCES

1. *Test Methods for Evaluating Solid Waste (SW-846)*, Vol. IB. US Environmental Protection Agency, Washington, DC, 3rd Ed., November 1986, proposed update II, Rev. 2, November, 1992.
2. Olufsen, B. S.; Bjorseth, A. in: *Handbook of Polycyclic Aromatic Hydrocarbons*, Bjorseth, A. Ed. Marcel Dekker, New York, 1983, pp 257-300.
3. Wise, S. A. in: *Handbook of Polycyclic Aromatic Hydrocarbons*, Bjorseth, A. Ed. Marcel Dekker, New York, 1983, pp 183-256.
4. Terabe, S.; Otsuka, K.; Ando, T. *Anal. Chem.* 1985, 57, 834.
5. Burton, D. E.; Sepaniak, M. J.; Maskarinec, M. P. *J. Chromatogr. Sci.* 1987, 25, 514.
6. Strasters, J. K.; Khaledi, M. G. *Anal. Chem.* 1992, 63, 2503.
7. Khaledi, M. G.; Smith, S. C.; Straster, J. K. *Anal. Chem.* 1991, 63, 1820.
8. Terabe, S.; Miyashita, Y.; Ishihama, Y.; Shibata, O. *J. Chromatogr.* 1993, 636, 47.
9. Gorse, J.; Balachunas, A. T.; Swaile, D. F.; Sepaniak, M. J. *High. Resolut. Chromatogr. Commun.* 1988, 11, 554.
10. Terabe, S.; Ishihama, Y.; Nishi, H.; Fukuyama, T. Otsuka, K. *J. Chromatogr.* 1991, 545, 359.
11. Terabe, S.; Ozaki, H.; Otsuka, K.; Ando, T. *J. Chromatogr.* 1985, 332, 211.
12. Nishi, H.; Fukuyama, T.; Matsuo, M.; Terabe, S. *J. Chromatogr.* 1990, 498, 313.
13. Cole, R. O.; Sepaniak, M. J.; Hinze, W.; Gorse, J.; Oldiges, K. *J. Chromatogr.* 1991, 557, 113.
14. Nishi, H.; Fukuyama, T.; Matsuo, M.; Terabe, S. *J. Chromatogr.* 1990, 515, 233.

15. Nishi, H.; Fukuyama, T.; Matsuo, M.; Terabe, S. *J. Microcol. Sep.* 1989, 1, 234.
16. Dabek-Zlotorzynska, E.; Lai, E. P. C. *J. Cap. Electrophoresis* 1996, 3, 31.
17. Nishi, H. Terabe, S. *J. Chromatogr. A* 1996, 735, 3.
18. Shi, Y.; Fritz, J. S. *Anal Chem.* 1995, 67, 3023.
19. Gil, M. I.; Ferreres, F.; Tomasbarberan, F. A. *J. Liq. Chromatogr.* 1995, 18, 3007.
20. Renougonnord, M. F.; David, K. *J. Chromatogr. A* 1996, 735, 249.
21. Vanorman, B. B.; Liversidge, G. G.; McIntire, G. L.; Olefirowicz, T. M.; Ewing, A.G. *J. Microcol. Sep.* 1990, 2, 176.
22. Zhang, C.; Heeren, F. V.; Thormann, W. *Anal. Chem.* 1995, 667, 2070.
23. Hylemon, P. B. in: *Sterols and Bile Acids*, Neuberger, A.; Van Deenen, L. L. M. Eds. Elsevier, Amsterdam, 1985, pp 372.
24. Otsuka, K.; Terabe, S. *J. Microcol. Sep.* 1989, 1, 150.

CHAPTER 6

MIGRATION TIME CORRECTION FOR ANALYSIS OF DERIVATIZED AMINO ACIDS AND OLIGOSACCHARIDES USING MICELLAR ELECTROKINETIC CHROMATOGRAPHY*

* A version of this chapter has been published. *J. Chromatogr. A* **2000**, 869, 375.

6.1 INTRODUCTION

Capillary electrophoresis is a powerful analytical tool that produces rapid and extremely high-resolution separations of complex mixtures [1-2]. In many applications, components in a sample are identified by comparing their migration time vs. the migration time of known standards. Migration time drifts can cause identification errors, particularly for components with small migration time differences. While component identities can be confirmed by co-migration with an authentic standard, this procedure requires at least two electrophoresis runs. It is preferable to ensure sufficient migration time reproducibility between runs so that a sample separation can be directly compared with a standard separation.

Several groups have proposed methods to improve migration time reproducibility. Lee and Yeung [3] used an adjusted migration index to improve the migration time precision. This method requires accurate knowledge of the internal diameter of the capillary, which is not easy to obtain with current capillary production technology. Bocek and coworkers [4] proposed the use of migration times of two standards and an unknown to determine the electrophoretic mobility (μ_{ep}) of the unknown. Jumppanen and Riekkola [5] developed a similar method using up to four markers of known μ_{ep} . Those authors [4-5] demonstrated significant improvement in migration time reproducibility with relative standard deviations as low as 0.01% after correction. However, for these methods the μ_{ep} of the markers must be known, which requires determination of the μ_{ep} of the markers in a specific separation system. Other methods such as relative migration time and relative

mobility have also been studied [6-7]. Palmer and Vandeginste [8] found that the relative mobility of the analyte to the reference standard gave better reproducibility than the relative migration time and actual mobility methods.

Dovich's group has considered three analyses that are particularly sensitive to variations in migration time. First, they have reported the use of CE to identify the phenylthiohydantoin (PTH)-amino acid derivatives produced by the classic Edman degradation reaction [9-11]. There are 22 components commonly observed in this reaction: 19 amino acids (cysteine is not stable in the reaction) plus three common impurities (diphenylthiourea, dimethylphenylthiourea, and diphenylurea). Most of these components are neutral and their separation requires the use of MEKC. Several components produce closely spaced peaks whose identification requires very precise migration times.

Second, they have performed similar studies based on a fluorescent Edman reagent that produces fluorescein thiohydantoin (FTH)-amino acids [12-13]. The identification of these components is more challenging than for the PTH-amino acids. The bulky fluorescein group dominates the mobility of each component. The best separation conditions require careful adjustment of the buffer pH to near the pK_a of fluorescein; the amino acid side-chains modulate the pK_a of the derivative, facilitating separation based on differences in ionization at the pH of the separation. The migration times are sensitive to slight changes in buffer pH and ionic strength.

Third, they have studied a set of metabolic products generated by biosynthesis and biodegradation of fluorescently labeled oligosaccharides [14-17]. Some of the biosynthetic products are very similar in structure, and their separation is based on

complexation with boric and phenylboronic acids and partitioning into SDS micelles. The separation of the components requires a relatively long time and produces a set of closely spaced peaks. The identification of these products is sensitive to slight changes in migration time.

In this chapter, I report two methods to correct for variations in migration time. The first method corrects for variation in electroosmotic mobility (μ_{eo}) while the second method corrects for variations in both μ_{eo} and μ_{ep} .

6.2 THEORY

In capillary electrophoresis, the migration time of an analyte x is given by:

$$t_x = \frac{LL_{eff}}{V[\mu_{eo} + \mu_{ep,x}]} \quad \text{Eq. (6.1)}$$

where L_{eff} is the effective length of the capillary from inlet to the detection window. L is the total length of the capillary. V is the applied potential. μ_{eo} is the electroosmotic mobility, and $\mu_{ep,x}$ is the electrophoretic mobility of the analyte.

6.2.1 Method 1: A single marker (m) is used to eliminate the effect of variations in electroosmotic flow from run to run. To perform this one-marker correction, I first obtain

a standard electropherogram containing the marker and the analyte of interest. The overall electrophoretic mobility of the marker is given by:

$$\mu_{overall,m} = \mu_{eo} + \mu_{ep,m} = \frac{LL_{eff}}{V\hat{t}_m} \quad \text{Eq. (6.2)}$$

where $\mu_{ep,m}$ is the electrophoretic mobility of the marker.

If only electroosmotic flow varies between runs, then the overall mobility of the marker under nonstandard conditions is given by:

$$\hat{\mu}_{overall,m} = \mu_{eo} + \Delta\mu_{eo} + \mu_{ep,m} = \frac{LL_{eff}}{V\hat{t}_m} \quad \text{Eq. (6.3)}$$

where $\hat{\mu}$ is the observed mobility under the nonstandard conditions, \hat{t} is the observed migration time, and $\Delta\mu_{eo}$ is the change in electroosmotic mobility.

The change in electroosmotic mobility is given by:

$$\hat{\mu}_{overall,m} - \mu_{overall,m} = \Delta\mu_{eo} = \frac{LL_{eff}}{V\hat{t}_m} - \frac{LL_{eff}}{V\hat{t}_m} \quad \text{Eq. (6.4)}$$

The corrected mobility of component x is given by:

$$\hat{\mu}_{overall, x} - \Delta\mu_{eo} = \frac{LL_{eff}}{V\hat{t}_x} - \left[\frac{LL_{eff}}{V\hat{t}_m} - \frac{LL_{eff}}{Vt_m} \right] = \frac{LL_{eff}}{Vt_{corrected, x}} \quad \text{Eq. (6.5)}$$

The corrected migration time is given by:

$$t_{corrected, x} = \left[\frac{1}{\hat{t}_x} - \left(\frac{1}{\hat{t}_m} - \frac{1}{t_m} \right) \right]^{-1} \quad \text{Eq. (6.6)}$$

6.2.2 Method 2: In the one-marker correction method, only the change in electroosmotic flow from run to run was considered. A two-marker method considers variations in both μ_{eo} and μ_{ep} . μ_{ep} might change due to a change in the mobility of the micelle in MEKC, a change in viscosity that accompanies a temperature change, *etc.*

Under standard conditions, the overall mobility is given by Equation 3. Under nonstandard conditions, the overall mobility is:

$$\hat{\mu}_{overall} = \mu_{eo} + \Delta\mu_{eo} + \gamma\mu_{ep} \quad \text{Eq. (6.7)}$$

where γ is the fractional change in μ_{ep} , by definition $\gamma = 1$ in the standard electropherogram. Here it is assumed that the μ_{ep} changes proportionally for all components, so that γ is the same for all components in any run.

The difference between the overall mobility of an analyte (x) and the overall mobility of marker 1 (m_1) in standard conditions is independent of the μ_{eo} :

$$\hat{\mu}_\tau - \mu_{m_1} = \mu_{ep,\tau} - \mu_{ep,m_1} \quad \text{Eq. (6.8)}$$

Similarly, the difference in overall mobility between the components under nonstandard conditions is given by:

$$\hat{\mu}_\tau - \hat{\mu}_{m_1} = \gamma [\mu_{ep,\tau} - \mu_{ep,m_1}] \quad \text{Eq. (6.9)}$$

γ is evaluated from the ratio of the differences in mobility:

$$\gamma = \frac{\hat{\mu}_{m_1} - \hat{\mu}_\tau}{\mu_{m_1} - \mu_\tau} = \frac{\frac{1}{\hat{t}_{m_1}} - \frac{1}{\hat{t}_\tau}}{\frac{1}{t_{m_1}} - \frac{1}{t_\tau}} \quad \text{Eq. (6.10)}$$

γ is constant for all components in the sample. In practice, it is calculated by comparing the migration times of the two markers that were added to the separation mixture:

$$\gamma = \frac{\frac{1}{\hat{t}_{m_1}} - \frac{1}{\hat{t}_{m_2}}}{\frac{1}{t_{m_1}} - \frac{1}{t_{m_2}}} \quad \text{Eq. (6.11)}$$

Ideally, these two markers differ widely in their migration times in order to improve the precision of the calculation.

The corrected migration time of an analyte is then determined by rearranging equation (6.10):

$$t_{corrected} = \left[\frac{1}{t_{m_1}} - \frac{1}{\gamma} \left(\frac{1}{\hat{t}_{m_1}} - \frac{1}{\hat{t}_r} \right) \right]^{-1} \quad \text{Eq. (6.12)}$$

6.3 EXPERIMENTAL

6.3.1 PTH-Amino Acids

The determination of PTH-amino acids was reported elsewhere [9-11]. Briefly, the fused-silica capillary was 40 cm in total length ($L_{eff} = 35$ cm), 50 μm i.d. and 185 μm o.d. This capillary was preconditioned by gravity flow of the running buffer for 24 h. The separation was performed at 10 kV running voltage with 15 s hydrodynamic injection. The running buffer (pH = 6.8) was composed of 10.7 mM sodium phosphate, 1.8 mM sodium borate, and 25 mM sodium dodecylsulfate (SDS).

The mixture of 19 PTH-amino acids, diphenylthiourea (DPTU), dimethylphenylthiourea (DMPTU), and diphenylurea (DPU) was purchased from Applied Biosystems (Foster City, CA). A working solution (2.5×10^{-5} M) of each PTH-amino acid was prepared by diluting the stock solution (1×10^{-4} M in acetonitrile) in running buffer. The fused-silica capillary was purchased from Polymicro Technologies Inc.

6.3.2 FTH-Amino Acids

The FTH amino acid standards were prepared by adding 20 μL of an aqueous solution containing 0.01 M of each individual amino acid (Sigma, Oakville Canada) and 20 μL of 1×10^{-3} M fluorescein isothiocyanate (Molecular Probes, Eugene OR) solution in HPLC-grade acetone (Aldrich, Milwaukee, WI USA) into 120 μL of a 0.2 M carbonate buffer at pH 9.1 [12-13]. The solution was mixed and then stored at room temperature in the dark for six to eight hours to complete the reaction. No wash or extraction steps were performed. The thiazolinone intermediate was converted to the FTH amino acid by adding 120 μL of neat trifluoroacetic acid (Caledon, Edmonton, Canada) to each reaction vial and reacting for 12 h in the dark. The mixture was then evaporated on a Speed Vac (Fisher, Edmonton Canada) to obtain a dry FTH-amino acid, which was dissolved in 500 μL of HPLC-grade acetonitrile (Aldrich) to give an approximate 4×10^{-5} M solution and stored at 4 $^{\circ}\text{C}$ until needed. The concentration of the stock solution was calculated assuming the reaction yields were 100%.

To prepare the working solution of mixed FTH-amino acids, a 5 μL aliquot of each stock solution was added to a vial, and the mixture was made up to 500 μL with acetonitrile to give a 4×10^{-7} M solution. The mixture was diluted 100-fold again with running buffer to obtain a solution containing 18 FTH-amino acids, each at approximately 4×10^{-9} M. Cysteine was not included in this solution because it was not stable in the reaction. Lysine was not included because of side reactions involving the ϵ -amine. Because no extraction was used, some by-products were present in this solution; they have not been identified.

The instrument for FTH-amino acid analysis was described elsewhere [17]. The separation buffer (pH 6.86) was composed of 15 mM sodium dihydrogen phosphate, 3.75 mM sodium tetraborate, 7.7 mM SDS, and 2.0 mM magnesium acetate. The working solution was electrokinetically injected at 540 V for 2 s and separated in a 60 cm long, 30 μm i.d., and 150 μm o.d. capillary at 18 kV.

6.3.3 Tetramethylrhodamine-Labeled Oligosaccharides

A tetramethylrhodamine (TMR) labeled disaccharide, $\beta\text{Gal}(1\rightarrow4)\beta\text{GlcNAc-O---TMR}$ (LacNAc), was used as a substrate. The biodegradation of LacNAc-O---TMR by galactosidase gives N-acetyl- β -D-glucosaminide-O---TMR (GlcNAc), and further degradation by hexosaminidase gives $\text{HO}(\text{CH}_2)_6\text{CONHCH}_2\text{CH}_2\text{NHCO---TMR}$ (Linker arm: -O---TMR). Biosynthesis by fucosyltransferases can result in the formation of $\alpha\text{Fuc}(1\rightarrow2)\beta\text{Gal}(1\rightarrow4)\beta\text{GlcNAc-O---TMR}$ (H-Type II), $\beta\text{Gal}(1\rightarrow4)[\alpha\text{Fuc}(1\rightarrow3)]\beta\text{GlcNAc-O---TMR}$ (Lewis X), and $\alpha\text{Fuc}(1\rightarrow2)\beta\text{Gal}(1\rightarrow4)[\alpha\text{Fuc}(1\rightarrow3)]\beta\text{GlcNAc-O---TM}$ (Lewis Y). Synthesis of the substrate and products has been described previously (14).

The instrument used for the determination of the fluorescent substrate and enzyme products has been described (16). Briefly, separation was carried out in a 50-60 cm long, 10 μm i.d., and 150 μm o.d. capillary at an electric field of 400 V/cm. The electrophoresis buffer contained 10 mM each of phosphate, tetraborate, phenylboronic acid, and SDS, at pH 9.3. The sheath fluid was identical to the running buffer.

6.4 RESULTS AND DISCUSSION

6.4.1 PTH-Amino Acids

Ten replicate runs of standard solutions containing the 19 PTH-amino acids, DMPTU, DPTU, and DPU, all at a concentration of 2.5×10^{-5} M, were obtained on the same day. The first electropherogram was taken as the standard, and subsequent electropherograms were normalized to the standard using the one-marker method. Figure 6.1 shows the relative standard deviation (RSD) values for the 22 analytes. Generally, the RSD values were reduced from about 1% without correction to less than 0.5% with 1-marker correction based on PTH-Y or DPTU.

The relative positions of the marker and analyte in the electropherogram affected the reproducibility of the corrected migration time. When PTH-Y was used as the marker (dashed curve), the early-migrating analytes had a RSD in migration time about 0.5%, but the RSD of migration time from the last six peaks increased monotonically from 0.5% to 1.3%. DPTU migrated in the middle of the electropherogram. When it was used as a marker (dotted curve) the relative precision of migration time for all analytes, except PTH-E and the last three peaks, was better than 0.4%.

The two-marker method corrects for drift in both electroosmotic and electrophoretic mobilities. DMPTU and DPU were used to correct the migration times in the same ten runs as above (solid curve). These components are common impurities generated in the Edman degradation reaction and make ideal markers for correction of

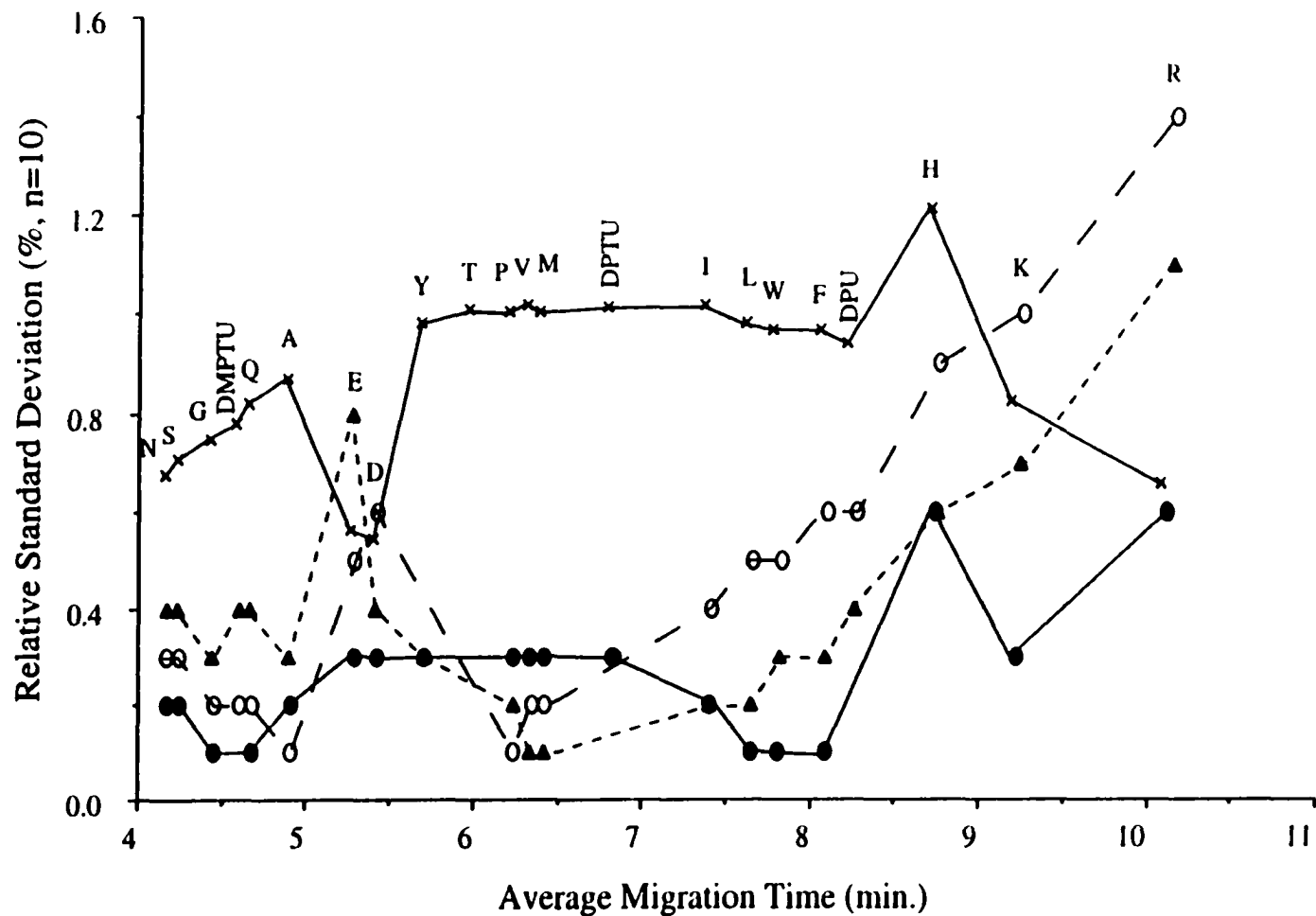


Figure 6.1 Relative standard deviation (RSD) of migration times for 19 PTH-amino acids, DMPTU, DPTU, and DPU before correction (x) and after one-marker correction based on PTH-Y (o) or DPTU (▲) and two-marker correction based on DMPTU and DPU (●). Letters represent PTH-amino acids with single letter abbreviation. Separation conditions are described in the text

migration time. The two-marker method significantly improved the reproducibility of migration times for all the analytes. After two-marker correction, the RSD of the migration times for all the analytes were about 0.4%, except for the PTH-H and PTH-R, which were about 0.6%.

Figure 6.2 presents four successive electropherograms obtained from the mixture. Figure 6.2A presents the raw data. Identification of any single component is difficult due to the variation in migration time. The single-marker migration time correction, Figure 6.2B, improves the migration time precision for the early migrating components, but actually degrades the migration time precision of the last few components. The two-component migration time correction, Figure 6.2C, does an outstanding job of correcting for migration time variations across the electropherograms, which simplifies identification of each component.

6.4.2 Between-Day Precision

To demonstrate the longer-term reproducibility of the migration times of PTH-amino acids, we calculated the RSD values of migration times from ten electropherograms that were obtained over a two month period. The RSD values from the raw data and after one- or two-marker corrections are shown in Figure 6.3. The raw migration times without correction gave RSDs from 3% to 10%. After the one-marker (DPTU) correction, the RSD values were generally reduced to about 1%. A V-shaped distribution of RSD values vs. average migration time was observed. As the migration time of the analytes approached the marker, DPTU, the RSD values became smaller.

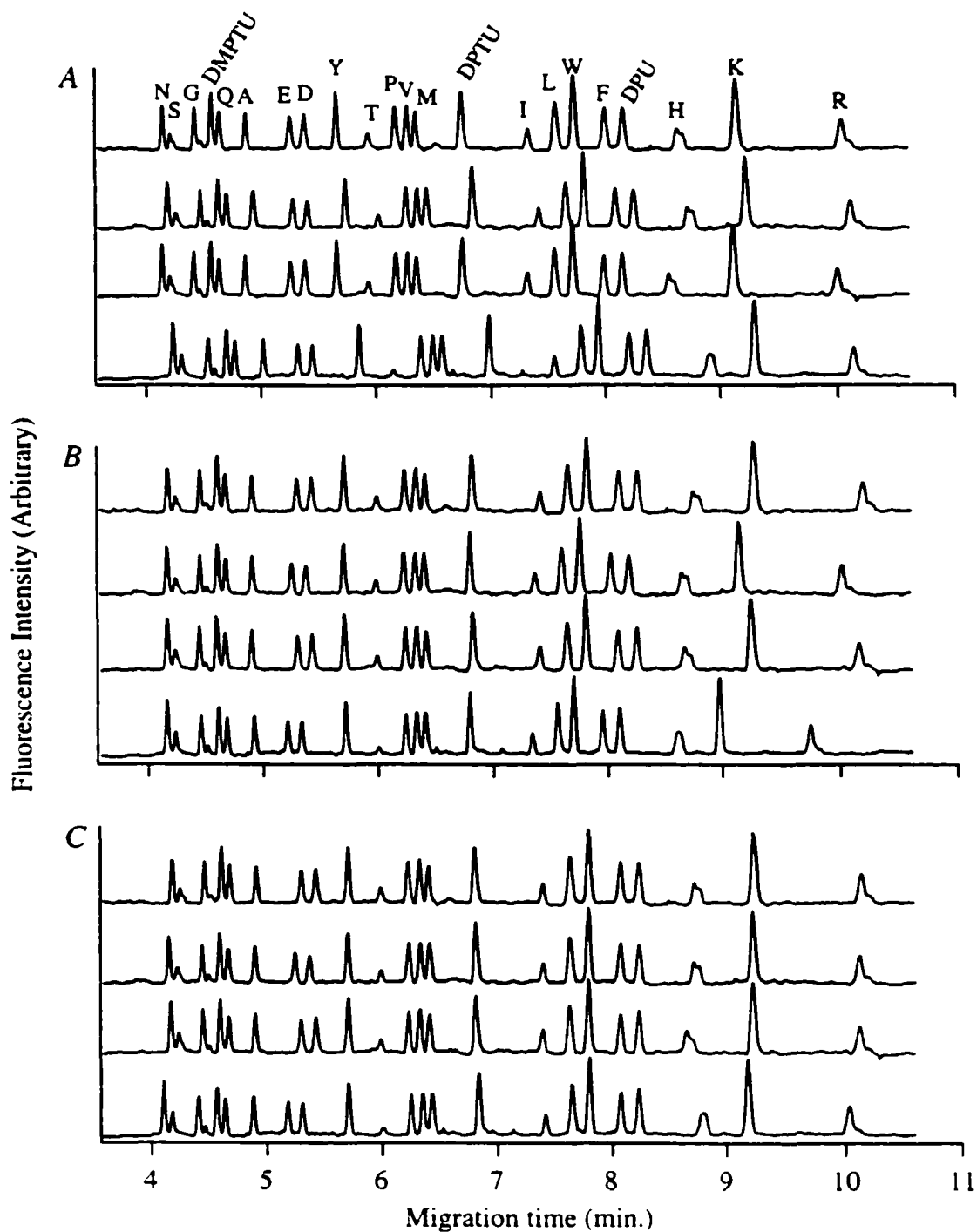


Figure 6.2 Comparison of electropherograms for raw data (A), one-marker corrected data (B), and two-marker corrected data (C) for separation of PTH-amino acids. PTH-Y was used as the marker for the one-component correction and DMPTU and DPU were used for the two-marker correction.

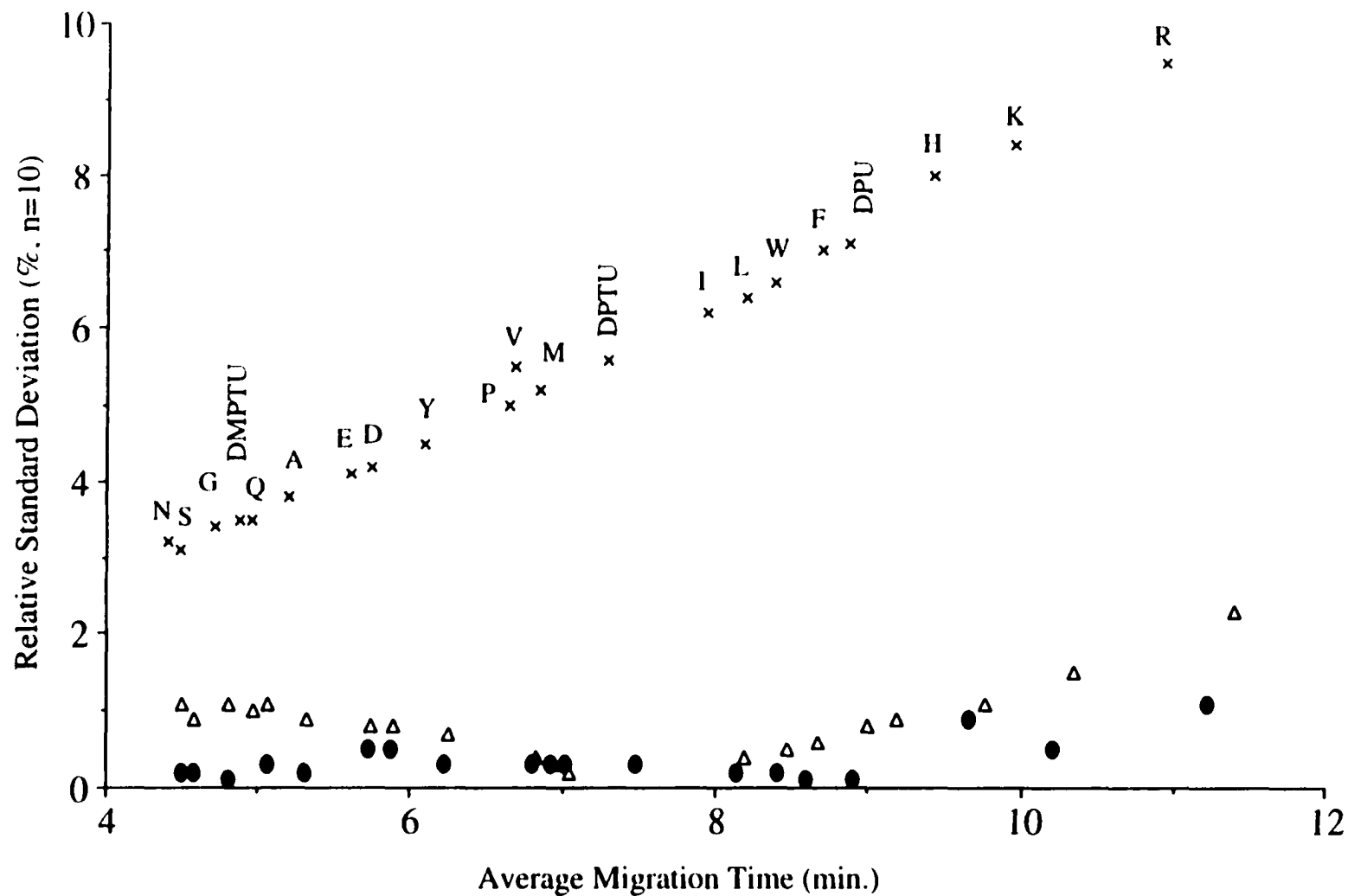


Figure 6.3 Relative standard deviation (RSD) of migration times of 19 PTH-amino acids, DMPTU, DPTU, and DPU from ten runs obtained over two months before correction (x), after one-marker (DPTU) correction (▲), and two-marker (DMPTU and DPU) (●). Separation conditions are the same as for the Figure 6.1 except the running voltage was 9kV.

When DMPTU and DPU were used in the two-marker method, the RSD values from these ten runs on different days were reduced to $< 0.5\%$ for all the analytes except for PTH-H and PTH-R which gave RSD values of 0.8% and 1%, respectively.

6.4.3 FTH-Amino Acids

The two correction methods were also applied for the analysis of FTH-amino acids. These compounds were much more difficult to analyze than the PTH-amino acids. The separation condition was based on the careful adjustment of the pH of the buffer near the pK_a for fluorescein; slight differences in ionization affected the separation. As a result, the migration times were quite sensitive to the buffer composition.

Four electropherograms were obtained from sequential runs. The RSD values obtained from the raw data, after the one-marker correction, and after the two-marker correction are shown in Figure 6.4. Before correction, the original migration time data gave RSD values from 2 to 4%. When peak B1 at 19.09 min. was used as the marker for the one-marker correction, the RSD of migration times were reduced to less than 1% for all except the last five peaks. The RSD of migration times for each peak improved as its migration time approached the marker B1 at 19.09 min.

Further improvement in the reproducibility of migration times for FTH-amino acids was obtained using the two-marker correction method. When the two peaks FTH-N and FTH-D at 15.05 and 28.67 min. were used as the markers, RSD values were generally reduced to less than 0.4% for all the FTH-amino acids, which was at least 8 times better than the uncorrected data.

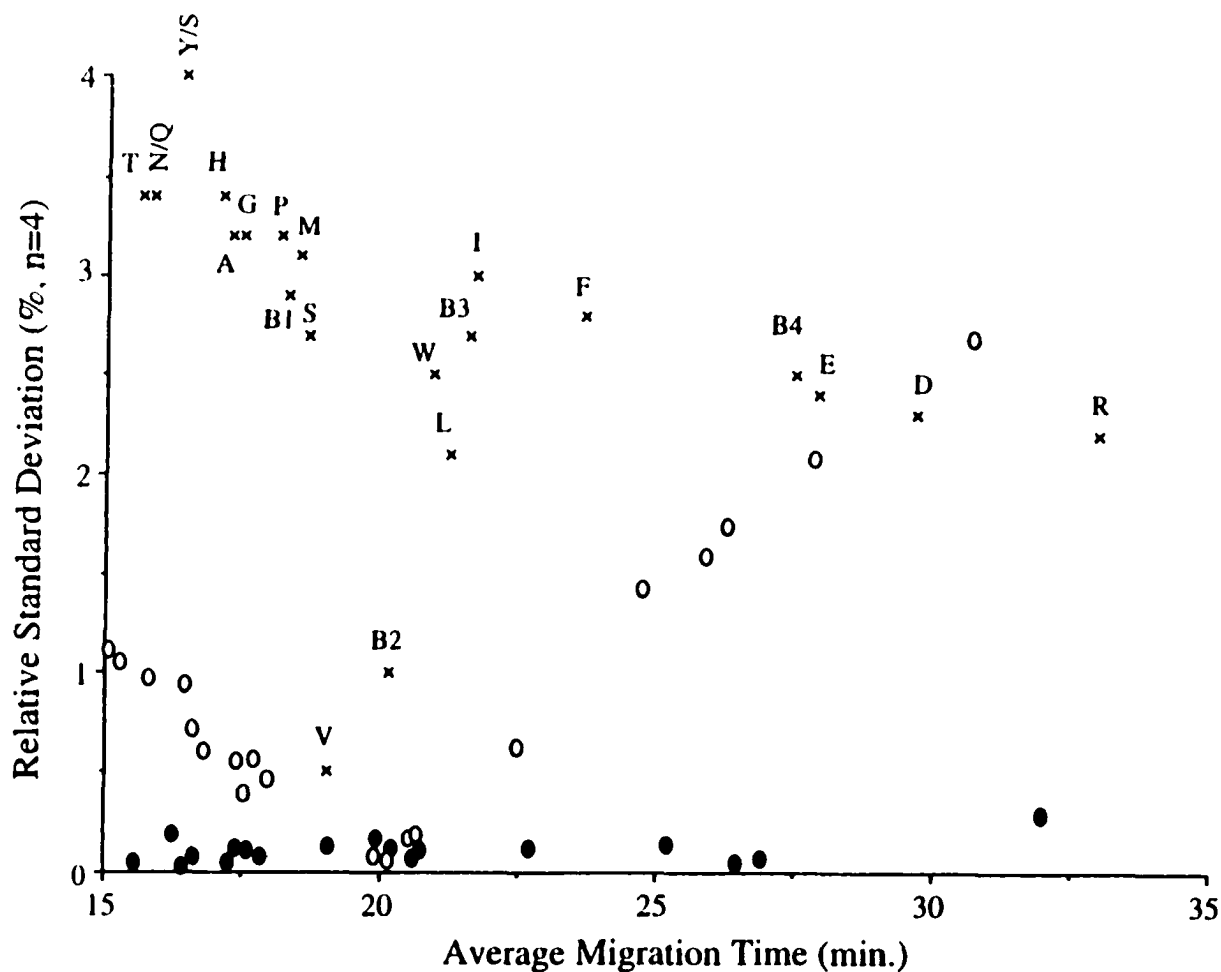


Figure 6.4 Relative standard deviation (RSD) of migration times for 19 FTH-amino acids, and unknown by-products without correction (x), with one-marker correction using the peak B1 at 19.09 min. (o), and two-marker correction using the two peaks (N, D) at 15.05 and 28.67 min. (●). B1, B2, B3, and B4 are unidentified by-products. Other letters represent FTH-amino acid with single letter abbreviation. Separation conditions are described in the text.

6.4.4 Oligosaccharide Analysis

As my last demonstration of the migration time correction methods, five runs of a standard solution containing five tetramethylrhodamine-labeled oligosaccharides were performed within one day. Approximately 3% RSD in peak migration time was observed from the raw data, Figure 6.5. The large variation of migration time is probably due to a change of temperature between runs; the experiments were performed in a poorly thermostatted room on a warm summer's day.

The variation in migration time is dramatically reduced using the correction methods. The RSD values for peaks 1, 2, 4, and 5 were reduced to less than 0.5% after one-marker correction using peak 3 as the marker. These are further reduced to less than 0.03% after two-marker correction with peak 3 and 5 as the markers.

6.5 CONCLUSION

The proposed correction methods dramatically reduces variations in migration time when applied to the separation of PTH-amino acids, FTH-amino acids, and oligosaccharides. However, the use of markers to improve migration time precision is not without problems. In particular, it may be difficult to chose markers that do not co-migrate with components in the standard mixture. Also, it is unlikely that the use of markers will be useful for large changes in buffer conditions that result in band-reversal.

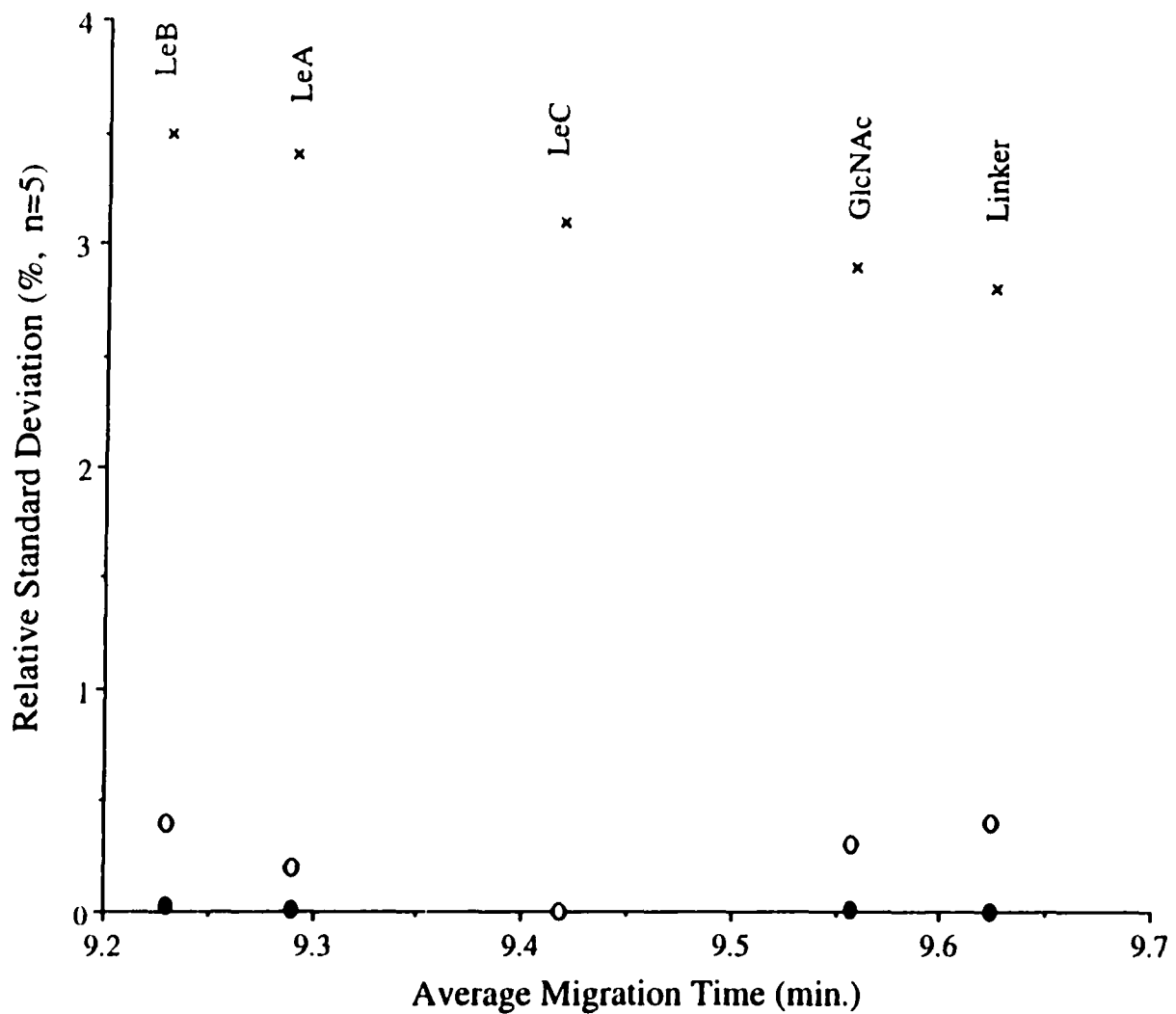


Figure 6.5 Relative standard deviation of migration times of five oligosaccharides separated using CE/LIF before (x) and after one-marker correction using peak 3 (o) and two-marker (●) correction using peak 3 and 5.

REFERENCES

1. Jorgenson, J. W.; Lukacs, K. D. *Anal. Chem.* 1981, 531, 298-1302.
2. Jorgenson, J. W.; Lukacs, K. D. *Science* 1983, 222, 266-272.
3. Lee, T.; Yeung, E. *Anal. Chem.* 1991, 63, 2842-2848.
4. Vespalec, R.; Gebauer, P.; Bocek, P. *Electrophoresis* 1992, 13, 677-682.
5. Jumppanen, J. H.; Riekkola, M. L. *Anal. Chem.* 1995, 67, 1060-1066.
6. Altria, K. D.; Harden, R. C.; Hart, M.; Hevizi, J.; Hailey, P. A.; Makwana, J. V.; Portsmouth, M. J. *J. Chromatogr.* 1993, 641, 147.
7. Chen, N.; Wang, L.; Zhang, Y. *J. Liq. Chromatogr.* 1993, 16, 3609.
8. Palmer, C.; Vandeginste, B. *J. Chromatogr.* 1995, 718, 153-165.
9. Waldren, K. C.; Dovichi, N. J. *Anal. Chem.* 1992, 64, 1396-1399.
10. Li, X.-F.; Waldron, K. C.; Black, J.; Lewis, D.; Ireland, I. D.; Dovichi, N. J. *Talanta* 1997, 44, 383-399.
11. Chen, M.; Waldren, K. C.; Zhao, Y.; Dovichi, N. J. *Electrophoresis* 1994, 15, 1290-1294.
12. Wu, S.; Dovichi, N. J. *Talanta* 1992, 39, 173-178.
13. Ireland, I. D.; Lewis, D. F.; Li, X.-F.; Renborg, A.; Kwong, S.; Chen, M.; Dovichi, N. J. *J. Protein Chem.* 1997, 16, 491-495.
14. Zhao, J. Y.; Dovichi, N. J.; Hingds Gaul, O.; Gosselin, S.; Palcic, M. M. *Glycobiology* 1994, 4, 239-242.
15. Zhang, Y.; Le, X. C.; Dovichi, N. J.; Compston, C. A.; Palcic, M. M.; Diedrich, P.; Hingds Gaul, O. *Anal. Biochem.* 1995, 227, 368-376.

16. Le, X. C.; Scaman, C.; Zhang, Y.; Zhang, J.; Dovichi, N. J.; Hindsgaul, O.; Palcic, M. M. *J. Chromatogr.* 1995, 716, 215-220.
17. Wu, S.; Dovichi, N. J. *J. Chromatogr.* 1989, 480, 141-155.

CHAPTER 7

CONCLUSIONS AND FUTURE WORK

CONCLUSIONS AND FUTURE WORKS

In the preceding chapters of this thesis, capillary electrochromatography (CEC), capillary electrophoresis (CE), and micellar electrokinetic chromatography (MEKC) utilizing crossed-beam thermo-optical UV absorbance detection (TOAD), as well as non-aqueous CE utilizing mass spectrometric (CEMS) detection have been explored for the separation and detection of a number of bioanalytes (i.e. phenylthiohydantoin - amino acids, testosterone metabolites, and *Fritillaria* alkaloids) and compounds of environmental interests (i.e. polycyclic aromatic hydrocarbons). The high separation efficiency ($\geq 100,000$ plates/m, an order of magnitude than conventional HPLC method) facilitates separation of mixtures of greater complexity. The TOAD and MS detections possess sufficient sensitivity to measure analyte concentration down to the order of 10^{-7} M and 10^{-8} M respectively to various compounds.

Some technical problems in CEC have been tackled and solved, including column-packing, frit fabrication, variations from column to column, column durability, and migration reproducibility of clean samples. Careful and well-controlled conditions are essential to ensure the manufacturing of CEC columns with high efficiencies. A simplified slurry-packing procedure was refined and demonstrated for packing CEC columns with 50 μm I.D.. CEC columns of comparable efficiency and reproducibility to commercially - available CEC columns have been produced. Evaluation of a single column over an extended period gave k' and N with precision of 0.6-5.6% RSD and 3.7-10% RSD respectively and with N values from 60,000 - 213,000 plates/m. The variation from column to column evaluated from 5 column gave precision within 0.28% - 0.94% RSD in migration time, 17% RSD in theoretical plates, and 6.9% in resolution.

Particular CEC methods with high efficiency and selectivity for analyses of mixture of polycyclic aromatic hydrocarbons, testosterone metabolites and phenylthiohydantoin amino acids were developed. Quantitative analysis using CEC was demonstrated. CEC with common HPLC type reverse phases is more suitable for separations of neutral hydrophobic compounds rather than charged molecules. The charged species have higher band broadening because of their narrow linear isotherm range. The application of CEC in neutral and hydrophobic compound separations should make CEC a viable alternative technique superior to both HPLC and CE.

Meanwhile, some intrinsic shortcomings have been recognized and addressed to provide guidance for the future work. There are fewer degrees of freedom for selectivity optimization in CEC than in HPLC. An attempt to increase the electroosmotic flow will cause an alteration of selectivity. The reproducibility of elution times is inherently vulnerable to sample matrix variations because of the small capacity and scale of the column.

One of the future prospects in CEC should focus on further instrument development. A new generation of equipment should perform accurate sample injection, produce reproducible flow, deal with small sample volumes, and be amenable to full automation. Gradient elution is one means to handle complex separations. The existing commercial instruments only allow isocratic operation. These instruments when modified to permit gradient CEC have drawbacks toward fully realizing the benefits of CEC. Controllable hydrodynamic sample injection for CEC may be an option in future instrument development because reproducible sample injection immune to sample matrix variation is critical to quantitative analysis.

Non-aqueous CE/MS for the screening of *Fritillaria* alkaloids shows a very bright future. The excellent efficiency and selectivity of CE with non-aqueous separation media allows baseline resolve 10 stereoisomeric alkaloids in much shorter analysis time than GC/MS or LC/MS methods. This method is distinguished by its fast speed and simplicity in sample preparation. Further directions should be toward improving the accuracy and precision in analysis of active components in crude extracts. The causes of unstable electrospray process in CE/MS as well as different interface designs should also be investigated toward alleviating the problem of unstable ESI process. Trials should be performed on coupling CE to the smaller MicroIonSpray interface to push the sensitivity to the ultimate limit.

Micellar electrochromatography using bile salts and organic modifiers has been shown as applicable, efficient and cost-effective in hydrophobic compound separations. The multiconformational bile salts aggregates in solution enhance partitioning of PAH in the micelles, which allows resolving 14 PAHs by MEKC. Bile salt aggregation maintained up to 70% organic solvent composition. Multiconformational bile salts aggregate in the presence of organic modifiers in solution. The resulting association with hydrophobic analytes require further study, which could aid in the understanding of the aggregation behavior of the bile salts, and therefore to manipulate and predict migration time order and selectivity of hydrophobic compounds using steroidal surfactants or other non-SDS detergent.

Finally, use of migration time markers enhances the precision of analyte migration times to various degrees demonstrated in MEKC of PTH - AAs, FTH - AAs, and oligosacchrides. The difficulty to choose markers that don't co-migrate with analyte

might be overcome by using dual-detector scheme that combines TOAD and fluorescence detection.